

**Functions of the Src Homology 3 and Guanylate Kinase Domains  
of the  $\beta$ -Subunit of Voltage-Gated Calcium Channels**

Erick Miranda Laferte

**Functions of the Src Homology 3 and Guanylate Kinase Domains  
of the  $\beta$ -Subunit of Voltage-Gated Calcium Channels**

Von der Naturwissenschaftlichen Fakultät  
der Gottfried Wilhelm Leibniz Universität Hannover  
Zur Erlangung des Grades

Doktor der Naturwissenschaften

-Dr. rer. Nat.-

genehmigte Dissertationen

von

Master en Bioquímica, Erick, Miranda Laferte  
geboren am 14 September 1974, in Havanna, Kuba

2009

Referent: Prof. Dr. Christoph Fahlke  
Korreferent: Prof. Dr. Anaclet Ngezahayo  
Prüfer: Prof. Dr. Theresia Kraft

Tag der Promotion: 21-August- 2009

**Abstract**

Voltage-gated calcium channels (VGCC) are multi-protein complex that are composed of a pore forming subunit  $Ca_v\alpha_1$  and different regulatory subunits.  $Ca_v\beta$  subunit is one of this modulatory subunits and it strongly regulates the voltage-dependent activation and inactivation of VGCCs. Different  $Ca_v\beta$  isoforms share two highly conserved domains flanked by shorter variable sequences: a Src homology 3 (SH3) domain and a guanylate kinase (GK) domain. Here we studied the functional role of both domains on the function and expression of heterologous VGCCs in *Xenopus* oocytes, using the cut open oocytes technique. The  $Ca_v\beta$ -SH3 and  $Ca_v\beta$ -GK domain proteins were purified from bacteria and they were injected into oocytes expressing  $Ca_v\alpha_1$  subunit. Our results demonstrated: 1) that  $Ca_v\beta$ -SH3 promotes channel endocytosis through dynamin interaction and that  $Ca_v\beta$  dimerization could be the signal that activates this pathway, 2) that  $Ca_v\beta$ -GK can recapitulate key modulatory properties of full length  $Ca_v\beta$  on channel activation and that it acts like a brake for channel inactivation. In general our findings have introduced a new perspective about the functions of the domains of  $Ca_v\beta$ , in which the GK domain regulates channel gating while the SH3 domain link the channel to intracellular process.

**Keywords:** voltage-gated calcium channel  $\beta$ -subunit, modular structure, endocytosis

## Zusammenfassung

Spannungsabhängige Kalziumkanäle (voltage-gated calcium channel: VGCC) sind Multiproteinkomplexe, die aus der porenbildenden Untereinheit  $Ca_v\alpha_1$  und unterschiedlichen regulatorischen Untereinheiten bestehen. Eine dieser modulierenden Untereinheiten ist die  $Ca_v\beta$ -Untereinheit. Sie steuert die spannungsabhängige Aktivierung und Inaktivierung der VGCCs. Verschiedene  $Ca_v\beta$ -Untereinheiten weisen zwei hoch konservierten Domänen - eine Src homology 3 (SH3) Domäne und eine Guanylasekinase (GK) Domäne - auf, die von kürzeren variablen Sequenzen umgeben sind. Mit der Cut-Open-Technik wurde der Einfluss beider Domänen auf Funktion und Expression von heterolog in *Xenopus* Oozyten exprimierten VGCCs untersucht. Die aus Bakterien aufgereinigten SH3- und GK-Proteine der  $Ca_v\beta$ -Untereinheit wurden direkt in Oozyten, die die  $Ca_v\alpha_1$ -Untereinheit exprimierten injiziert. Unsere Ergebnisse zeigen: 1) dass  $Ca_v\beta$ -SH3 die Endozytose des Kanals über eine Interaktion mit Dynamin fördert und dass die  $Ca_v\beta$ -Dimerisierung möglicherweise das aktivierende Signal dieses Signaltransduktionsweges ist und 2) dass  $Ca_v\beta$ -GK modulierende Schlüsseleigenschaften auf die Kanalaktivierung des vollständigen  $Ca_v\beta$  übernehmen kann und dass  $Ca_v\beta$  die Kanalinaktivierung verlangsamt. Unsere Ergebnisse haben eine neue Perspektive über die Funktion der  $Ca_v\beta$  Domänen eröffnet. Einerseits reguliert die GK-Domäne das Schaltverhalten des Kanals, während die SH3-Domäne ihrerseits eine Verbindung zu intrazellulären Prozessen herstellt.

**Stichwörter:** Spannungsabhängige Kalziumkanäle  $Ca_v\beta$  Untereinheiten, modulare Struktur  
Endozytose

## Contents

<b>2. Introduction</b> .....	9
2.1 Subunit composition of voltage-gated calcium channels.....	10
2.2 Classification of VGCCs.....	10
2.3 $\text{Ca}_v\alpha_1$ subunits.....	12
2.4 $\text{Ca}_v\alpha_2\delta$ subunits.....	15
2.5 $\text{Ca}_v\gamma$ subunits.....	16
2.6 $\text{Ca}_v\beta$ subunits.....	16
2.6.1 Structure of the $\text{Ca}_v\beta$ subunits.....	17
2.6.2 Functions of the $\text{Ca}_v\beta$ subunits.....	18
<b>3. Discussion</b> .....	22
3.1 $\text{Ca}_v\beta_{2a}$ -SH3 promotes endocytosis via dynamin interaction.....	22
3.2 $\text{Ca}_v\beta_{2a}$ -GK suffices to modulate gating of the channel.....	30
<b>4. Conclusions</b> .....	35
<b>5. References</b> .....	36
<b>List of Publications</b> .....	49
<b>6. The Src homology 3 domain of the <math>\beta</math>-subunit of voltage gated calcium channels promotes endocytosis via dynamin interaction</b> .....	50
6.1 Abstract.....	51
6.2 Introduction.....	52

6.3 Materials and Methods.....	54
6.3.1 Recombinant Proteins.....	54
6.3.2 Binding assay.....	55
6.3.3 Xenopus Oocytes preparation, injection and electrophysiological recordings.....	56
6.3.4 Surface expression measurements in Xenopus Oocyte.....	57
6.4 Results.....	58
6.4.1 $\beta_{2a}$ -SH3 reduces the number of channels expressed in the plasma membrane.....	58
6.4.2 $\beta_{2a}$ -SH3 induced reduction of $Q_{on}$ depends on dynamin.....	59
6.4.3 $\beta_{2a}$ -SH3 and full length $Ca_v\beta_{2a}$ down-regulate the distantly related Shaker potassium channel expressed in Xenopus oocytes.....	65
6.4.4 Full length $Ca_v\beta_{2a}$ reduces the number of plasma membrane $Ca_v1.2$ channels lacking the AID but not WT channels.....	65
6.5 Discussion.....	70
6.6 References.....	74
6.7 Supplemental Data.....	77
<b>7. The guanylate kinase domain of the <math>\beta</math>-subunit of voltage-gated calcium channels suffices to modulate gating.....</b>	<b>81</b>
7.1 Abstract.....	82
7.2 Introduction.....	83
7.3 Materials and Methods.....	86
7.3.1 Construction of cDNA and protein expression.....	86
7.3.2 Binding assay.....	87
7.3.3 Oocytes injection and electrophysiological recordings.....	87
7.4 Results.....	89
7.4.1 Refolding and binding assay of $Ca_v\beta$ -GK domain.....	89
7.4.2 $Ca_v\beta_{2a}$ -GK increases peak current amplitude and shifts the current-voltage relationship of $Ca_v1.2$ channels.....	92

7.4.3 $\text{Ca}_v\beta_{2a}$ -GK inhibits inactivation of $\text{Ca}_v2.3$ WT channels.....	96
7.4.4 $\text{Ca}_v\beta_{1b}$ -GK resembles $\text{Ca}_v\beta_{2a}$ in inhibiting inactivation of $\text{Ca}_v2.3$ WT channels.....	98
7.4.5 Full-length $\text{Ca}_v\beta$ proteins switch $\text{Ca}_v2.3$ -inactivation phenotype depending on the time of injection.....	98
7.5 Discussion.....	104
7.6 References.....	108
7.7 Supplemental Data.....	113
<b>8. Dimerization of the Src homology 3 domain of the voltage-gated calcium channel <math>\beta</math>-subunit regulates endocytosis.....</b>	<b>123</b>
8.1 Abstract.....	124
8.2 Introduction.....	125
8.3 Materials and Methods.....	127
8.3.1 cDNA constructs and recombinant proteins.....	127
8.3.2 Immunoprecipitations.....	127
8.3.3 Pull-down assay.....	127
8.3.4 <i>Xenopus</i> Oocytes preparation, injection and electrophysiological recordings.....	128
8.3.5 Blue native polyacrylamide gel electrophoresis.....	129
8.4 Results and Discussion.....	130
8.4.1 $\text{Ca}_v\beta_{2a}$ -SH3 dimerizes through a single disulfide bond.....	130
8.4.2 $\text{Ca}_v\beta_{2a}$ -SH3 C113A dimerization-deficient mutant associates with dynamin but does not promote endocytosis.....	132
8.4.3 Concatameric $\text{Ca}_v\beta_{2a}$ -SH3 113A rescues endocytosis.....	134
8.4.4 $\text{Ca}_v\beta$ forms dimers.....	135
8.4.5 Speculation.....	137
8.5 References.....	141
<b>Acknowledgments.....</b>	<b>145</b>



**Curriculum Vitae..... 146**

## Abbreviations

AID:  $\alpha$  interaction domain

BN-PAGE: Blue native polyacrylamide gel electrophoresis

Ca<sub>v</sub> $\alpha$ <sub>1</sub>: Voltage-gated calcium channels  $\alpha$ <sub>1</sub> subunit

Ca<sub>v</sub> $\alpha$ <sub>2</sub>: Voltage-gated calcium channels  $\alpha$ <sub>2</sub> subunit

Ca<sub>v</sub> $\beta$ : Voltage-gated calcium channels  $\beta$  subunit

Ca<sub>v</sub> $\delta$ : Voltage-gated calcium channels  $\delta$  subunit

Ca<sub>v</sub> $\gamma$ : Voltage-gated calcium channels  $\gamma$  subunit

DHP: Dihydropyridine

DTT: Dithiothreitol

Dyn<sub>829-842</sub>: Dynamin peptide encompassing residues 829-842

GK: Guanylate Kinase

GST: Glutathione S- transferase

HA: Hemagglutinin

HVA: Low voltage activated calcium channels

LVA: Low voltage activated calcium channels

MAGUK: Membrane associated guanylate kinase

PRD: Proline rich domain

Q<sub>on</sub>: Total charge movement

SDS-PAGE: Sodium dodecyl sulphate polyacrylamide gel electrophoresis

SH3: Src Homology-3

VGCCs: Voltage-gated calcium channels

YFP: Yellow Fluorescent protein

## List of Figures and Tables

Figure 2.1	Proposed schematic structure of VGCCs.....	11
Figure 2.2	Membrane topology VGCCs.....	14
Figure 2.3	Structural organization of $\text{Ca}_v\beta$ .....	19
Figure 3.1	Model of the proposed mechanism of VGCCs endocytosis promoted by $\text{Ca}_v\beta$ .....	29
Figure 6.1	$\beta_{2a}$ -SH3 reduces charge movement in <i>Xenopus</i> oocytes expressing $\text{Ca}_v1.2$ .....	60
Figure 6.2	$\beta_{2a}$ -SH3-induced reduction of charge movement is not abolished by bafilomycin.....	63
Figure 6.3	$\beta_{2a}$ -SH3-induced reduction of charge movement relies on interaction with dynamin.....	64
Figure 6.4	$\beta_{2a}$ -SH3 binds in vitro to dynamin but not to $\text{Ca}_v1.2$ .....	66
Figure 6.5	$\beta_{2a}$ -SH3 and full length $\text{Ca}_v\beta_{2a}$ reduce ionic currents mediated by <i>Shaker</i> potassium channels expressed in <i>Xenopus</i> oocytes...	67
Figure 6.6	Full length $\text{Ca}_v\beta_{2a}$ internalizes calcium channels devoid of the AID site but not WT channels.....	69
Figure 6.7	Model for $\text{Ca}_v\beta$ and dynamin interaction.....	72
Figure 6.S1	Normalized membrane conductance as function of membrane potential and mean $\pm$ S.E.M of parameters defining the Boltzmann distribution that best fitted the data for <i>Xenopus</i> oocytes expressing <i>Shaker</i> IR.....	79
Figure 6.S2	$G/G_{\max}$ vs $V_m$ plot from <i>Xenopus</i> oocytes expressing <i>Shaker</i> ...	80
Figure 7.1	Domain structure, purification and binding assay of $\text{Ca}_v\beta$ constructs.....	90
Figure 7.2	Refolded $\text{Ca}_v\beta_{2a}$ -GK and $\text{Ca}_v\beta_{2a}$ -SH3-GK shift the current- voltage relationship of $\text{Ca}_v1.2$ -mediated currents.....	94
Figure 7.3	$\text{Ca}_v\beta_{2a}$ -GK covalently linked to $\text{Ca}_v1.2$ WT, but not to $\text{Ca}_v1.2$ W470S, increases peak current amplitudes and shifts the current-voltage relationship.....	95

Figure 7.4	Ca <sub>v</sub> β-GK slows down inactivation of Ca <sub>v</sub> 2.3-mediated currents.....	97
Figure 7.5	Ca <sub>v</sub> β-GK shifts mid-point voltage for the steady-state inactivation of Ca <sub>v</sub> 2.3-mediated currents.....	99
Figure 7.6	Ca <sub>v</sub> β <sub>1b</sub> -GK slows down inactivation of Ca <sub>v</sub> 2.3-mediated currents and shifts the steady-state inactivation toward more depolarized potentials.....	100
Figure 7.7	Ca <sub>v</sub> 2.3-inactivation phenotype induced by full-length Ca <sub>v</sub> β <sub>1b</sub> and Ca <sub>v</sub> β <sub>2a</sub> C3,4S depends on the time of injection.....	102
Figure 7.S1	Sucrose Gradient analysis of molecular standars.....	115
Figure 7.S2	Sucrose Gradient analysis of Ca <sub>v</sub> β <sub>2a</sub> -GK.....	116
Figure 7.S3	Sucrose Gradient analysis of Ca <sub>v</sub> β <sub>1b</sub> -GK.....	117
Figure 7.S4	Ca <sub>v</sub> β <sub>2a</sub> -SH3-GK is as effective as full length Ca <sub>v</sub> β <sub>2a</sub> in modulating activation of Ca <sub>v</sub> 1.2-mediated currents.....	118
Figure 7.S5	Mutation of a fully conserved tryptophan within the AID sequence yields Ca <sub>v</sub> 2.3 channels insensible to full length Ca <sub>v</sub> β <sub>2a</sub> and refolded Ca <sub>v</sub> β <sub>2a</sub> -GK.....	119
Figure 8.1	BN-PAGE analysis of wild type Ca <sub>v</sub> β <sub>2a</sub> -SH3 and Ca <sub>v</sub> β <sub>2a</sub> -SH3 C113A.....	131
Figure 8.2	Association with dynamin and endocytosis activity of wild type Ca <sub>v</sub> β <sub>2a</sub> -SH3 and Ca <sub>v</sub> β <sub>2a</sub> -SH3 C113A dimerization-deficient mutant.....	133
Figure 8.3	Association with dynamin and endocytosis activity of wild type Ca <sub>v</sub> β <sub>2a</sub> -SH3 and Ca <sub>v</sub> β <sub>2a</sub> -SH3 C113A concatamers.....	136
Figure 8.4	BN-PAGE and pull down assays of Ca <sub>v</sub> β <sub>2a</sub> .....	138
Figure 8.5	Model for the functional switch of Ca <sub>v</sub> β from calcium channel modulator to endocytosis activator.....	139
Table 2.1	Nomenclature, classification and tissue distribution of Ca <sub>v</sub> α <sub>1</sub> subunits.....	13

Table 6.S1	Mean $\pm$ S.E.M of parameters defining the Boltzmann distribution that best fitted the Normalized $Q_{on}$ vs $V_m$ plots for <i>Xenopus</i> oocytes expressing $Ca_v1.2$ .....	77
Table 6.S2	Mean $\pm$ S.E.M of parameters defining the mono-exponential function that best described the time course of normalized $Q_{on}$ for <i>Xenopus</i> oocytes expressing $Ca_v1.2$ .....	78
Table 7.S1	Parameters defining the sum of two Boltzmann distributions that best fitted normalized tail currents for the indicated $Ca_v1.2$ subunit combinations.....	120
Table 7.S2	Average $t_{1/2}$ and parameters defining the Boltzmann distribution and the percentage of non-inactivating current component that best fitted steady-state inactivation for the indicated $Ca_v2.3$ subunit combinations.....	121

## **2. Introduction**

The intracellular and extracellular environments of a living cell are separated by a plasma membrane that by itself is impermeable to water, hydrophilic molecules and ions. Diverse proteins inserted inside of this membrane are responsible for the transport of these hydrophilic compounds. These proteins belong to two major groups: transporters and channels (Hill, 1993a)

Ion channels are pores, which by opening allow the passive flow of specific ions in the direction of their electrochemical gradient. Opening of a channel can be accomplished in several ways, one of them is through a change in the membrane potential, and channels that open following this mechanism are called voltage-gated ion channels.

Voltage-gated ion channels belong to a super family of ion channels that have in common the presence of a voltage sensor that led the opening of the pore after a membrane depolarization. Voltage-gated calcium channels (VGCCs) belong to this family, they mediate the influx of  $\text{Ca}^{2+}$  ions into eukaryotic cells in response to membrane depolarization. Changes in intracellular calcium concentrations regulate various cellular functions including: neurotransmission, muscular excitation-contraction coupling, hormone secretion and gene expression (Catterall, 2000). VGCCs have been found mainly in all excitatory eukaryotic cells but they are also present in low levels in not excitatory tissues. They play a crucial role in calcium signalling cascade (Dolphin, 2003a).

## **2.1 Subunit composition of voltage-gated calcium channels.**

Fatt and Katz in 1953 were the first that identified the VGCCs. Approximately thirty years later, the first calcium channel protein was isolated. They are heteromultimers consisting of a main pore forming subunit that associates with different auxiliary subunits to form functional channels. The pore forming subunit was named  $Ca_v\alpha_1$  and it contains all determinants for functional voltage gated ion channels. The auxiliary regulatory subunits were named  $Ca_v\beta$ ,  $Ca_v\alpha_2$ ,  $Ca_v\delta$  and  $Ca_v\gamma$  (Fig.2.1) (Flockerzi et al., 1986; Sieber et al., 1987; Takahashi et al., 1987; Leung et al., 1988).

## **2.2 Classification of VGCCs**

The first classification of the VGCCs was based on their electrophysiological properties. It was found that some calcium channels need only a small membrane depolarization to be activated while others need a higher change in the membrane potential. Based on this distinctive characteristic VGCCs were classified into two groups: low voltage activated (LVA) and high voltage activated (HVA) calcium channels (Carbone and Lux, 1984). Because of their little conductance LVA channels were also called T channels (T for Tiny).

Further studies led to the identification of the pharmacological properties of VGCCs. Channels sensitive to 1,4-dihydropyridine (DHP) were called L-type (Hess et al., 1984). Additionally channels sensitive to  $\omega$ -conotoxin GVIA were classified as N-type channels and those sensitive to  $\omega$ -agatoxin IVA as P-type. Other  $\omega$ -agatoxin IVA sensitive channels were identified in cerebellar granule cells and termed Q-type, but they were combined with P-type and they were called P/Q. There is another group of

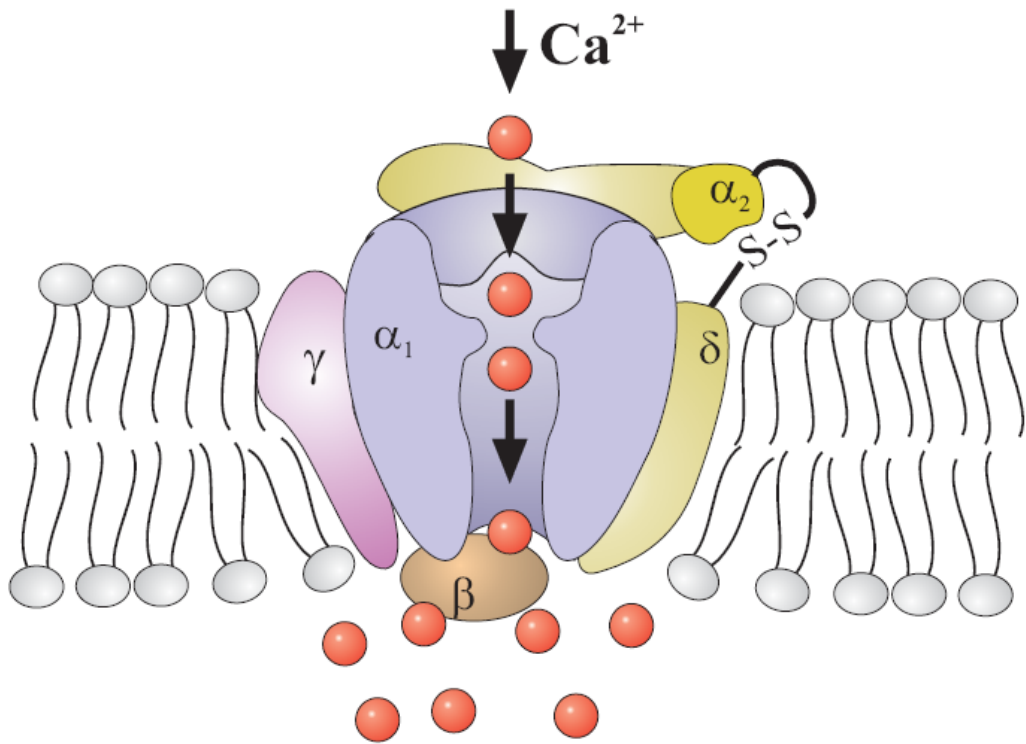


**Figure 2.1 Proposed schematic structure of VGCCs.** The  $Ca_v\alpha_1$  is the pore forming subunit through which calcium ions can pass in the direction of their electrochemical gradient upon channel opening.  $Ca_v\beta$ ,  $Ca_v\alpha_2$ ,  $Ca_v\delta$  and  $Ca_v\gamma$  are regulatory subunits that modulate channel activity.



channels that are insensitive to these toxin and that were called R-type (McCleskey et al., 1987; Mintz et al., 1992; Randall et al., 1995).

After the cloning of the  $\text{Ca}_v\alpha_1$  subunit a nomenclature was established on the base of the differences in the amino acids sequences of each isoform (Table 2.1) (Dolphin, 2003a). In the last years, with the increase on the number of cloned  $\text{Ca}_v\alpha_1$  subunits, a new classification was proposed in which a number is give to each isoform (Table 2.1) (Ertel et al., 2000).

### **2.3 $\text{Ca}_v\alpha_1$ subunits**

$\text{Ca}_v\alpha_1$  is the pore forming subunit of the VGCCs. It is a polypeptide chain with 24 transmembrane segments. These segments are organized into four homologous repeats or domains, each containing six transmembrane segments (Fig 2.2). The four domains are linked through large cytoplasmic loops that are capable of interact with a number of modulatory proteins including the  $\text{Ca}_v\beta$  subunit (Stotz et al., 2003).

The sequence of  $\text{Ca}_v\alpha_1$  reveals the presence of positive lysine and arginine residues in the S4 segment of each domain, which are supposed to form the voltage sensor that promotes the voltage activation. The pore is principally permeable to calcium and barium and the selectivity filter is attributed to four glutamate residues in close proximity in the loop linking the S5-S6 segments and that line the pore (Dolphin, 2006).

HVA	DHP Sensitive	L	$\alpha_{1S}$	Ca <sub>v</sub> 1.1	Skeletal Muscle
			$\alpha_{1C}$	Ca <sub>v</sub> 1.2	heart, smooth muscle
			$\alpha_{1D}$	Ca <sub>v</sub> 1.3	Neurons, secretory cells, heart
			$\alpha_{1F}$	Ca <sub>v</sub> 1.4	Retina, sensory neurons
	DHP Insensitive	P/Q	$\alpha_{1A}$	Ca <sub>v</sub> 2.1	Neurons
		N	$\alpha_{1B}$	Ca <sub>v</sub> 2.2	Neurons
		R	$\alpha_{1E}$	Ca <sub>v</sub> 2.3	Neurons
LVA	-	T	$\alpha_{1G}$	Ca <sub>v</sub> 3.1	Brain
			$\alpha_{1H}$	Ca <sub>v</sub> 3.2	Brain
			$\alpha_{1I}$	Ca <sub>v</sub> 3.3	Brain

**Table 2.1** Nomenclature, classification and tissue distribution of Ca<sub>v</sub>α<sub>1</sub> subunits

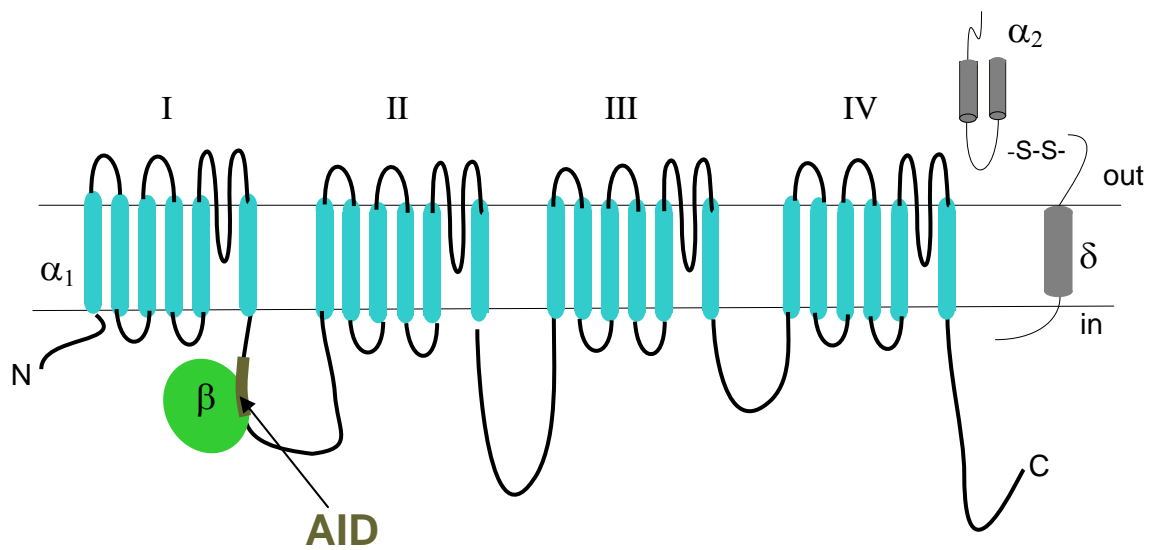


**Figure 2.2 Membrane topology VGCCs.** Blue barrels represent the transmembrane segments of  $\text{Ca}_v\alpha_1$ . In green is showed  $\text{Ca}_v\beta$  subunit and in grey  $\text{Ca}_v\alpha_2\delta$  subunit. AID represents the  $\alpha$  interaction domain present in the loop I-II

The loop joining the domains I and II (loop I-II) is an important region for VGCC regulation. It contains an eighteen amino acids long consensus sequence, highly conserved among HVA VGCCs, the so called  $\alpha$  interaction domain (AID). The AID sequence constitutes the primary binding site for the  $\text{Ca}_v\beta$  subunit, the major regulatory subunit of VGCCs (Pragnell et al., 1994). Independent of its role like a binding pocket for  $\text{Ca}_v\beta$ , several studies have found other functions to this loop. Leroy et al. (2005) and Dafi et al. (2004) described that mutations in this region affect the voltage-dependent inactivation of the channels and Bichet et al. (2000) reported that it contains an endoplasmic reticulum retention signal.

The N-terminus and the C-terminus of the channels are intracellular located. The function of the N-terminus is not very well understood, but a mutant channel with truncations in this region exhibit a better membrane expression than the wild type (Wei et al., 1996). This supports the idea that this region contributes to intracellular trafficking of  $\text{Ca}_v\alpha_1$ . The role of the C terminus has been associated with the  $\text{Ca}^{2+}$  dependent inactivation mechanism in L-type channels and with voltage-dependent inactivation in other members of the family (Pitt et al., 2001).

#### **2.4 $\text{Ca}_v\alpha_2\delta$ subunits**

$\text{Ca}_v\alpha_2\delta$  subunits are encoded by four genes ( $\text{Ca}_v\alpha_2\delta 1$  through  $\text{Ca}_v\alpha_2\delta 4$ ) with molecular masses between 140 and 170 kDa.  $\text{Ca}_v\alpha_2$  and  $\text{Ca}_v\delta$  are proteolytically cleaved from one single polypeptide chain, which is later linked by a disulfide bond to yield the mature  $\text{Ca}_v\alpha_2\delta$  subunit (Fig 2.2) (De Jongh et al. 1990). This subunit has modulatory effects on the time course and voltage dependence on current activation and

inactivation, and on the trafficking of  $\text{Ca}_v\alpha_1$  subunits to the plasma membrane (Bangalore et al., 1996; Felix et al., 1997; Qin et al., 1998).

### **2.5 $\text{Ca}_v\gamma$ subunits**

$\text{Ca}_v\gamma$  are encoded by eight genes ( $\text{Ca}_v\gamma 1$  through  $\text{Ca}_v\gamma 8$ ). They have molecular masses of approximately 32 kDa. This subunit was originally found associated with the skeletal muscle L-type channels (Bosse et al., 1990; Jay et al., 1990) but recently some  $\text{Ca}_v\gamma$  isoforms have been found in other tissues (Klugbauer et al., 2000). The regulatory functions of this subunit remain unclear but some small inhibitory effects on channel activation have been observed (Freise et al., 2000; Arikath et al., 2003).

### **2.6 $\text{Ca}_v\beta$ subunits**

$\text{Ca}_v\beta$  is the main regulatory subunit of VGCCs. Until now four different non allelic genes encoding for this proteins have been identified and cloned, each one with different splices variants that make even higher the total number of  $\text{Ca}_v\beta$  (Hullin et al., 1992; Birnbaumer et al., 1998).

Diverse studies have revealed the tissue distribution of the  $\text{Ca}_v\beta$ .  $\text{Ca}_v\beta_1$  is expressed in skeletal muscle, cardiac tissue and nervous system.  $\text{Ca}_v\beta_2$  and  $\text{Ca}_v\beta_3$  exist preferentially in cardiac muscle but also at low levels in neurons,  $\text{Ca}_v\beta_4$  is present in the nervous system (Hullin et al., 1992; Perez Reyes et al., 1992; Castellanos et al., 1993; Birnbaumer et al., 1998; Dolphin et al., 2003b). Analysis of the co-distribution of the  $\text{Ca}_v\alpha_1$  and  $\text{Ca}_v\beta$  subunits suggests that they could coexist in diverse combinations in different tissues, but some pairs could predominate over others,

depending of the subunit concentration and the difference in the affinities between them (Dolphin, 2003b).

### **2.6.1 Structure of the $Ca_v\beta$ subunits**

The molecular masses of  $Ca_v\beta$  subunits range between 52 and 78 kDa. Sequence alignments of several  $Ca_v\beta$  isoforms reveal the presence of five regions: two central (II and IV) highly conserved among all  $Ca_v\beta$ , flanked by three regions (I, III and V) variable in sequence and length (Fig. 2.3A).

The crystallographic structures of three different  $Ca_v\beta$  isoforms revealed that the first conserved domain encompasses a Src homology-3 (SH3) domain and the second a Guanylate Kinase (GK) domain. (Fig.2.3B)(Chen et al., 2004; Opatowsky et al., 2004; Van Petegem et al., 2004). These domains are found in members of the membrane-associated guanylate kinase (MAGUK) family of scaffolding proteins. Typical MAGUKs also contain at the N-terminus one to three PDZ domains.  $Ca_v\beta$  was then identified as a novel member of MAGUK family.

The crystallographic structures of  $Ca_v\beta$  were also solved in a complex with the AID peptide of the  $Ca_v\alpha_1$  subunit (Fig. 2.3B).They show that the GK domain is interacting with the AID while SH3 does not contribute to this association and it is facing to the opposite side of the GK-AID interaction surface (Chen et al., 2004; Opatowsky et al., 2004; Van Petegem et al., 2004).

The SH3 domains are modules controlling protein-protein interactions by binding to proline rich domains (PRD) presents in specific ligand proteins. In  $\text{Ca}_v\beta$  many of the canonical SH3 residues necessary for the interaction with PRD are buried into the structure puzzling a possible function for this domain (Chen et al., 2004; Opatowsky et al., 2004; Van Petegem et al., 2004).

The GK domain, like in many other MAGUK proteins, does not have enzymatic activity due to the fact that the glycine-rich ATP binding motif present in true Guanylate Kinase is not conserved in  $\text{Ca}_v\beta$ -GK (Dolphin, 2003b).

### **2.6.2 Functions of the $\text{Ca}_v\beta$ subunits**

The association of one single molecule of  $\text{Ca}_v\beta$  subunit to  $\text{Ca}_v\alpha_1$  suffices for modulation of the channel (Dalton et al., 2005). This association is reversible at the level of plasma membrane but the signal that promotes dissociation from the channel is unknown (Hidalgo et al., 2006).

$\text{Ca}_v\beta$  subunits promote and increase the current density of VGCCs. This effect can be attributed to an increase on channel activation and/or on plasma membrane expression (Dolphin, 2006). All  $\text{Ca}_v\beta$  subunits shift the voltage-dependence activation of the VGCCs toward higher hyperpolarizing voltages, which means that in the presence of  $\text{Ca}_v\beta$  subunit the channel can achieve the same open probability with less membrane depolarization (Josephson and Varadi, 1996; Kamp et al., 1996).  $\text{Ca}_v\beta$  increase the trafficking of the channels to the plasma membrane, probably masking some

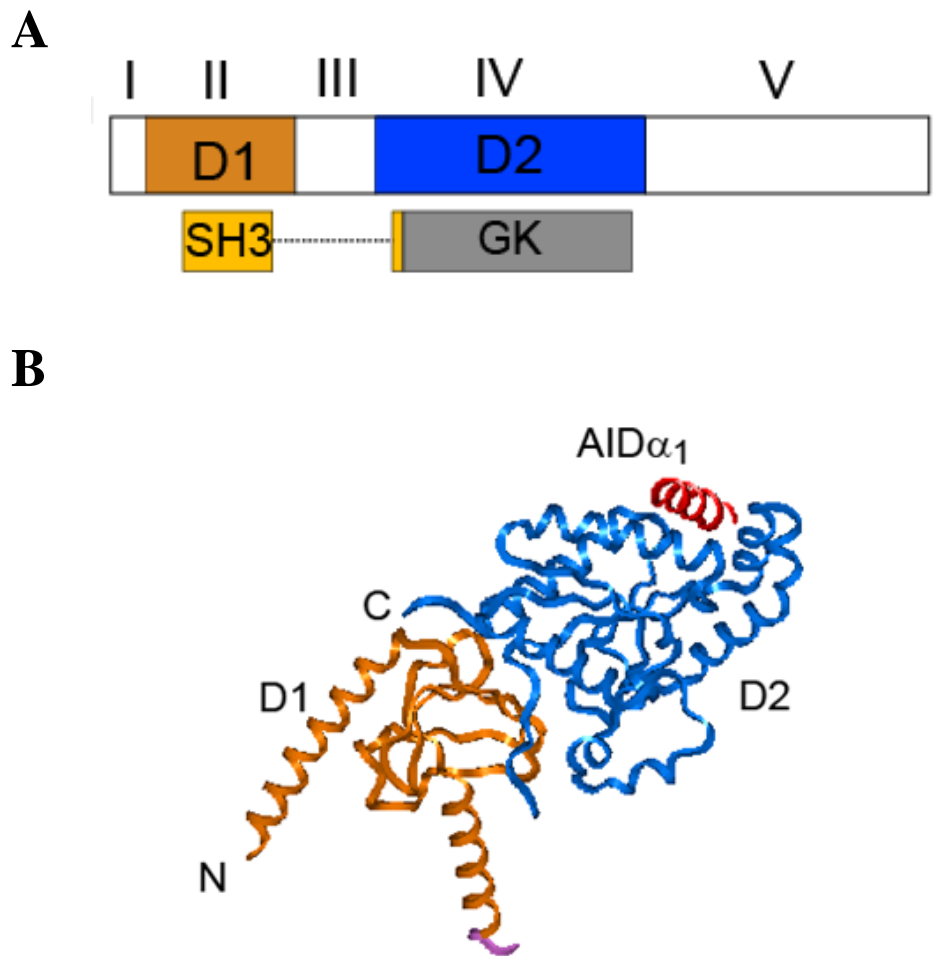


**Figure 2.3 Structural organization of  $\text{Ca}_v\beta$ .** **A** Representation of  $\text{Ca}_v\beta$  primary structure showing the conserved D1 and D2 regions flanked by the variable regions, D1 encompass a SH3 domain and D2 a GK domain. **B** Three dimensional structure of  $\text{Ca}_v\beta$ : D1 correspond to SH3 domain, D2 to GK domain, C to C-terminal, N to N-terminal and  $\text{AID}\alpha_1$  to the AID sequence from  $\text{Ca}_v\alpha_1$ .



endoplasmic reticulum retention signals presents in the loop I-II of the  $Ca_v\alpha_1$  subunits (Bichet et al., 2000).

$Ca_v\beta$  effects channel inactivation in an isoform specific manner. All  $Ca_v\beta$  isoforms except  $Ca_v\beta_{2a}$  inhibits inactivation while the other ones facilitate (Olcese et al., 1994). This particular property of  $Ca_v\beta_{2a}$  is attributed to palmytoilation of two cysteine residues at position three and four in N-terminus region of this protein (Chien et al., 1996; Qin et al., 1998; Hurley et al., 2000; Restituito et al., 2000).

In summary,  $Ca_v\beta$  has a crucial role on the regulation of VGCCs function. It exhibits a modular structure consisting of two highly conserved protein-protein interaction domains, an SH3 and a GK domain. While the GK domain interacts directly with AID the SH3 domain does not participate at all in the binding to AID. This structural arrangement suggests that GK is responsible for channel modulation while no function for the SH3 domain can be deduced. It is likely that this domain interact with other cellular partners. Until now no functional role has been described for any of these domains.

The aim of this work was to investigate the functional role of the SH3 and GK domains of  $Ca_v\beta$  and their effect on modulation of VGCCs using a combination of electrophysiological, biochemical and molecular biology techniques. We demonstrated that while the SH3 domain promotes endocytosis by interacting with dynamin, an endocytic protein, the GK domain suffices for channel's modulation. These results

provided a new functional map for  $\text{Ca}_v\beta$  and added a new function to this regulatory subunit emphasizing its multifunctional nature.

### 3. Discussion

$\text{Ca}_v\beta$  is a two-domain protein composed of a SH3 and a GK domain. It binds with high affinity to the AID sequence within the loop I-II of the  $\text{Ca}_v\alpha_1$  subunit and regulates many electrophysiological properties of the channel functions. Despite of several attempts, any of the functions of the full length  $\text{Ca}_v\beta$  have been related with any of its domains. Here we studied the functions of these domains analysing the effect of the injection of recombinant  $\text{Ca}_v\beta$ -SH3 and  $\text{Ca}_v\beta$ -GK domains into *Xenopus* oocytes expressing  $\text{Ca}_v\alpha_1$  and using several biochemical and molecular biology methods.

#### 3.1 $\text{Ca}_v\beta$ -SH3 promotes endocytosis via dynamin interaction

We purified from bacteria a recombinant  $\text{Ca}_v\beta_{2a}$ -SH3 that eluted as a mono-disperse peak from a size exclusion chromatography with a molecular weight corresponding to a monomeric form.

We studied the effect of the injection of recombinant  $\text{Ca}_v\beta_{2a}$ -SH3 domain into oocytes expressing  $\text{Ca}_v1.2$ , using cut open oocytes technique. This technique allows us to measure ionic and gating currents. Total charge movement ( $Q_{on}$ ) were calculated as the integral of the gating currents and they represent the total number of charges that are moved leading to channel opening (Benzanilla and Stefani, 1998). Every channel has a fix number of charges that move in response to depolarization and, hence  $Q_{on}$  it is proportional to the number of channels (Equation 3.1) (Hill, 1993b).

$$Q_{on} = N \times q \quad \text{Equation 3.1}$$

Where N is the total number of channel on the plasma membrane and q are the charges of an unitary channel that move in response to depolarization

After the injection of  $Ca_v\beta_{2a}$ -SH3 we observed a dramatic decrease in  $Q_{on}$  (Fig 6.1C). This decrease proceeds without changes in the voltage or time dependence of  $Q_{on}$  (Fig. 6.1F and G) and it likely reflected a reduction in the number of channels in the cell surface. Channel surface expression using immunoassay experiment with oocytes expressing HA-tagged  $Ca_v1.2$  channels showed that the drop of  $Q_{on}$  corresponds to a decrease in the number of channels on the plasma membrane (Fig 6.2A).

An arrest of channels exocytosis or enhanced endocytosis may be responsible for the reduction in the number of channels expressed on the plasma membrane upon  $Ca_v\beta_{2a}$ -SH3 injection. We discriminated between these two possibilities performing the experiments in the presence of bafilomycin or Dynamin K44A, the first is a blocker of the exocytosis and the second is a negative dominant mutant that produces an arrest of the endocytosis (Herskovits et al., 1993; Damke et al., 1994). Using this approach we could see that the effect was still active in the presence of bafilomycin (Fig 6.2B and C) but that it was inhibited by Dynamin K44A (Fig 6.3B and C) and we could conclude that the dramatic decrease observed in the number of channel after the injection of  $Ca_v\beta_{2a}$ -SH3 was due to an activation of the endocytosis of the channels.

Any previous publication had reported this endocytic effect of  $Ca_v\beta_{2a}$ -SH3 or full length  $Ca_v\beta_{2a}$  and we did not know the possible mechanism. Three different

crystallographic structure of  $\text{Ca}_v\beta$  in a complex with the AID show that  $\text{Ca}_v\beta$ -SH3 does not associate directly with the AID sequence of  $\text{Ca}_v\alpha_1$ , but they can not exclude that the SH3 domain interact with other regions of the channel (Chen et al., 2004; Opatowsky et al., 2004; Van Petegem et al., 2004). We decided, as a first step to understand the causes of this effect, to test if the recombinant  $\text{Ca}_v\beta_{2a}$ -SH3 can directly interact with  $\text{Ca}_v1.2$  subunit expressed in mammalian cells.

Using pull-downs assay we were not able to detect interaction of  $\text{Ca}_v\beta_{2a}$ -SH3 with  $\text{Ca}_v1.2$ . This result excluded the possibility that  $\text{Ca}_v\beta$ -SH3 associate with other segments of the channel different to AID and it corroborated the hypothesis that  $\text{Ca}_v\beta$ -SH3 could associate with other cytoplasmic proteins (Chen et al., 2004; Opatowsky et al., 2004; Van Petegem et al., 2004).

The SH3 domains are modules that interact with PRD containing proteins (Solomaha et al., 2005). Dynamin is one of these proteins that contain a PRD and it has an important role in cellular endocytosis (Takei et al., 2005; Newton et al., 2006). It is a multidomain protein with a molecular mass of approximately 100 kDa and with GTPase activity that it is responsible of excising the endocytic vesicle from the plasma membrane (Hinshaw, 2000; Mark et al., 2001).

Because dynamin is a protein involved in the endocytosis and it contains a PRD (Grabs et al., 1997; Gad et al., 2000), we decided to study if the recombinant  $\text{Ca}_v\beta_{2a}$ -SH3 is able to interact *in vitro* with dynamin.

Using a pull-down assay we detected binding of the two proteins (Fig 6.4A). This interaction could be inhibited by pre-incubating the mix of both proteins with a GST fusion protein containing a peptide derived from the PRD of dynamin residues 829-843 (GST-Dyn<sub>829-842</sub>) (Fig 6.4B). This suggests that the association dynamin-Ca<sub>v</sub>β<sub>2a</sub>-SH3 is through the PRD of dynamin.

Ca<sub>v</sub>β-SH3 contains all the canonical residues necessary to interact with PRD domains, nevertheless, simulated docking predictions indicated that Ca<sub>v</sub>β-SH3 is unlikely to interact with PRD unless a considerable rearrangement occurs (Chen et al., 2004). However, our results suggest that the interaction between dynamin PRD and Ca<sub>v</sub>β-SH3 may be mediated by non canonical residues in Ca<sub>v</sub>β-SH3 or alternatively, exposition of canonical residues may be tuneable by a yet unknown regulatory protein or event.

In order to know if the interaction dynamin-Ca<sub>v</sub>β<sub>2a</sub>-SH3 was responsible of the endocytic effect promoted by Ca<sub>v</sub>β<sub>2a</sub>-SH3. We co-injected a mix of Ca<sub>v</sub>β<sub>2a</sub>-SH3 and GST-Dyn<sub>829-842</sub> into oocytes expressing Ca<sub>v</sub>1.2 and we found that the endocytosis promoted by Ca<sub>v</sub>β<sub>2a</sub>-SH3 domain was inhibited ((Fig 6.3D), this proved that the interaction Dynamin-Ca<sub>v</sub>β<sub>2a</sub>-SH3 was the responsible of the activation of the endocytosis.

The association of dynamin with SH3 domains containing proteins has been related with endocytosis and, even when the mechanism is not very well understood, it is

know that this association modulate the GTPase activity of dynamin and its oligomerization state (Yoshida et al., 2005)

Dimerization is probably a crucial step in the endocytosis process. It has been reported that some of the SH3 containing proteins that interact with dynamin and that are involved in endocytosis form homo or heterodimers *in vivo* (Wigge et al., 1997; Ringstad et al., 2001). Using Blue Native PAGE (BN-PAGE) we demonstrated that at least *in vitro* Ca<sub>v</sub>β<sub>2a</sub>-SH3 dimerizes through a disulfide bond and a single substitution of cysteine to alanine at position 113 abolish dimerization and result in the dimerization-deficient mutant Ca<sub>v</sub>β<sub>2a</sub>-SH3 C113A (Fig 8.1).

We examined the ability of Ca<sub>v</sub>β<sub>2a</sub>-SH3 C113A to decrease Q<sub>on</sub> after injection in oocytes. This mutant exhibited a reduced capability to promote endocytosis, but still was able to interact with dynamin (Fig 8.2). This finding suggested that dimerization of Ca<sub>v</sub>β<sub>2a</sub>-SH3 is an important step to activate endocytosis. In order to prove this hypothesis we designed a concatameric Ca<sub>v</sub>β<sub>2a</sub>-SH3 C113A by joining through a linker two single molecules. We found that this protein could rescue the endocytic function of the wild-type Ca<sub>v</sub>β<sub>2a</sub>-SH3 (Fig 8.3C), demonstrating that Ca<sub>v</sub>β<sub>2a</sub>-SH3 dimerization is crucial to promote the effect.

Because an endocytic function has never been described as a property of full length Ca<sub>v</sub>β, it was of crucial relevance for us to evaluate the effect of the full length protein. We found through measurements of Q<sub>on</sub> and cell surface assays that full length Ca<sub>v</sub>β<sub>2a</sub> can reduce the number of channels in the plasma membrane but just when the Ca<sub>v</sub>α<sub>1</sub>-

Ca<sub>v</sub>β primary interaction site is disrupted (Ca<sub>v</sub>1.2 ΔAID mutant) (Fig 6.6). Ca<sub>v</sub>β<sub>2a</sub> co-injected with loop I-II also failed to promote endocytosis of the Ca<sub>v</sub>1.2 ΔAID mutant (Fig 8.4C), suggesting that Ca<sub>v</sub>β<sub>2a</sub> has to be free of any interaction with Ca<sub>v</sub>α<sub>1</sub> to promote this effect. *In vitro* pull down assays showed also that Ca<sub>v</sub>β<sub>2a</sub> binds to dynamin and that like in the case of Ca<sub>v</sub>β<sub>2a</sub>-SH3 this interaction is antagonized by GST-Dyn<sub>829-842</sub> (Fig 6.5).

Due to the fact that Ca<sub>v</sub>β<sub>2a</sub>-SH3 and full length Ca<sub>v</sub>β promote channel endocytosis without direct interaction with the channel protein, we examined their effects onto the distantly related Shaker potassium channel that lacks binding activity to the Ca<sub>v</sub>β (Bichet et al., 2000). Injection of Ca<sub>v</sub>β<sub>2a</sub>-SH3 to oocytes expressing the Shaker channel resulted in not changing in channel activation (Fig 6.S1) but ionic currents were dramatically reduced (Fig 6.5A) after protein injection, suggesting a decrease in the number of channel in the plasma membrane. This current reduction was also partially blocked by pre-incubation of Ca<sub>v</sub>β<sub>2a</sub>-SH3 with GST-Dyn<sub>829-842</sub>. Ca<sub>v</sub>β also reduce Shaker's ionic currents to a similar degree as Ca<sub>v</sub>β<sub>2a</sub>-SH3 without changes in voltage dependent. This current was also antagonized by GST-Dyn<sub>829-842</sub>. These results corroborated that binding of Ca<sub>v</sub>β<sub>2a</sub>-SH3 or full length Ca<sub>v</sub>β to the protein to be sequestered is not necessary.

Previous studies have reported the existence of homo-dimers in other members of the MAGUK family (Christopherson et al., 2003; Weifeng et al., 2008). Since our findings demonstrate that dimerization is a crucial step on the endocytosis process promoted by



Ca<sub>v</sub>β<sub>2a</sub>-SH3, we explored the ability of full length Ca<sub>v</sub>β<sub>2a</sub> to form dimers *in vitro* and *in vivo*.

Using BN-PAGE and pull-down assays, we detected the presence of a dimeric form of this protein (Fig 8.4A and B) but we found also that full length Ca<sub>v</sub>β<sub>2a</sub>C113A is not a dimerization defective mutant, suggesting a dimeric conformation stabilized by additional interactions. We proposed that like in the case of Ca<sub>v</sub>β<sub>2a</sub>-SH3 dimerization of the full length protein is responsible of the endocytic effect. Unfortunately up to now we failed to produce a Ca<sub>v</sub>β dimerization-deficient mutant that can prove our hypothesis.

It has been reported that just one Ca<sub>v</sub>β molecule suffices to regulated most of the electrophysiological properties of VGCCs, and that probably the stoichiometry Ca<sub>v</sub>α<sub>1</sub>-Ca<sub>v</sub>β is one-to-one (Dalton et al., 2005). Based in our results, we envision that dimerization could be the switch for controlling Ca<sub>v</sub>β functions and that it provides new regulatory characteristics to this protein. Hidalgo et al. (2006) have demonstrated that the interaction Ca<sub>v</sub>α<sub>1</sub>-Ca<sub>v</sub>β in the plasma membrane is reversible, this mechanism could provide a source of free Ca<sub>v</sub>β that can dimerize. We proposed a model where Ca<sub>v</sub>β binds to the channel as a monomer and when unbound may dimerize, interact with dynamin and promote endocytosis (Fig 3.1).

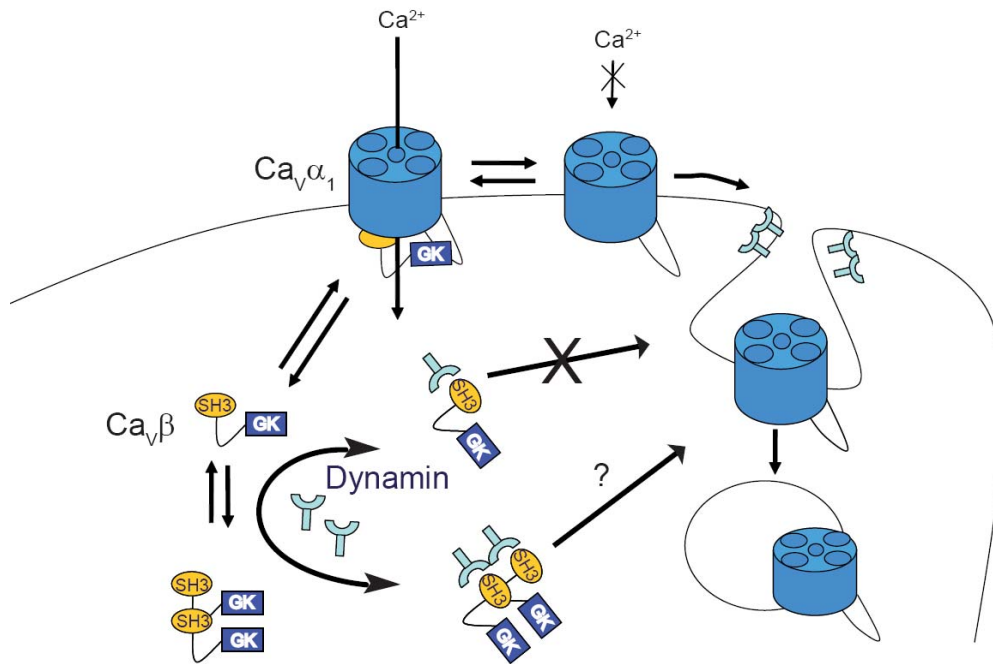


**Figure 3.1 Model for the functional switch of  $\text{Ca}_v\beta$  from calcium channel modulator to endocytosis activator.**  $\text{Ca}_v\beta$  binds as a monomer to the AID site located within the intracellular loop joining domain I and II of  $\text{Ca}_v\alpha_1$ . (For simplicity the other loops were removed). Dissociation of  $\text{Ca}_v\beta$  allows its interaction with dynamin and dimerization. Only interaction of the dimeric form of  $\text{Ca}_v\beta$  with dynamin would lead to endocytosis. The mechanism by which this interaction results in vesicle internalization remains to be investigated.

### 3.2 $\text{Ca}_v\beta$ -GK suffices to modulate gating of the channel

The crystallographic structure of  $\text{Ca}_v\beta$  provides the information, that  $\text{Ca}_v\beta$ -GK is the domain interacting directly with the AID. Despite several attempts, the ability of isolated  $\text{Ca}_v\beta$ -GK to mimic  $\text{Ca}_v\beta$  functions remained controversial (McGee et al., 2004; Takahashi et al., 2004; Maltez et al., 2005; He et al., 2007; Richards et al., 2007).

First we assessed the ability of the  $\text{Ca}_v\beta_{2a}$ -GK expressed in mammalian cells to interact with the AID sequence present into the loop I-II of  $\text{Ca}_v1.2$ . We were able through a pull-down assay to detect that both proteins interact with each other (Fig 7.1D). This agrees with the information that provides the crystallographic structure (Chen et al., 2004; Opatowsky et al., 2004; Van Petegem et al., 2004) and it suggests that probably  $\text{Ca}_v\beta$ -GK suffices to modulate the channel.

We studied the effect of the refolded  $\text{Ca}_v\beta$ -GK modules on *Xenopus* oocytes expressing two types of  $\alpha_1$  pore-forming subunits,  $\text{Ca}_v1.2$  and  $\text{Ca}_v2.3$ , and compared it to the action of recombinant full length  $\text{Ca}_v\beta$  isoforms. We expressed and purified from bacteria the GK of  $\text{Ca}_v\beta_{1b}$  and  $\text{Ca}_v\beta_{2a}$ . They were accumulated in inclusion bodies from where they were refolded (Fig 7.1C).

We found that injection of  $\text{Ca}_v\beta_{2a}$ -GK into oocytes expressing  $\text{Ca}_v1.2$  produces similar effect on channel activation that  $\text{Ca}_v\beta_{2a}$ , resulting in a leftward shift in the current-voltage relationship (Fig 7.2B), but in the case of  $\text{Ca}_v\beta_{2a}$ -GK this effect was just seen when the channel expression levels were reduced to the minimum, maybe because the

concentration of the injected protein was very low and/or its stability into the oocytes is low too (Fig 7.2A).

To overcome these two problems we generated a construct where the  $\text{Ca}_v\beta_{2a}$ -GK was covalently linked to  $\text{Ca}_v1.2$  ( $\text{Ca}_v1.2$ -  $\text{Ca}_v\beta_{2a}$ -GK) and compared with  $\text{Ca}_v1.2$  linked to  $\text{Ca}_v\beta_{2a}$  ( $\text{Ca}_v1.2$ - $\text{Ca}_v\beta_{2a}$ ) (Fig 7.3A). With a similar approach it was previously demonstrated that just one single  $\text{Ca}_v\beta$  molecule is enough to modulate the channel (Dalton et al., 2005).

When covalently linked to  $\text{Ca}_v1.2$ ,  $\text{Ca}_v\beta_{2a}$ -GK was as efficient as  $\text{Ca}_v\beta_{2a}$  in increasing the ionic current to charge movement ratio ( $I/Q$ ) and leftward shifting the current-voltage relationship. This effect was abolished when the  $\text{Ca}_v\alpha_1$ - $\text{Ca}_v\beta$  primary interaction site was disrupted through a point mutation and it proves that  $\text{Ca}_v\beta$ -GK suffices to modulate channel activation (Fig 7.3B and C).

That isolate  $\text{Ca}_v\beta$ -GK can recapitulate the modulatory properties of full length  $\text{Ca}_v\beta$  on channel activation is a new finding. It implies that the association  $\text{Ca}_v\alpha_1$ -GK mediated by the AID is enough to regulate channel activation and that this interaction is critical for channel modulation as it was suggested by Van Petegem et al. (2008).

The possible effect of  $\text{Ca}_v\beta$ -GK on channel inactivation was also very interesting to study. It has been reported that different  $\text{Ca}_v\beta$  isoforms have distinctive effect on this property. While  $\text{Ca}_v\beta_{2a}$  is unique in its ability to inhibit inactivation, the other  $\text{Ca}_v\beta$  isoforms facilitate it.  $\text{Ca}_v\beta_{2a}$  slow-down inactivation, increases the fraction of non-

inactivating current and it shifts the steady-state inactivation curve towards more positive potentials (Olcese et al., 1994; Qin et al., 1996; Sokolov et al., 2000; Restituito et al., 2000; Hering et al., 2000; Jones et al., 2000). Other isoforms, like for example  $\text{Ca}_v\beta_{1b}$ , accelerate channel inactivation and shift to more negative potentials the voltage-dependent inactivation (Olcese et al., 1994). These distinguishing modulatory properties of  $\text{Ca}_v\beta_{2a}$  have been broadly attributed to palmitoylation of the two contiguous cysteine residues at position 3 and 4 in the N-terminus region ( $\text{Ca}_v\beta_{2a}$  C3,4S) (Chien et al., 1996; Qin et al., 1998; Hurley et al., 2000; Restituito et al., 2000).

We found that the injection of  $\text{Ca}_v\beta_{2a}$ -GK and  $\text{Ca}_v\beta_{1b}$ -GK into oocytes expressing  $\text{Ca}_v2.3$  produces, in both case, a slow-down of the inactivation and a shift of the steady-state inactivation to more positive potentials, results that are similar to those obtained with  $\text{Ca}_v\beta_{2a}$ . That demonstrates that  $\text{Ca}_v\beta$ -GK acts as a brake to inhibit voltage-dependent inactivation. An important corollary from this conclusion is that inhibition of the inactivation is the intrinsic characteristic of  $\text{Ca}_v\beta$ , and that facilitation of the inactivation promoted by  $\text{Ca}_v\beta_{1b}$  and other isoforms requires the presence of additional structural determinants outside of the GK domain.

Our results also suggest that the palmitoylation of the N-terminus region of  $\text{Ca}_v\beta_{2a}$  seems just to have a secondary role on the modulatory properties of this protein on channel inactivation. Maybe, palmitoylation just masks and avoids that some amino acids residues outside of the GK domain, and that could be necessary for facilitate channel inactivation; undergo posttranslational modification, but until that moment any

previous report supported the idea that channel inactivation can be regulated by posttranslational modifications on  $\text{Ca}_v\beta$ .

On previous reports that describe facilitation of channel inactivation promoted by some  $\text{Ca}_v\beta$  isoforms,  $\text{Ca}_v2.3$  channels have been co-expressed with cRNAs encoding  $\text{Ca}_v\beta_{1b}$  or the palmytolation deficient mutant  $\text{Ca}_v\beta_{2a}$  C3,4S (Olcese et al., 1994; Qin et al., 1996; Qin et al., 1998; Sokolov et al., 2000; Restituto et al., 2000; Hering et al., 2000; Jones et al., 2000). In these experiments the molecules of  $\text{Ca}_v\beta$  subunits are for some days into the oocytes and in this time they could suffer multiples posttranslational modifications.

We decided to study the effect on channel inactivation of recombinant  $\text{Ca}_v\beta_{1b}$  and  $\text{Ca}_v\beta_{2a}$  C3,4S proteins that were injected just some hours before of perform the electrophysiological recordings (late-injection) into oocytes expressing  $\text{Ca}_v2.3$ . Under this condition these proteins probably will not undergo any posttranslational modification and this could reflect a variation in the inactivation phenotype. We found that the late-injection of these proteins inhibited the inactivation compared with oocytes expressing  $\text{Ca}_v2.3$  alone (Fig 7.7). This it is a dramatic different compared with the phenotype that these proteins confer when they are co-express with the channel. To be sure that this different was not due to an unfolding of the recombinant proteins, we co-injected them together with the cRNA encoding  $\text{Ca}_v2.3$  (co-injection) and indeed we found that inactivation was facilitated like in the co-expression experiment (Fig 7.7). We concluded that after posttranslational modifications during

biogenesis of the channel complex,  $Ca_v\beta$  can switch the phenotype conferred to  $Ca_v2.3$  from slow-inactivating to fast-inactivating.

All these results demonstrate that  $Ca_v\beta$ -GK acts as inhibitory brake for channel inactivation and therefore the facilitation of inactivation conferred by isoforms like  $Ca_v\beta_{1b}$ , requires of additional structural determinants that undergo posttranslational modifications and that counteract with this GK-brake like effect.

As new protein partners are being discovered, the functional role of  $Ca_v\beta$  is expanding rapidly (28;29). Here we found that the SH3 module of  $Ca_v\beta$  binds to the endocytotic protein dynamin and promotes endocytosis and we also reported that the GK module regulates calcium channel function. Together these findings introduce a new perspective of  $Ca_v\beta$ . Calcium entry through VGCCs upon membrane depolarization ensues a transient change in intracellular calcium concentration that regulates diverse cellular functions. Integration of these different cellular processes must be tightly coordinated in living cells and the domain architecture of  $Ca_v\beta$  with two functionally independent modules appears particularly well suited to orchestrate calcium signaling. We suggest that while GK regulates calcium entrance, the SH3 domain links channel activity to other cellular processes.

#### **4. Conclusions**

Our findings have introduced a new perspective about the functions of the domains of  $\text{Ca}_v\beta$ . Calcium entry through VGCCs on membrane depolarization ensures a transient change in intracellular calcium concentration that regulates diverse cellular functions. Integration of these different cellular processes must be tightly coordinated in living cells, and the architecture of  $\text{Ca}_v\beta$ , with its two functionally independent domains, appears particularly well suited for orchestrating calcium signaling. We suggest that whereas  $\text{Ca}_v\beta$ -GK regulates calcium entrance, the  $\text{Ca}_v\beta$ -SH3 can down-regulate the channels from the plasma membrane under certain physiological conditions and at the same time links channel activity to other cellular processes by binding to additional cytoplasmic proteins.



## 5. References

1. Arikath J, Chen CC, Ahern C, Allamand V, Flanagan JD, Coronado R, Gregg RG, Campbell KP (2003)  $\gamma$ 1 subunit interactions within the skeletal muscle L-type voltage-gated calcium channels. *J. Biol. Chem.* 278:1212-1219.
2. Bangalore R, Mehrke G, Gingrich K, Hofmann F, Kass RS (1996) Influence of L-type  $\text{Ca}^{2+}$  channel  $\alpha_2/\delta$  subunit on ionic and gating current in transiently transfected HEK 293 cells. *Am. J. Physiol.* 270:H1521-1528.
3. Benzanilla F, Stefani E (1998) Gating Currents. *Methods Enzymol.* 293:331-352.
4. Bichet D, Cornet V, Geib S, Carlier E, Volsen S, Hoshi T, Mori Y, De Waard M (2000) The loop I-II of the  $\text{Ca}^{2+}$  channel  $\alpha_1$  subunit contains an endoplasmic reticulum retention signal antagonized by the  $\beta$  subunit. *Neuron* 25:177-190.
5. Birnbaumer L, Qin N, Olcese R, Tareilus E, Platano D, Costantin J, Stefani E (1998) Structure and functions of calcium channel  $\beta$  subunit. *J Bioenerg. Biomembr.*30:357-375.
6. Bosse E, Regulla S, Biel M, Ruth P, Meyer HE, Flockerzi V, Hofmann F (1990) The cDNA and deduced amino acid sequence of the  $\gamma$  subunit of L-type calcium channel from rabbit skeletal muscle. *FEBS Lett* 267:153-156.

7. Carbone E, Lux HD (1984) A low voltage-activated, fully inactivating Ca channel in vertebrate sensory neurons. *Nature* 310:501-502.
8. Castellano A, Wei X, Birnbaumer L, Perez-Reyes E (1993) Cloning and expression of a neuronal calcium channel  $\beta$  subunit. *J. Biol. Chem* 268:12359-12366.
9. Catterall WA (2000) Structure and regulation of voltage-gated calcium channels. *Annu. Rev. Cell Dev. Biol.* 16:521-555.
10. Chen YH, Li MH, Zhang Y, He LL, Yamada Y, Fitzmaurice A, Shen Y, Zhang H, Tong L, Yang J (2004) Structural basis of the  $\alpha 1$ - $\beta$  subunit interaction of voltage-gated  $\text{Ca}^{2+}$  channels. *Nature* 429: 675-680.
11. Chen AJ, Carr KM, Shirokov RE, Rios E, Hosey MM (1996) Identification of palmitoylation sites within the L-type calcium channel  $\beta 2a$  subunit and effects on channel function. *J. Biol. Chem.* 271:26465-26468.
12. Christopherson KS, Sweeny NT, Craven SE, Kang R, El-Husseini AD, Brecht DS (2003) Lipid and protein-mediated multimerization of PSD-95: implications for receptor clustering and assembly of synaptic protein networks. *J. Cell Sci.* 116:3213-3219.

13. Dafi O, Berrou L, Dodier Y, Raybaud A, Sauve R, Parent L (2004) Negatively charged residues in the N- terminal of the AID helix confer slow voltage dependent inactivation gating to CaV 1.2. *Biophys. J.* 87:3181-3192.
14. Dalton S, Takahashi SX, Jayalakshmi M, Colecraft HM (2005) A single Ca<sub>v</sub>β can reconstitute both traffic and macroscopic conductance of voltage-dependent calcium channels. *J. Physiol.* 567: 757- 769.
15. Damke H, Baba T, Warnock DE, Schmid SL (1994) Induction of mutant dynamin specifically blocks endocytic coated vesicle formation. *J. Cell Biol.* 127:915-934.
16. De Jongh KS, Warner C, Catterall WA (1990). Subunits of purified calcium channel alpha2 and delta are encoded by the same gene. *J. Biol. Chem.* 265:14738-14741.
17. Dolphin AC (2003a) G protein modulation of voltage-gated calcium channels. *Pharmacol. Rev.* 55:607–627.
18. Dolphin AC (2003b) β subunits of voltage-gated calcium channels. *Journal of Bioenergetics and Biomembranes.* 35: 599-620.
19. Dolphin AC (2006) A short history of voltage-gated calcium channels. *British Journal of Pharmacology* 147:56-62.

20. Ertel EA, Campbell KP, Harpold MM, Hoffman F, Mori Y, Perez-Reyes E, Schwartz A, Snutch TP, Tanabe T, Birnbaumer L, Tsien RW, Catterall WA (2000) Nomenclature of voltage-gated calcium channels. *Neuron* 25:533-535.
21. Fatt P, Katz B (1953) The electrical properties of crustacean muscle fibres. *J. Physiol.* 120:171-204.
22. Felix R, Gurnett CA, De Waard M, Campbell KP (1997) Dissection of functional domains of voltage-dependent  $\text{Ca}^{2+}$  channel  $\alpha_2/\delta$  subunit. *J. Neurosci.* 17:6884-6891.
23. Flockerzi V, Oeken H, Hofmann F (1986) Purification of a functional receptor for calcium channels blockers from rabbit skeletal muscle microsomes. *Eur. J. Biochem.* 161:217-224.
24. Freise D, Held B, Wissenbacz U, Pfeifer A, Trost C, Himmerkus N, Schweig U, Freichel M, Biel M, Hofmann F, Hoth M, Flockerzi V (2000) Absence of the  $\gamma$  subunit of the skeletal muscle dihydropyridine receptor increases L-type calcium channel currents and alters channel inactivation properties. *J. Biol. Chem.* 275:14476-14481.
25. Gad H, Ringstad N, Löw P, Kjaerulff O, Gustafsson J, Wenk M, Di Paolo G, Nemoto Y, Crum J, Ellisman MH, DE Camelli P, Shupliakov O, Brodin L (2000) Fission and uncoating of synaptic chlatrin-coated vesicles are perturbed

- by disruption of interactions with the SH3 domain of endophilin. *Neuron* 27:301-312.
26. Grabs D, Slepnev VI, Songyang Z, David C, Lynch M, Cantley LC, De Camelli P (1997) The SH3 domain of amphiphysin binds to the proline rich domain of dynamin at a single site that define a new SH3 binding consensus sequence. *J. Biol. Chem.* 272:13419-13425.
27. Hanlon MR, Berrow NS, Dolphin AC, Wallace BA (1999) Modelling of a voltage-dependent Ca<sup>2+</sup> channel beta subunit as a basis for understanding its functional properties. *FEBS Letters* 445:366-370.
28. He LL, Zhang Y, Chen YH, Yamada Y, Yang J (2007) Functional modularity of the beta-subunit of voltage-gated Ca<sup>2+</sup> channels. *Biophys. J.* 93: 834-845.
29. Hess P, Lansman JB, Tsien RW (1984) Different modes of Ca channel gating behaviour favoured by dihydropyridine Ca agonist and antagonist. *Nature* 311:538-534.
30. Hering S, Berjukow S, Sokolov S, Marksteiner R, Weiss RG, Kraus R, Timin EN (2000) Molecular determinants of inactivation in voltage-gated calcium channels. *J. Physiol* 528:237-249.

31. Herskovits JS, Burgess CC, Obar RA, Vallee RB (1993) Effects of mutant rat dynamin on endocytosis. *J. Cell Biol.* 122:565-578.
32. Hidalgo P, Gonzalez-Gutierrez G, Garcia-Olivares J, Neely A (2006) The  $\alpha_1$ - $\beta$  subunit interaction that modulates calcium channel activity is reversible and requires a competent  $\alpha$ -interaction domain. *J. Biol. Chem.* 281: 24104-24110.
33. Hill B (1993a) Ionic channels of excitable membranes. Sinauer Associate  
Second Edition: 1-3.
34. Hill B (1993b) Ionic channels of excitable membranes. Sinauer Associate  
Second Edition: 317-320.
35. Hinshaw JE, (2000) Dynamin and its role in membrane fission. *Annu. Rev. Cell. Dev. Biol.* 16:483-519.
36. Hoffmann F, Lacinova L, Klugbauer N (1999) Voltage-dependent calcium channels: from structure to function. *Rev. Physiol. Biochem. Pharmacol.* 139:33-87.
37. Hullin R, Singer-Lahat D, Freichel M, Biel M, Dascal N, Hofmann F, Flockerzi V (1992) Calcium channel  $\beta$  subunit heterogeneity: functional expression of cloned cDNA from heart, aorta and brain. *EMBO J.* 11:885-890.

38. Hurley JH, Cahil AL, Currie KP, Fox AP (2000) The role of dynamic palmitoylation in calcium channel inactivation. *Proc Natl Acad Sci USA* 97:9293-9298.
39. Jay S, Ellis SB, McCue AF, Williams ME, Vedvick TS, Harpold MM, Campbell KP (1990) Primary structure of the  $\gamma$  subunit of the DHP-sensitive calcium channel from skeletal muscle. *Science* 248:490-492.
40. Jones LP, Wei SK, Yue DT (1998) Mechanism of auxiliary subunit modulation of neuronal  $\alpha_1E$  calcium channels. *J. Gen. Physiol* 112:125-143.
41. Josephson IR, Varadi G (1996) The  $\beta$  subunit increases  $Ca^{2+}$  currents and gating charge movements of human cardiac L-type  $Ca^{2+}$  channels. *Biophys J.* 70:1285-1293.
42. Kamp TJ, Perez-Garcia MT, Marban E (1996) Enhancement of ionic and charge movement by co-expression of calcium channel  $\beta_{1a}$  subunit with  $\alpha_{1c}$  subunit in a human embryonic kidney cell line. *J. Physiol.* 492:89-96.
43. Klugbauer N, Dai S, Specht V, Lacinova L, Marais E, Bohn G, Hofmann F (2000) A family of  $\gamma$ -like calcium channel subunits *FEBS Lett.* 470:189-197.
44. Leroy J, Richards MW, Butcher AJ, Nieto-Rostro M, Pratt WS, Davies A, Dolphin AC (2005) Interaction via a key tryptophan in the I-II linker of N-type

- calcium channels is required for beta1 but not for palmitoylated beta2, implicating an additional binding site in the regulation of channel voltage-dependent properties. *J. Neurosci* 25:6984-6996.
45. Leung AT, Imagawa T, Block B, Franzini-Armstrong C, Campbell KP (1988) Biochemical and ultrastructural characterization of the 1,4 dihydropyridine receptor from rabbit skeletal muscle. Evidence for a 52 kDa subunit. *J Biol Chem* 263:994-1001.
46. Maltez JM, Nunziato DA, Kim J, Pitt GS (2005) Essential Ca(V)beta modulatory properties are AID-independent. *Nat. Struct. Mol. Biol.* 12:372-377.
47. Mark B, Stowell MH, Vallis Y, Mills IG, Gibson A, Hopkins CR, McMahon HT (2001) GTPase activity of dynamin and resulting conformation change are essential for endocytosis. *Nature.* 410:231-235.
48. McCleskey EW, Fox AP, Feldman DH, Cruz LJ, Olivera BM, Tsien RW, Yoshickami D (1987) Omega-conotoxin: direct and persistent blockade of specific types of calcium channel in neuron but not muscle. *Proc. Natl. Acad. Sci. USA:* 84:4327-4331.



49. McGee AW, Nunziato DA, Maltez JM, Prehoda KE, Pitt GS, Bredt DS (2004) Calcium channel function regulated by the SH3-GK module in beta subunits. *Neuron* 42: 89-99.
50. Mintz IM, Venema VJ, Swiderek KM, Lee TD, Bean BP, Adams ME (1992) P-type calcium channels blocked by the spider toxin  $\omega$ -aga-IVA. *Nature* 355:827-829.
51. Newton AJ, Kirchhausen T, Murthy N (2006) Inhibition of dynamin completely blocks compensatory synaptic vesicle endocytosis. *Proc. Natl. Acad. Sci. USA*: 103:17955-17960.
52. Olcese R, Qin N, Schneider T, Neely A, Wei X, Stefani E, Birnbaumer L (1994) The amino termini of calcium channel set rates of inactivation independently of their effect on activation. *Neuron* 13:1433-1438.
53. Opatowsky Y, Chen CC, Campbell KP, Hirsch JA (2004) Structural analysis of the voltage-dependent calcium channel beta subunit functional core and its complex with the alpha 1 interaction domain. *Neuron* 42:387-399.
54. Perez-Reyes E, Castellano A, Kim HS, Bertrand P, Bagstrom E, Lacerda AE, Wei XY, Birnbaumer L (1992) Cloning and expression of cardiac/brain  $\beta$  subunits of the L-type calcium channel. *J. Biol. Chem.* 267:1792-1797.

55. Pitt GS, Zuhlke R, Hudmon A, Schulman H, Reuter H, Tsien RW (2001) Molecular basis of calmodulin tethering and Ca<sup>2+</sup> dependent inactivation of L-type Ca<sup>2+</sup> channels. *J. Biol. Chem.* 276:30794-30802.
56. Pragnell M, De Waard M, Mori M, Tanabe T, Snutch TP, Campbell KP (1994) Calcium channel  $\beta$  subunit binds to a conserved motif in the I-II cytoplasmic linker of the  $\alpha_1$  subunit. *Nature* 368:67-70.
57. Qin N, Olcese R, Zhou J, Cabello O, Birnbaumer L, Stefani E (1996) Identification of a second region of the beta-subunit involved in regulation of calcium channel inactivation. *Am. J. Physiol.* 271:C1539-C1545.
58. Qin N, Olcese R, Stefani E, Birnbaumer L (1998) Modulation of human neuronal  $\alpha_1E$ -type calcium channel by  $\alpha_2/\delta$  subunit. *Am. J. Physiol.* 274:C1324-1331.
59. Qin N, Platano D, Olcese R, Constantin JL, Stefani E, Birnbaumer L (1998) Unique regulatory properties of the type 2a calcium channel  $\beta$  subunit caused by palmitoylation. *Prot. Natl Acad. Sci. USA* 95:4690-4695.
60. Randall A, Tsien RW (1995) Pharmacological dissection of multiple types of Ca<sup>2+</sup> channel currents in rat cerebellar granule neurons. *J. Neurosci.* 15:2995-3012.

61. Restituito S, Cens T, Barrere C, Geib S, Galas S, De Waard M, Charnet P (2000) The  $\beta$ 2a subunit is a molecular groom for the calcium channel inactivation gate. *J. Neuroscience* 20:9046-9052.
62. Richards MW, Leroy J, Pratt WS, Dolphin AC (2007) The HOOK-domain between the SH3- and the GK-Domains of  $Ca_v\beta$  subunits contains key determinants controlling calcium channel inactivation. *Channels* 1: 92-101.
63. Ringstad N, Nemoto Y, DeCamilli P. (2001) Differential Expression of Endophilin 1 and 2 Dimers at Central Nervous System Synapses. *J. Biol. Chem.* 276:40424-40430.
64. Sieber M, Nastainczyk W, Zubor V, Wernet W, Hofmann F (1987) The 165 kDa peptide of the purified skeletal muscle dihydropyridene receptor contains the known regulatory sites of the calcium channel. *Eur. J. Biochem.* 167:117-122.
65. Sokolov S, Weiss RG, Timin EN, Hering S (2000) Modulation of slow inactivation in class A calcium channels by beta subunits. *J. Physiol. (Lond)* 527:445-454.
66. Solomaha E, Szeto FL, Mohammed AY, Palfrey HC (2005) Kinetics of Src Homology 3 Domain association with the proline rich domain of dynamins. *J. Biol. Chem.* 280:23147-23156.

67. Stotz SC, Jarvis SE, Zamponi GW (2003) Functional roles of cytoplasmic loops and pore lining transmembrane helices in the voltage-dependent inactivation of HVA calcium channels. *J. Physiol.* 554:263-273.
68. Takahashi SX, Miriyala J, Colecraft HM (2004) Membrane-associated guanylate kinase-like properties of beta-subunits required for modulation of voltage-dependent Ca<sup>2+</sup> channels. *Proc. Natl. Acad. Sci. USA* 101:7193-7198.
69. Takahashi M, Seagar MJ, Jones JF, Reber BF, Catterall WA (1987) Subunit structure of dihydropyridine-sensitive calcium channels from skeletal muscle. *Proc. Natl. Acad. Sci. USA.*84:5478-5482.
70. Takei K, Yoshida Y, Yamada H (2005) Regulatory mechanisms of dynamin dependent endocytosis. *J. Biochem.* 137:243-247.
71. Van Petegem F, Clark KA, Chatelain FC, Minor DL (2004) Structure of a complex between a voltage-gated calcium channel  $\beta$ -subunit and an  $\alpha$ -subunit domain. *Nature* 429:671-675.
72. Van Petegem F, Duderstadt KE, Wang M, Minor DL (2008) Alanine-scanning mutagenesis defines a conserved energetic hotspot in the Ca<sub>v</sub> $\alpha_1$  AID-Ca<sub>v</sub> $\beta$  interaction site that is critical for channel modulation. *Structure* 16:280-294.

73. Wei X, Neely A, Olcese R, Lang W, Stefani E, Birnbaumer L (1996) Increase in Ca<sup>2+</sup> channel expression by deletions at the amino terminus of cardiac  $\alpha_{1c}$  subunit. *Receptors and Channels* 4:205-215.
74. Weifeng X, Schlüter OM, Steiner P, Czervionke BL, Sabatini B, Malenka RC (2008) Molecular dissociation of the role of PSD-95 in regulating synaptic strength and LTD. *Neuron* 57:248-262.
75. Wigge P, Köhler K, Vallis Y, Doyle CA, Owen D, Hunt SP, McMahon HT (1997) Amphiphysin heterodimers: potential role in clathrin-mediated endocytosis. *Mol. Biol. Cell.* 8:2003-2015.
76. Yoshida Y, Kinuta M, Abe T, Liang S, Araki K, Cremona O, Di Paolo G, Moriyama Y, Yasuda T, De Camilli P, Takei K (2004) The stimulatory action of amphiphysin on dynamin function is dependent on lipid bilayer curvature. *EMBO J.* 23:3483-3491.

## List of Publications

**Miranda-Laferte E\***, Gonzalez-Gutierrez\*. G, Neely A and Hidalgo P (2007). The Src homology 3 domain of the  $\beta$ -subunit of voltage-gated calcium channels promotes endocytosis via dynamin interaction. *J. Biol. Chem.* 282(4): 2156-2162. (\*First author with equal contribution)

Gonzalez-Gutierrez G, **Miranda-Laferte E**, Nothmann D, Schmidt S, Neely A and Hidalgo P (2008).The guanylate kinase domain of the  $\beta$ -subunit of voltage-gated calcium channels suffices to modulate gating. *Proc. Natl. Acad. Sci. USA.* 105(37):14198-14203.

**Miranda-Laferte E**, Gonzalez-Gutierrez G, Schmidt S, Neely A and Hidalgo P. (2009) Dimerization of the Src Homology 3 domain of the voltage-gated calcium channel  $\beta$ -subunit regulates endocytosis. Manuscript to be submitted to *EMBO Reports*.

**6. The Src homology 3 domain of the  $\beta$ -subunit of voltage gated calcium channels promotes endocytosis via dynamin interaction**

Giovanni Gonzalez-Gutierrez<sup>\*1</sup>, Erick Miranda-Laferte<sup>‡1</sup>, Alan Neely<sup>\*</sup> and Patricia Hidalgo<sup>‡</sup>

<sup>‡</sup>Abteilung Neurophysiologie, Medizinische Hochschule Hannover, 30625 Hannover, Germany

<sup>\*</sup>Centro de Neurociencia de Valparaíso, Universidad de Valparaíso 2349400 Chile

<sup>1</sup>These authors contributed equally to this work

**J. Biol. Chem. 2007 Vol. 282, No 38: 2156-2162**

© 2007 by The American Society for Biochemistry and Molecular Biology, Inc.

## **6.1 Abstract**

**High voltage-gated calcium channels enable calcium entry into cells in response to membrane depolarization. Association of the auxiliary  $\beta$ -subunit to the  $\alpha$ -interaction-domain in the pore-forming  $\alpha_1$ -subunit is required to form functional channels. The  $\beta$ -subunit belongs to the membrane associated guanylate kinase class of scaffolding proteins containing a Src homology 3 and a guanylate kinase domain. While the latter is responsible for the high affinity binding to the  $\alpha$ -interaction-domain, the functional significance of the Src homology 3 domain remains elusive. Here, we show that injection of isolated  $\beta$ -subunit Src homology 3 domain into *Xenopus laevis* oocytes expressing the  $\alpha_1$ -subunit reduces the number of channels in the plasma membrane. This effect is reverted by coexpressing  $\alpha_1$  with a dominant-negative mutant of dynamin, a GTPase involved in receptor-mediated endocytosis. Full length  $\beta$ -subunit also downregulates voltage-gated calcium channels but only when lacking the  $\alpha$ -interaction-domain. Moreover, isolated Src homology 3 domain and the full length  $\beta$ -subunit were found to interact *in vitro* with dynamin and to internalize the distantly related *Shaker* potassium channel. These results demonstrate that the  $\beta$ -subunit regulates the turnover of voltage-gated calcium channels and other proteins in the cell membrane. This effect is mediated by dynamin and depends on the association state of the  $\beta$ -subunit to the  $\alpha_1$ -pore forming subunit. Our findings define a novel function for the  $\beta$ -subunit through its Src homology 3 domain and establish a link between voltage-gated calcium channels activity and the cell endocytic machinery.**



## **6.2 Introduction**

Cellular processes including muscle contraction, endocrine secretion, synaptic transmission and gene expression (1) depend on the regulated influx of calcium through voltage-gated calcium channels (VGCCs). VGCCs are multi-protein complexes containing a pore-forming subunit ( $\text{Ca}_v\alpha_1$ ) and a variable number of auxiliary subunits. Association of the auxiliary  $\beta$ -subunit ( $\text{Ca}_v\beta$ ) to a site shared by all  $\text{Ca}_v\alpha_1$ , the so called AID ( $\alpha$ -interaction domain), is mandatory to form a fully functional VGCC. Homology modelling (2) and the recent high resolution crystal structures of three  $\text{Ca}_v\beta$  isoforms (3-5) identified  $\text{Ca}_v\beta$  as a novel member of the membrane-associated guanylate kinase (MAGUK) class of scaffolding proteins containing a Src homology 3 (SH3) and a guanylate kinase (GK) domain (Fig. 6.1A). As shown by the crystal structure of  $\text{Ca}_v\beta$  complexed to AID, the  $\text{Ca}_v\beta$ -GK binds to the AID whereas  $\text{Ca}_v\beta$ -SH3 interacts with GK. Although SH3 domains are known to mediate protein-protein interactions by binding to proline rich motifs in ligand proteins (6), no interactions mediated by the  $\text{Ca}_v\beta$ -SH3 have been described yet. Moreover, the functional integrity of  $\text{Ca}_v\beta$ -SH3 domain is uncertain since the residues homologous to the ones critical for binding PXXP motifs in canonical SH3 modules are occluded in the crystal structure of  $\text{Ca}_v\beta$ . Intriguingly, canine and human cardiac cells express splicing variants encoding short versions of the  $\text{Ca}_v\beta$  that only encompass the variable N-terminal region and the SH3 domain (7;8) (V1 and C1 in Fig. 6.1A, respectively).

Here, we studied the effect of isolated  $\text{Ca}_v\beta$ -SH3 on calcium channel function and expression. The SH3 domain of the rat  $\beta_{2a}$  isoform of  $\text{Ca}_v\beta$  ( $\beta_{2a}$ -SH3) was expressed

*The SH3 domain of the  $\beta$ -subunit of VGCCs promotes endocytosis via dynamin interaction*

in bacteria, purified and injected into *Xenopus* oocytes expressing the cardiac  $\text{Ca}_v\alpha_1$  ( $\text{Ca}_v1.2$ ) subunit isoform. We found that the  $\beta_{2a}$ -SH3 induces removal of channels from the plasma membrane in a dynamin dependent fashion. This function is preserved by full length  $\text{Ca}_v\beta$  in the absence of  $\text{Ca}_v\alpha_1$  subunit or when binding to it is disrupted by deleting the AID site. Our results define a novel interaction and outline a new function for the calcium channel  $\beta$ -subunit.

## **6.3 Materials and Methods**

### **6.3.1 Recombinant Proteins**

The cDNA encoding the SH3 domain of the rat  $\beta$ 2a isoform (Swiss-Prot entry:Q8VGC3) encompassing residues 24 to 136 was subcloned between BamHI and EcoRI restriction sites by conventional PCR methods into pRSETB vector (Invitrogen) to introduce a polyhistidine tag at the N-terminal. The molecular mass predicted by the amino acid sequence of the  $\text{Ca}_v\beta_{2a}$ -SH3 His tagged protein is 16.7 kDa. The  $\text{Ca}_v\beta_{2a}$ -SH3 His tagged was expressed in BL-21 (DE-3) E.coli bacteria by 2-hour induction with 0.5 mM Isopropyl- $\beta$ -D-thiogalactopyranoside at 37 °C. Cells were harvested by centrifugation, flash frozen and stored until use at -80°C. Right before protein purification the cells were resuspended in phosphate buffer (50 mM sodium phosphate buffer and 300 mM NaCl, pH 7.0) containing EDTA-free protease inhibitor cocktail (Roche Applied Science) and disrupted by ultrasonication. After centrifugation, the protein was purified from the cleared cell lysate by using a cobalt based metal-affinity chromatography (Talon, BD Biosciences) according to the manufacturer's instructions, followed by size-exclusion chromatography onto a superdex™ S-200 column 26/60 (GE Healthcare Life Sciences) pre-equilibrated with Buffer containing 20 mM Tris buffer, 300 mM NaCl, 1 mM EDTA, pH 8.0. The fractions containing the protein were pooled, concentrated up to 1-2 mg/ml by centrifugation using Amicon Ultra tubes 10.000 MWCO (Millipore), aliquoted, flash frozen and stored at -80 °C until use. The full length  $\text{Ca}_v\beta_{2a}$  was prepared as described (9). The apparent molecular mass of  $\text{Ca}_v\beta_{2a}$ -SH3 His tagged determined from the size exclusion chromatography calibration curve was obtained from the partition coefficient value ( $K_{av}$ ) calculated from its elution volume as described (10), where  $K_{av}$  is equal to  $(V_e - V_o)/(V_t - V_o)$ ,

and:  $V_e$  is the elution volume of the protein;  $V_o$  is the void volume of the column calibrated with Blue dextran and  $V_t$  is the total bed volume. A set of globular protein standards was used as indicated in the figure. Mass spectrometry analysis was performed in the Mass spectrometry laboratory, Zentrums Pharmakologie und Toxikologie, Medizinische Hochschule Hannover. The protein was digested by trypsin and the peptides were analyzed in Ultraflex MALDI-TOF/TOF Mass Spectrometer (Bruker Daltonics).

The GST-Dyn<sub>829-842</sub> peptide was prepared as follows: two overlapping oligonucleotides were designed according to the dynamin sequence (Swiss-Prot entry: Q05193), to encode the peptide sequence from residues 829 to 842 (829-PPQVPSRPNRAPPG). After annealed, the oligonucleotides were ligated into pGEX vector (GE Healthcare Life Sciences) to fuse a GST at the N-terminal (GST-Dyn<sub>829-842</sub> peptide). The GST alone and GST-Dyn<sub>829-842</sub> peptide were expressed in bacteria and purified as described (10). Dynamin mutation and Ca<sub>v</sub>1.2  $\Delta$ AID deletion were done by standard overlapping PCR using complementary oligonucleotides

### **6.3.2 Binding assay**

Pull down assays using His-tagged Ca<sub>v</sub> $\beta$ <sub>2a</sub>-derivatives as baits were performed as described (10). Briefly His-Ca<sub>v</sub> $\beta$ <sub>2a</sub> derivatives were coupled to cobalt based agarose for one hour at 4°C and incubated for another hour with pre-cleared tsA201 cell extract obtained 24-48 hours after transfection with dynamin or with YFP-Ca<sub>v</sub>1.2 expression vector. The beads were pelleted, washed five times and bound fractions eluted with SDS-PAGE loading buffer and resolved on SDS-PAGE. In the binding assays to

dynamin the gel was transferred to nitrocellulose membrane and subjected to immunoblot analysis using anti dynamin antibody (BD biosciences). Binding to YFP-Cav1.2 was visualized by fluorescence scanning using a Typhoon imager (GE Healthcare Life Sciences)

### **6.3.3 *Xenopus* Oocytes preparation, injection and electrophysiological recordings**

*Xenopus laevis* oocytes were prepared, injected and maintained as in previous report (10). All capped cRNA were synthesized using the MESSAGE-machine (Ambion, Austin TX, USA), resuspended in 10  $\mu$ l water and stored in 2  $\mu$ l aliquots at  $-80$  °C until use. The Cav1.2-subunit used in this study bears a deletion of 60 amino acids at the amino terminal end that increase expression (11). Electrophysiological recordings on Cav1.2 expressing oocytes were performed two to five hours after protein injection (50 nl of the protein stock solution, 1-2 mg/ml, per oocyte) and five to seven days after cRNA injection using the cut-open oocyte technique with a CA-1B amplifier (Dagan Corp., Minneapolis MN USA) as described (9). The external solution contained in mM, 10 Ba<sup>2+</sup>, 96 n-Methylglucamine, and 10 pH 7.0 and the internal solution 120 n-Methylglucamine, 10 EGTA, and 10 HEPES, pH 7.0. Data acquisition and analysis were performed using the pCLAMP system and software (Axon Instruments Inc., Foster City CA USA). Currents were filtered at 2 kHz and digitized at 10 kHz. Linear components were eliminated by P/-4 prepulse protocol. The normalized charge movement-voltage plot and the average current-voltage plot were obtained as described (12) using a CA-1B amplifier (Dagan). Currents were filtered at 1 kHz and digitized at 20 kHz. Ionic currents mediated by *Shaker* potassium channel were recorded one day after cRNA injection with two-electrode voltage clamp technique

using a Dagan TEV 200A or Warner OC725A and filtered at 10 kHz. For the Bafilomycin treatment, oocytes were incubated with 500 nM Bafilomycin A<sub>1</sub> (Sigma-Aldrich) 24 hours prior to protein injection (9). The *Shaker* channel used, Sh IR (Inactivation Removed) bears an N-terminal deletion that removes fast inactivation (13).

#### **6.3.4 Surface expression measurements in *Xenopus* Oocyte**

Surface expression of Ca<sub>v</sub>1.2 channels bearing the HA epitope (Ca<sub>v</sub>1.2-HA) was measured by immunoassay as described (9). Briefly, five to seven days after Ca<sub>v</sub>1.2 RNA injection, oocytes were separated in two groups; for electrophysiological recordings and for immunoassay. Oocytes were incubated in blocking buffer containing 1% BSA followed by incubation with 1  $\mu$ g/ml rat monoclonal anti-HA antibody (3F10, Roche Molecular Biochemicals). After washing, oocytes were incubated with HRP-coupled secondary antibody (goat anti-rat FAB fragments, Jackson ImmunoResearch), extensively washed and individual oocytes placed in 50  $\mu$ l of SuperSignal ELISA femto substrate (Pierce) in 96 wells microplates (Optiplate, PerkinElmer) and chemiluminescence quantified 30 seconds later with a luminometer (Viktor2, PerkinElmer).

## **6.4 Results**

### **6.4.1 $\beta_{2a}$ -SH3 reduces the number of channels expressed in the plasma membrane.**

The purified SH3 domain of the  $\text{Ca}_v\beta_{2a}$  with an expected molecular mass of 16.7 kDa elutes as a monodisperse peak from a size exclusion chromatography (Fig. 6.1B). The size exclusion chromatography calibration curve yielded an apparent molecular mass of 20.8 kDa that is compatible with a monomeric conformation of the protein. Mass spectrometry analysis on the purified  $\beta_{2a}$ -SH3 confirmed its identity (data not shown).  $\beta_{2a}$ -SH3 was injected in *Xenopus* oocytes expressing  $\text{Ca}_v1.2$  and gating and ionic currents were measured using the cut-open oocyte voltage clamp technique. Injection of  $\beta_{2a}$ -SH3 into oocytes causes a dramatic decrease in charge movement ( $Q_{\text{on}}$ , Fig. 6.1C) that develops with a time constant of 0.9 hours (Fig. 6.1D).  $Q_{\text{on}}$  stems from the conformational changes leading to channel opening (14) and, hence it is proportional to the number of channels. Since decrease in  $Q_{\text{on}}$  proceeds without changes in the voltage or time dependence (Fig. 6.1E-G), it likely reflects a reduction in the number of channels in the cell surface (9). In contrast, injection of full length  $\text{Ca}_v\beta$ , does modify channel gating as expected (15) (Fig. 6.1E). We corroborated that the drop of  $Q_{\text{on}}$  upon  $\beta_{2a}$ -SH3 injection stems from a decrease in the number of channels in the plasma membrane by immunoassay (9). Channel surface expression was measured in oocytes expressing HA-tagged  $\text{Ca}_v1.2$  channels and compared to  $Q_{\text{on}}$  measurements on the same group of oocytes as shown in Fig. 6.2A.

Impaired assembly and forward trafficking or enhanced backward trafficking may be responsible for the reduction in the number of channels expressed in the plasma membrane upon  $\beta_{2a}$ -SH3 injection. To discriminate between these two possibilities we

examined the effect of  $\beta_{2a}$ -SH3 when incorporation of new proteins into the plasma membrane was inhibited by bafilomycin. We have previously shown that indeed bafilomycin treatment interrupt incorporation of new  $Ca_v1.2$  channels in oocytes and causes a net reduction of channel density due to constitutive turnover (9). Injection of  $\beta_{2a}$ -SH3 in bafilomycin treated oocytes resulted in 35% reduction in  $Q_{on}$  (Fig 6.2C) that compares to the 29% observed in control conditions (Fig. 6.2B). Thus, down-regulation induced by  $\beta_{2a}$ -SH3 was not prevented by bafilomycin, indicating that this domain interferes with the backward trafficking rather than with the incorporation of newly formed channels.

#### **6.4.2 $\beta_{2a}$ -SH3 induced reduction of $Q_{on}$ depends on dynamin.**

Removal of membrane proteins from the surface implicates endocytosis. Several SH3-containing proteins participate in the regulation of this process by associating with dynamin, a GTPase that excises endocytic vesicles from the plasma membrane (16-19). The proline rich domain (PRD) of dynamin binds to SH3 domains in the partner protein and this interaction recruits dynamin to the plasma membrane. Moreover, endocytosis of ion channels and receptors through a dynamin dependent process has been reported (20-22). Therefore, we investigated the potential role of dynamin in  $\beta_{2a}$ -SH3 induced channel internalization. We first verified the presence of endogenous dynamin in *Xenopus* oocytes by western blot analysis using anti-dynamin antibody and



*The SH3 domain of the  $\beta$ -subunit of VGCCs promotes endocytosis via dynamin interaction*

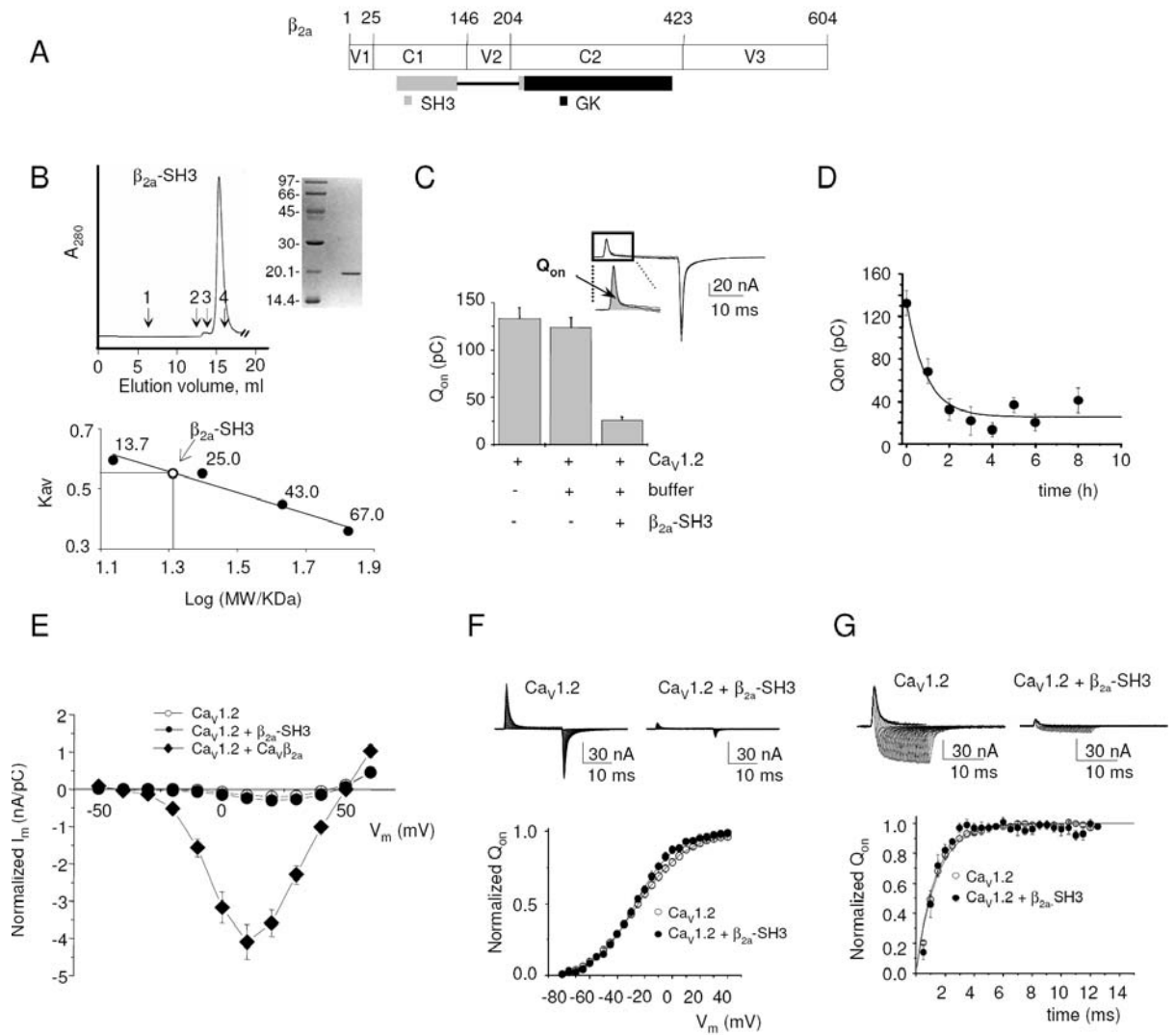


**Fig 6.1.  $\beta_{2a}$ -SH3 reduces charge movement in *Xenopus* oocytes expressing  $\text{Ca}_v1.2$ .** *A*,  $\text{Ca}_v\beta$  domains: V1, V2 and V3 denote variable regions, C1 and C2 conserved SH3 and GK like domains, respectively. Numbers refer to amino acid sequence in the  $\beta_{2a}$  rat isoform used in this study. *B*, Size exclusion chromatography profile of purified  $\beta_{2a}$ -SH3 domain and molecular mass calibration curve on Superdex 200 10/30 column (GE Healthcare Life Sciences). 1, void volume and 2, 3 and 4 denotes the elution volume of Albumin (67 kDa), Ovalbumin (43 kDa), and Ribonuclease A (13.7 kDa), respectively. The inset shows a SDS-PAGE performed on purified  $\beta_{2a}$ -SH3 with numbers corresponding to the molecular mass of standards in kDa. *C*, Average  $Q_{on}$  from  $\text{Ca}_v1.2$ -expressing oocytes before ( $132.6 \pm 11.6$  pC,  $n=18$ ) and after  $\beta_{2a}$ -SH3 ( $26.0 \pm 3.8$  pC,  $n=25$ ) or buffer injection ( $123.6 \pm 10.5$  pC,  $n=22$ ) as control.  $Q_{on}$  was measured by integrating gating current during a step near  $I_{Ba}$  reversal potential as shown in the inset. Voltage near  $I_{Ba}$  reversal potential was determined empirically by stepping to several potential in 2 mV increments. *D*, Time course of the  $\beta_{2a}$ -SH3-induced decrease in  $Q_{on}$  in  $\text{Ca}_v1.2$ -expressing *Xenopus* oocytes. Each point corresponds to the average of  $Q_{on}$  measured as in Fig. 1c for several oocytes recorded at different times following the injection of  $\beta_{2a}$ -SH3. Averages for each time point includes measurements up to 30 minutes before the indicated time and  $t = 0$  corresponds to the average  $Q_{on}$  from non-injected oocytes. The data was fitted to  $Q_{on} = Q_o (\exp[-t/\tau]) + Q_{min}$  where  $Q_o$  is the estimated  $Q_{on}$  at time = 0 in pC (108 pC),  $Q_{min}$  is the residual  $Q_{on}$  (25.7 pC) and  $\tau$  time constant in hours (0.90 hours). *E*, Average current-voltage plot normalized by  $Q_{on}$  from  $\text{Ca}_v1.2$ -expressing oocytes before protein injection ( $\circ$ ) and after  $\beta_{2a}$ -SH3 ( $\bullet$ ) or  $\text{Ca}_v\beta2a$  ( $\blacklozenge$ ) injection. *F*, Representative gating currents traces and voltage-dependence of  $Q_{on}$  from  $\text{Ca}_v1.2$ -expressing oocytes before ( $\circ$ ) and after  $\beta_{2a}$ -SH3 injection ( $\bullet$ ) during 20 ms voltage pulses from -80 mV to +40 mV in 5 mV increments from a holding potential of -90 mV recorded in 2 mM external  $\text{Co}^{2+}$ . *G*, Representative gating currents traces and time-dependence of  $Q_{on}$  from  $\text{Ca}_v1.2$ -expressing oocytes before ( $\circ$ ) and after  $\beta_{2a}$ -SH3 injection ( $\bullet$ ) during pulses to +40 mV of variable duration (0.5 to 12.5 ms in 0.5 increments) from a holding of -90 mV. Proteins were injected 1-5 h before recordings. See details in supplemental Table 6.S1 and 6.S2.

detected a protein of molecular mass similar to a heterologous expressed HA-tagged dynamin I (Fig. 6.3A). Coexpressing  $\text{Ca}_v1.2$  with dynamin did not have a direct impact on channel expression and  $\beta_{2a}$ -SH3 induced reduction of  $Q_{on}$  was equivalent (compare Fig. 6.1C and 6.3B). We then examined the effect of expressing a dominant-negative mutant of dynamin lacking GTPase activity that inhibits endocytosis (dynamin K44A) (23). Co-expression with dynamin K44A reduced oocytes survival rate and yielded smaller  $Q_{on}$  than  $\text{Ca}_v1.2$  alone or with dynamin WT. Although causes for these changes are unclear, we still observed that  $\beta_{2a}$ -SH3-induced reduction of  $Q_{on}$  was blunted by expression of dynamin K44A (Fig. 6.3C).

To further test the role of dynamin, we fused a 14 amino acid residues peptide spanning the proline rich region of dynamin I to GST protein to produce GST-Dyn<sub>829-842</sub> peptide. This peptide is known to disrupt the interaction between dynamin and SH3 domains and to inhibit endocytosis in synaptic vesicles (24;25). Figure 6.3D shows that pre-incubation of  $\beta_{2a}$ -SH3 with GST-Dyn<sub>829-842</sub> peptide, but not with GST alone, inhibits its potency to reduce  $Q_{on}$ . Furthermore,  $\beta_{2a}$ -SH3 binds *in vitro* to dynamin (Fig. 6.4A) and, consistently with the electrophysiological data, this binding is partially blocked by GST-Dyn<sub>829-842</sub> peptide but not by GST (Fig. 6.4B). We tested the ability of  $\beta_{2a}$ -SH3 to bind to the full length channel. Using a similar pull down assay, we did not observe binding of  $\beta_{2a}$ -SH3 to  $\text{Ca}_v1.2$  fused to the Yellow Fluorescent Protein (YFP- $\text{Ca}_v1.2$ ; Fig. 6.4C). In contrast and as expected,  $\text{Ca}_v\beta$  and the functional core of  $\text{Ca}_v\beta$  (26) encompassing the SH3 and GK domains (C1 to C2 in Fig. 6.1A) bound to the channel.

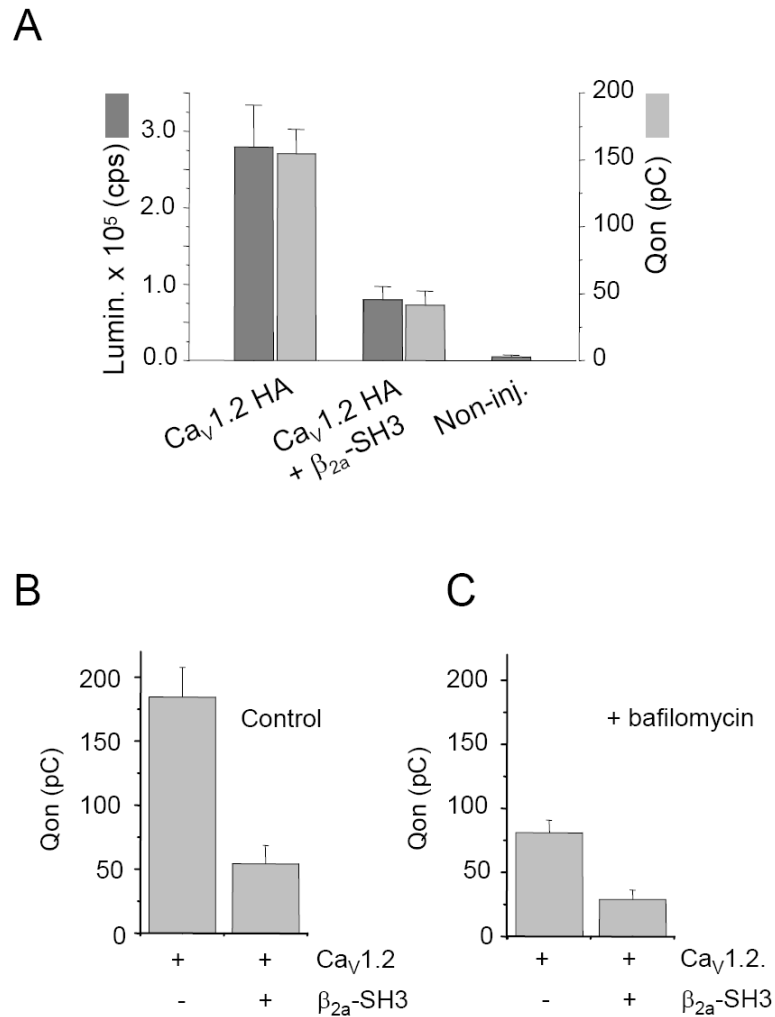


**Fig 6.2.  $\beta_{2a}$ -SH3-induced reduction of charge movement is not abolished by bafilomycin.** *A*, Chemiluminescence and  $Q_{on}$  of oocytes expressing Ca<sub>v</sub>1.2-HA alone or after  $\beta_{2a}$ -SH3 injection. Chemiluminescence was integrated for 0.2 s and expressed as 10<sup>5</sup> count per second (cps).  $Q_{on}$  was measured as in Fig. 1c. Non inj., non-injected oocytes. *B*, Average  $Q_{on}$  measured from *Xenopus* oocytes expressing Ca<sub>v</sub>1.2 in control conditions before ( $184.3 \pm 23.3$  pC,  $n = 9$ ) and after  $\beta_{2a}$ -SH3 injection ( $54.0 \pm 14.6$  pC,  $n = 8$ ). *C*, Average  $Q_{on}$  measured from *Xenopus* oocytes expressing Ca<sub>v</sub>1.2 treated with 500 nM Bafilomycin for 24 hours before ( $80.9 \pm 9.8$  pC,  $n = 8$ ) and after  $\beta_{2a}$ -SH3 injection ( $28.9 \pm 7.3$  pC,  $n = 7$ ). In both cases the reduction in  $Q_{on}$  following  $\beta_{2a}$ -SH3 injection is significant (t-test,  $p < 0.01$ ).

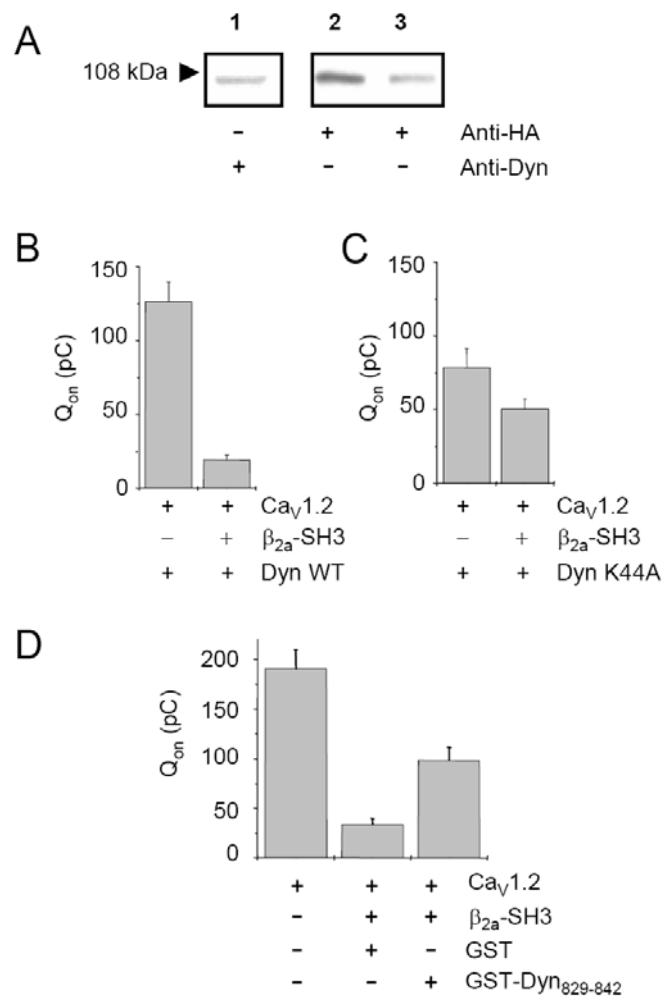


**Fig 6.3.  $\beta_{2a}$ -SH3-induced reduction of charge movement relies on interaction with dynamin.** *A*, Western blot analysis from *Xenopus* oocytes homogenates. Lane 1, non injected control oocytes, lane 2, oocytes injected with HA-tagged dynamin-WT cRNA and lane 3, with HA-tagged dynamin-K44A cRNA. Membranes were analyzed with anti-dynamin or anti-HA antibodies as indicated. *B*, Average  $Q_{on}$  from oocytes coexpressing Ca<sub>v</sub>1.2 and dynamin-WT before ( $126.3 \pm 13.5$  pC,  $n=24$ ) and after  $\beta_{2a}$ -SH3 injection ( $19.2 \pm 3.2$  pC,  $n=28$ ). *C*, Average  $Q_{on}$  from oocytes coexpressing Ca<sub>v</sub>1.2 and dynamin-K44A before ( $78.3 \pm 12.8$  pC,  $n=19$ ) and after  $\beta_{2a}$ -SH3 injection ( $50.6 \pm 6.9$  pC,  $n=19$ ). *D*, Average  $Q_{on}$  from Ca<sub>v</sub>1.2-expressing oocytes before ( $190.8 \pm 18.8$  pC,  $n=25$ ) and after injection of  $\beta_{2a}$ -SH3 pre-incubated in equal weight ratio with either GST ( $33.3 \pm 6.1$  pC,  $n=37$ ) or GST-Dyn<sub>829-842</sub> peptide ( $98.3 \pm 13.1$  pC,  $n=32$ ) as indicated.

#### **6.4.3 $\beta_{2a}$ -SH3 and full length $\text{Ca}_V\beta_{2a}$ down-regulate the distantly related Shaker potassium channel expressed in *Xenopus* oocytes.**

Because  $\beta_{2a}$ -SH3 promotes channel internalization without binding to the channel protein, we examined the effect of  $\beta_{2a}$ -SH3 onto the distantly related *Shaker* potassium channel that lack binding activity to the  $\text{Ca}_V\beta$ -subunit (27). Injection of  $\beta_{2a}$ -SH3 to oocytes expressing the *Shaker* channel resulted in no changes in channel gating (supplemental Fig. 6.S1) but ionic currents were reduced by approximately 60% one hour after protein injection (Fig. 6.5A). This current reduction was also partially blocked by pre-incubation of  $\beta_{2a}$ -SH3 with GST-Dyn<sub>829-842</sub> peptide but not with GST (Fig. 6.5B). Full length  $\text{Ca}_V\beta_{2a}$  preserves the ability of  $\beta_{2a}$ -SH3 to downregulate *Shaker* channels expressed in oocytes.  $\text{Ca}_V\beta_{2a}$  reduced ionic currents to similar degree as  $\beta_{2a}$ -SH3 (Fig. 6.5C) without changes in the voltage dependency (supplemental Fig. 6.S2). This current decrease was also antagonized by GST-Dyn<sub>829-842</sub> peptide. Moreover,  $\text{Ca}_V\beta_{2a}$  bound *in vitro* to dynamin and this interaction was inhibited by GST-Dyn<sub>829-842</sub> peptide (Fig. 6.5D). These results indicate that  $\text{Ca}_V\beta$  still acts through the dynamin dependent endocytic pathway.

#### **6.4.4 Full length $\text{Ca}_V\beta_{2a}$ reduces the number of plasma membrane $\text{Ca}_V1.2$ channels lacking the AID but not WT channels.**

A corollary from the above results is that free  $\text{Ca}_V\beta$  may also be able to reduce surface expression of  $\text{Ca}_V1.2$  channels when the  $\text{Ca}_V\alpha_1$ - $\text{Ca}_V\beta$  primary interaction site is disrupted. To test this possibility we deleted the AID site of  $\text{Ca}_V1.2$  (residues 459 to 475) to obtain  $\text{Ca}_V1.2$ - $\Delta$ AID channels. This mutated channel yields gating currents

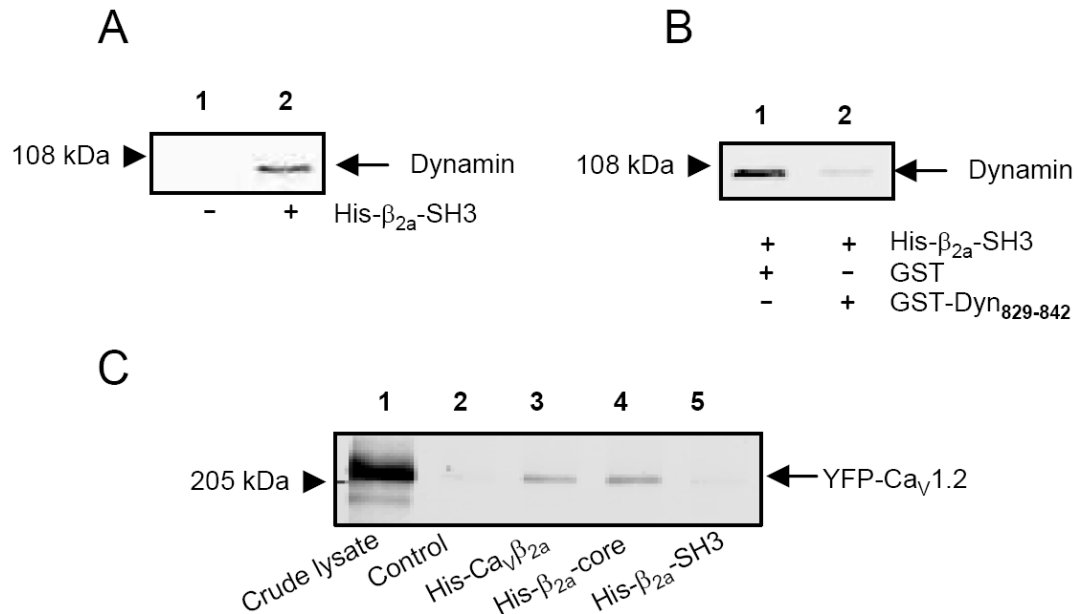


**Fig 6.4.  $\beta_{2a}$ -SH3 binds in vitro to dynamin but not to Ca<sub>v</sub>1.2.** *A*, Anti-dynamin western-blot. His- $\beta_{2a}$ -SH3 coupled to Co<sup>2+</sup> beads was incubated with lysate from cells expressing dynamin I (lane 2). Control binding with uncoupled Co<sup>2+</sup> beads (lane 1). *B*, As in *A*, except that either GST (lane 1) or GST-Dyn<sub>829-842</sub> peptide (lane 2) was added during incubation with dynamin-containing lysate. *C*, Binding of His-tagged Ca<sub>v</sub> $\beta_{2a}$  derivatives to YFP-Ca<sub>v</sub>1.2. Lane 1, crude lysate from cells expressing YFP-Ca<sub>v</sub>1.2; lane 2, control binding with uncoupled Co<sup>2+</sup> beads; lane 3, binding to full length Ca<sub>v</sub> $\beta_{2a}$ ; lane 4, to  $\beta_{2a}$ -core and lane 5, to  $\beta_{2a}$ -SH3. YFP-Ca<sub>v</sub>1.2 bands were visualized by fluorescence scanning using Typhoon-9410 imaging system (GE Healthcare Life Sciences). Binding experiments were repeated three, two and five times in *A*, *B* and *C*, respectively.

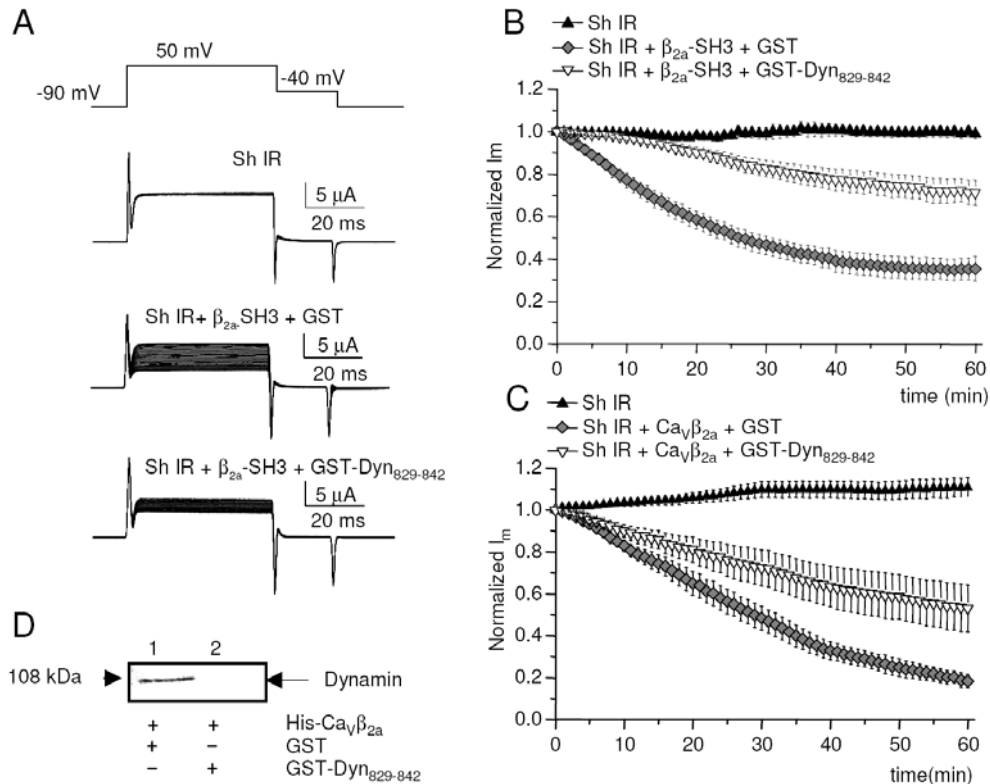


**Fig 6.5.  $\beta_{2a}$ -SH3 and full length Ca<sub>v</sub> $\beta_{2a}$  reduce ionic currents mediated by *Shaker* potassium channels expressed in *Xenopus* oocytes.** *A*, Representative ionic currents traces from oocytes expressing *Shaker* IR (Sh IR) before (top) and after  $\beta_{2a}$ -SH3 injection either pre-incubated with GST (middle) or with GST-Dyn<sub>829-842</sub> peptide (bottom). Each panel corresponds to 60 traces recorded once per minute during the pulse protocol depicted on top. *B*, Normalized current amplitudes over time for Sh IR-expressing oocytes before ( $\square$ ) ( $n=7$ ) and after injection of  $\beta_{2a}$ -SH3 pre-incubated with either GST ( $\bullet$ ) ( $n=11$ ) or GST-Dyn<sub>829-842</sub> ( $\blacktriangle$ ) ( $n=6$ ). *C*, Time course of current reduction measured as in *B* from Sh IR-expressing oocytes before ( $\square$ ) ( $n=7$ ) and after injection of Ca<sub>v</sub> $\beta_{2a}$  pre-incubated with a six fold excess (w/w) of either GST ( $\bullet$ ) ( $n=8$ ) or GST-Dyn<sub>829-842</sub> ( $\blacktriangle$ ) ( $n=9$ ). *D*, Anti-dynamin western-blot (as in Fig. 4B). His-Ca<sub>v</sub> $\beta_{2a}$  was coupled to Co<sup>2+</sup> beads and incubated with dynamin I cell lysate plus GST (lane 1) or GST-Dyn<sub>829-842</sub> peptide (lane 2).



that, with respect to their voltage and time dependence, are indistinguishable from wild type  $\text{Ca}_v1.2$  (Fig. 6.6 A,B), but as expected,  $\text{Ca}_v\beta_{2a}$  loses its ability to potentiate ionic currents (Fig. 6.6C). As recently corroborated by chemiluminescent enzyme immunoassay (9), surface expression of  $\text{Ca}_v1.2$  channels in oocytes is not altered by injection of  $\text{Ca}_v\beta_{2a}$  protein (Fig. 6.6D). In contrast, in oocytes expressing  $\text{Ca}_v1.2$ - $\Delta\text{AID}$  injection of  $\text{Ca}_v\beta_{2a}$  reduces  $Q_{\text{on}}$  to the same extent as did  $\beta_{2a}$ -SH3 in oocytes expressing wild type  $\text{Ca}_v1.2$  (Fig. 6.6E). To further prove that channels lacking the AID are indeed expressed in the plasma membrane and that  $\text{Ca}_v\beta$  decreases the number of channels at the cell surface, we performed the surface expression assay with  $\text{Ca}_v1.2$ - $\Delta\text{AID}$  HA-tagged channels.  $\text{Ca}_v\beta_{2a}$  injection decreased  $Q_{\text{on}}$  and chemiluminescence signal in  $\text{Ca}_v1.2$ - $\Delta\text{AID}$  expressing oocytes (Fig. 6.6F).

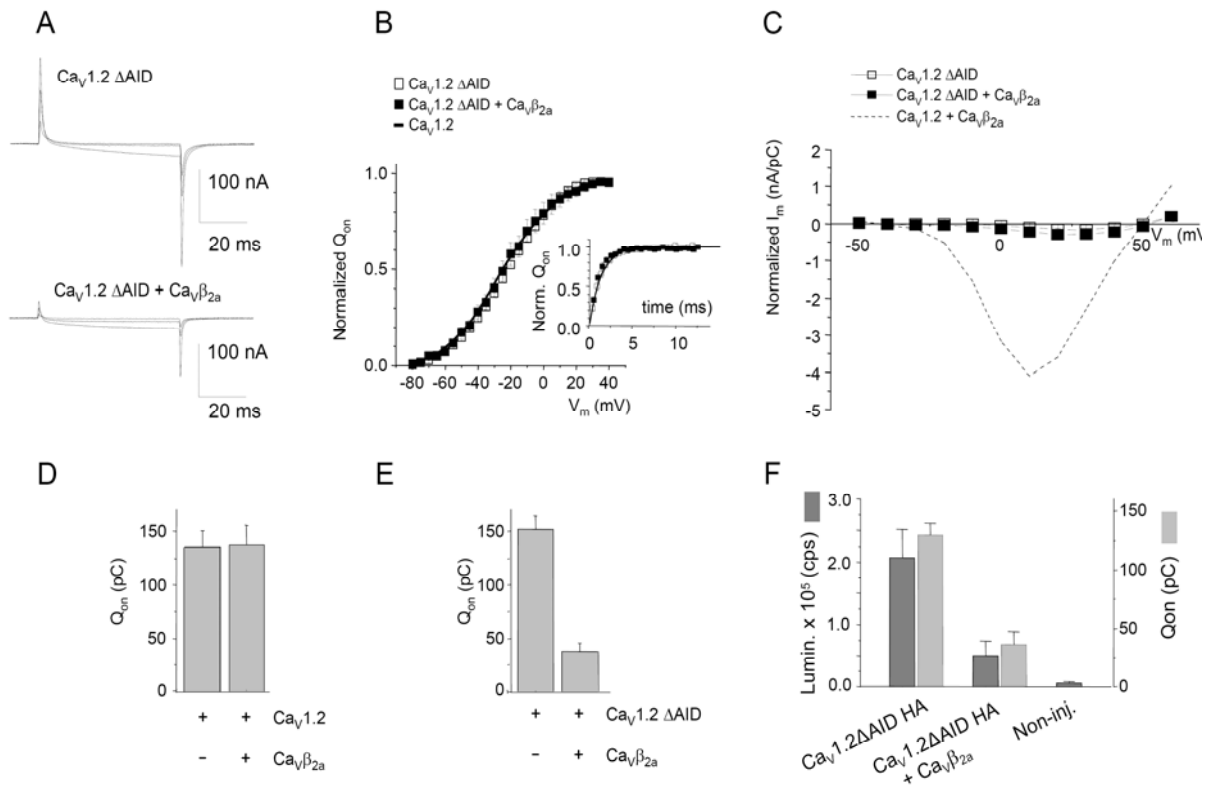


**Fig 6.6. Full length  $Ca_v\beta_{2a}$  internalizes calcium channels devoid of the AID site but not WT channels.** *A*, Representative ionic and gating currents traces from oocytes expressing  $Ca_v1.2\Delta AID$  channels during 60 ms voltage pulses to  $-30$ ,  $0$  and  $+30$  mV from a holding potential of  $-80$  mV. *B*, Voltage- and time-dependence (inset) of  $Q_{on}$  from  $Ca_v1.2$ - (continuous line) and  $Ca_v1.2\Delta AID$ -expressing oocytes before ( $\square$ ) and after  $Ca_v\beta_{2a}$  injection ( $\blacksquare$ ) measured as in Fig. 1F and G. See details in supplemental Table S1 and S2. *C*, Average current-voltage plot normalized by  $Q_{on}$  from  $Ca_v1.2\Delta AID$ -expressing oocytes before ( $\square$ ) and after  $Ca_v\beta_{2a}$  injection ( $\blacksquare$ ). For comparison, the data from  $Ca_v1.2$ -WT with  $Ca_v\beta_{2a}$  was included (dotted line). *D*, Average  $Q_{on}$  from  $Ca_v1.2$  expressing oocytes before ( $135.4 \pm 14.4$  pC,  $n=27$ ) and after ( $137.3 \pm 17.4$  pC,  $n=31$ )  $Ca_v\beta_{2a}$  injection. *E*, Average  $Q_{on}$  from  $Ca_v1.2\Delta AID$ -expressing oocytes before ( $151.2 \pm 12.4$  pC,  $n=32$ ) and after  $Ca_v\beta_{2a}$  injection ( $37.4 \pm 7.8$  pC,  $n=39$ ). *F*, Chemiluminescence and  $Q_{on}$  on oocytes expressing  $Ca_v1.2\Delta AID$ -HA alone ( $20.7 \pm 0.4 \times 10^5$  cps,  $n=23$  and  $129.5 \pm 9.9$  pC,  $n=14$ ) or after  $Ca_v\beta_{2a}$  injection ( $0.5 \pm 0.23 \times 10^5$  cps,  $n=23$  and  $26.5 \pm 18.3$  pC,  $n=12$ ). Non-inj., non-injected oocytes ( $0.06 \pm 0.02 \times 10^5$  cps,  $n=35$ ).

## **6.5 Discussion**

We here show that SH3 domain of the  $\beta$ -subunit of the voltage-gated calcium channels promotes internalization of membrane proteins in a dynamin dependent manner. In addition, we found that  $\text{Ca}_V\beta$ -SH3 binds in vitro to dynamin and, since this association is inhibited by GST-Dyn<sub>829-842</sub> peptide, we propose that this interaction is mediated by the PRD of dynamin. Nevertheless, simulated docking predictions indicate that  $\text{Ca}_V\beta$ -SH3 is unlikely to interact with PXXP motifs unless a considerable structural rearrangement occurs (4). The dynamin PRD- $\text{Ca}_V\beta$ -SH3 interaction may be mediated by non-canonical PXXP binding residues in  $\text{Ca}_V\beta$ -SH3 or alternatively exposition of canonical residues may be tuneable by a yet unknown regulatory protein or event. The interaction between recombinant  $\beta_{2a}$ -SH3 and dynamin may reflect an *in vivo* phenomenon given that a SH3-only form of the  $\text{Ca}_V\beta$  protein is expressed in cardiac cells (8).

Binding of  $\text{Ca}_V\beta$ -SH3 to the protein being sequestered is not required, since no interaction between the  $\beta_{2a}$ -SH3 and the whole  $\text{Ca}_V1.2$  channel was observed and certainly no association occurs with the *Shaker* channel.  $\text{Ca}_V\beta$ -SH3 has been reported to associate only with isolated regions or truncated  $\text{Ca}_V\alpha_1$  channels (28;29). Thus, it is conceivable that other cytoplasmic regions within the whole channel hinder this association.

In the presence of the full length  $\text{Ca}_V\beta$ -subunit, calcium channels lacking the AID site, but no WT channels, are down-regulated, as though binding to  $\text{Ca}_V\beta$  prevents the

channel complex to be internalized. Since association of the  $\text{Ca}_v\beta$  to VGCCs insures normal channel activity, this would constitute an efficient quality control mechanism in which the same protein insures functional fitness and survival of the channel in the plasma membrane (Fig. 6.7). Our recent finding that the  $\text{Ca}_v\alpha_1$ - $\text{Ca}_v\beta$  interaction is reversible at the level of the plasma membrane (9) supports this mechanism. The ability of this auxiliary subunit to influence internalization of other membrane proteins anticipates that replacement of complete signal transduction assemblies may be triggered by the presence of free  $\text{Ca}_v\beta$ . Whereas the whole picture is certainly still incomplete, our findings outline a novel signaling pathway for the regulation of intracellular calcium concentration.

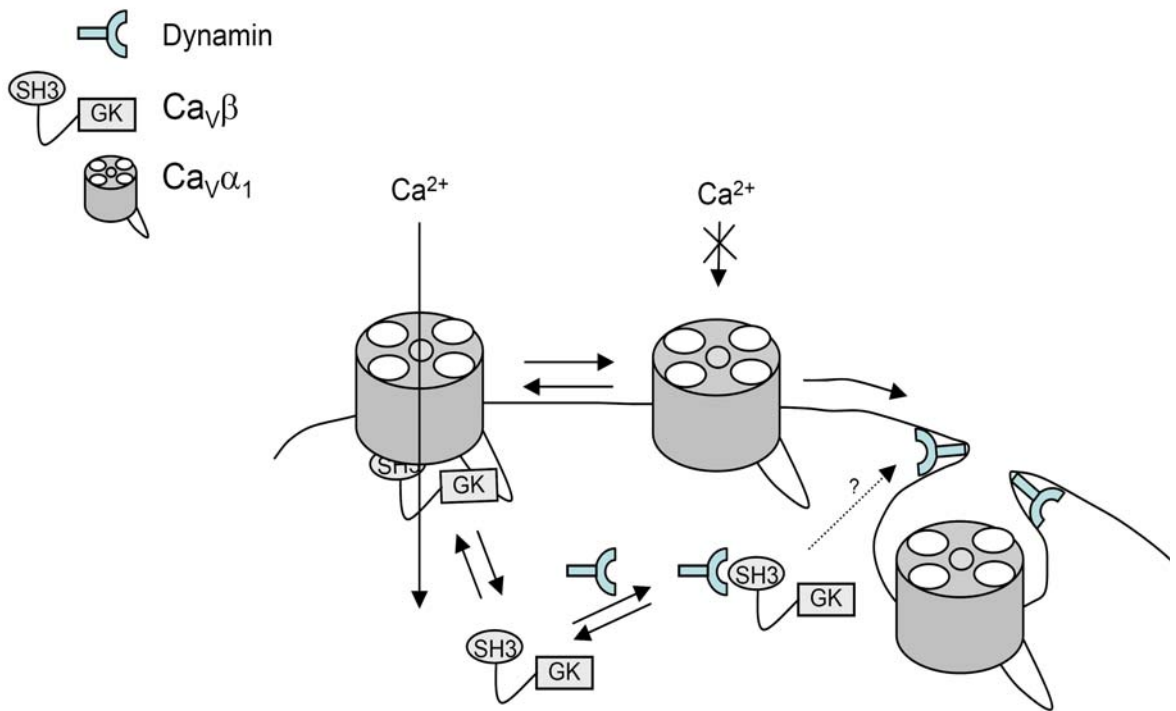


**Fig 6.7. Model for Ca<sub>v</sub>β and dynamin interaction.** The cartoon depicts that association of Ca<sub>v</sub>β to Ca<sub>v</sub>1.2 masks the SH3-module. Upon dissociation from Ca<sub>v</sub>α<sub>1</sub> the SH3 domain becomes available to interact with dynamin leading to down-regulation of calcium currents through endocytosis. How the interaction with Ca<sub>v</sub>β-SH3 recruits dynamin to its anchor site remains to be investigated.

***Acknowledgements***

We thank Dr. Christoph Fahlke and Dr. David Naranjo for insightful discussion, Ute Scholl for kindly providing us with the dynamin constructs, Dr. Matthias Gaestel for kindly sharing the luminometer Victor2 and Dr. Andreas Pich for the mass spectrometry. This work was supported by grants from the Deutsche Forschung Gemeinschaft (DFG) (FOR 450, TP1, to PH.) and Fondo para el Desarrollo de Ciencia y Tecnologia (FONDECYT -1020899) and Anillo de Ciencia y Tecnologia (ACT-46) to AN. The authors declare no competing financial interests.

<sup>2</sup>The abbreviations used are: VGCC, voltage-gated calcium channel; AID,  $\alpha$ -interaction-domain;  $\text{Ca}_v\beta$ ,  $\beta$ -subunit of voltage-gated calcium channels;  $\text{Ca}_v\alpha_1$ , pore-forming  $\alpha$ -subunit of voltage-gated calcium channels; SH3, Src-homology 3 domain; GK, guanylate kinase domain;  $\beta_{2a}$ -SH3, Src-homology 3 domain from  $\beta_{2a}$  isoform;  $\text{Ca}_v1.2$ , cardiac isoform of the  $\alpha$ -subunit of voltage-gated calcium channels; GST-Dyn<sub>829-842</sub>, Dynamin peptide encompassing residues 829 to 842; Q<sub>on</sub>, charge movement.

## 6.6 References

1. Arikath, J. and Campbell, K. P. (2003) *Curr. Opin. Neurobiol.* **13**, 298-307
2. Hanlon, M. R., Berrow, N. S., Dolphin, A. C., and Wallace, B. A. (1999) *FEBS Lett.* **445**, 366-370
3. Opatowsky, Y., Chen, C. C., Campbell, K. P., and Hirsch, J. A. (2004) *Neuron* **42**, 387-399
4. Chen, Y. H., Li, M. H., Zhang, Y., He, L. L., Yamada, Y., Fitzmaurice, A., Shen, Y., Zhang, H., Tong, L., and Yang, J. (2004) *Nature* **429**, 675-680
5. Van Petegem F., Clark, K. A., Chatelain, F. C., and Minor, D. L., Jr. (2004) *Nature* **429**, 671-675
6. Sparks, A. B., Rider, J. E., Hoffman, N. G., Fowlkes, D. M., Quillam, L. A., and Kay, B. K. (1996) *Proc. Natl. Acad. Sci. U. S. A* **93**, 1540-1544
7. Foell, J. D., Balijepalli, R. C., Delisle, B. P., Yunker, A. M., Robia, S. L., Walker, J. W., McEnery, M. W., January, C. T., and Kamp, T. J. (2004) *Physiol Genomics* **17**, 183-200
8. Cohen, R. M., Foell, J. D., Balijepalli, R. C., Shah, V., Hell, J. W., and Kamp, T. J. (2005) *Am. J Physiol Heart Circ. Physiol* **288**, H2363-H2374
9. Hidalgo, P., Gonzalez-Gutierrez, G., Garcia-Olivares, J., and Neely, A. (2006) *J. Biol. Chem.* **281**, 24104-24110
10. Neely, A., Garcia-Olivares, J., Voswinkel, S., Horstkott, H., and Hidalgo, P. (2004) *J. Biol. Chem.* **279**, 21689-21694
11. Wei, X., Neely, A., Olcese, R., Lang, W., Stefani, E., and Birnbaumer, L. (1996) *Receptors Channels.* **4**, 205-215
12. Dzhura, I. and Neely, A. (2003) *Biophys. J.* **85**, 274-289

13. Hoshi, T., Zagotta, W. N., and Aldrich, R. W. (1990) *Science* **250**, 533-538
14. Bezanilla, F. and Stefani, E. (1998) *Methods Enzymol.* **293**, 331-352
15. Neely, A., Wei, X., Olcese, R., Birnbaumer, L., and Stefani, E. (1993) *Science* **262**, 575-578
16. Hinshaw, J. E. (2000) *Annu. Rev. Cell Dev. Biol.* **16**, 483-519
17. Marks, B., Stowell, M. H., Vallis, Y., Mills, I. G., Gibson, A., Hopkins, C. R., and McMahon, H. T. (2001) *Nature* **410**, 231-235
18. Gout, I., Dhand, R., Hiles, I. D., Fry, M. J., Panayotou, G., Das, P., Truong, O., Totty, N. F., Hsuan, J., Booker, G. W., and . (1993) *Cell* **75**, 25-36
19. Okamoto, P. M., Herskovits, J. S., and Vallee, R. B. (1997) *J. Biol. Chem.* **272**, 11629-11635
20. Carroll, R. C., Beattie, E. C., Xia, H., Luscher, C., Altschuler, Y., Nicoll, R. A., Malenka, R. C., and von Zastrow, M. (1999) *Proc. Natl. Acad. Sci. U. S. A* **96**, 14112-14117
21. Zeng, W. Z., Babich, V., Ortega, B., Quigley, R., White, S. J., Welling, P. A., and Huang, C. L. (2002) *Am. J. Physiol Renal Physiol* **283**, F630-F639
22. Shimkets, R. A., Lifton, R. P., and Canessa, C. M. (1997) *J. Biol. Chem.* **272**, 25537-25541
23. Herskovits, J. S., Burgess, C. C., Obar, R. A., and Vallee, R. B. (1993) *J. Cell Biol.* **122**, 565-578
24. Shupliakov, O., Low, P., Grabs, D., Gad, H., Chen, H., David, C., Takei, K., De Camilli, P., and Brodin, L. (1997) *Science* **276**, 259-263
25. Shpetner, H. S., Herskovits, J. S., and Vallee, R. B. (1996) *J. Biol. Chem.* **271**, 13-16



26. Opatowsky, Y., Chomsky-Hecht, O., Kang, M. G., Campbell, K. P., and Hirsch, J. A. (2003) *J. Biol. Chem.* **278**, 52323-52332
27. Bichet, D., Cornet, V., Geib, S., Carlier, E., Volsen, S., Hoshi, T., Mori, Y., and De Waard, M. (2000) *Neuron* **25**, 177-190
28. Maltez, J. M., Nunziato, D. A., Kim, J., and Pitt, G. S. (2005) *Nat. Struct. Mol. Biol.* **12**, 372-377
29. Takahashi, S. X., Miriyala, J., Tay, L. H., Yue, D. T., and Colecraft, H. M. (2005) *J. Gen. Physiol* **126**, 365-377

## 6.7 Supplemental Data

**Table 6.S1**

	Ca <sub>v</sub> 1.2	Ca <sub>v</sub> 1.2 + $\beta_{2a}$ -SH3	Ca <sub>v</sub> 1.2 $\Delta$ AID	Ca <sub>v</sub> 1.2 $\Delta$ AID + Ca <sub>v</sub> $\beta_{2a}$
Q <sub>max</sub> (pC)	150 ± 24	21 ± 4	102 ± 13	47 ± 10
V <sub>1/2</sub> (mV)	-26.0 ± 1.9	-25.8 ± 1.2	-22.6 ± 1.3	-23.6 ± 3.5
Z	1.39 ± 0.06	1.71 ± 0.05	1.50 ± 0.05	1.61 ± 0.15
n	6	8	8	8

Mean ± S.E.M of parameters defining the Boltzmann distribution that best fitted the Normalized Q<sub>on</sub> vs V<sub>m</sub> plots for *Xenopus* oocytes expressing Ca<sub>v</sub>1.2 (Fig. 6.1F) and Ca<sub>v</sub>1.2.AID (Fig. 6.6B) with and without injection of the corresponding protein. The following equation was adjusted to the data:

$$Q_{on}(V) = Q_{max} / 1 + \exp \left[ zF (V_{1/2} - V_m) / RT \right] \quad \text{eq. 6.S1}$$

where Q<sub>max</sub> is the maximum Q<sub>on</sub>, V<sub>1/2</sub> is the voltage at which the Q<sub>on</sub> is 50% of Q<sub>max</sub>, V<sub>m</sub> is the membrane potential and z the effective valence.

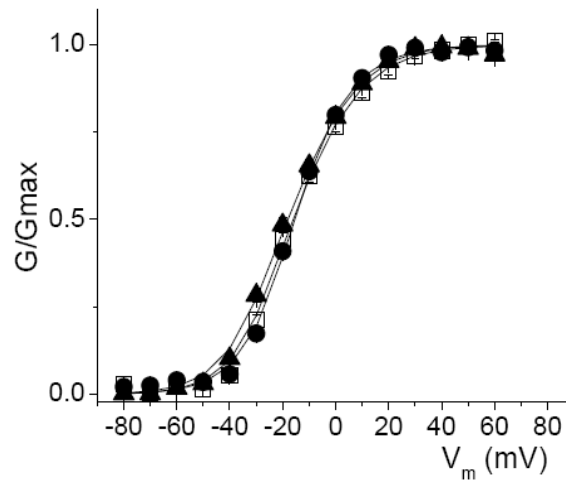
**Table 6.S2**

	Ca <sub>v</sub> 1.2	Ca <sub>v</sub> 1.2 + $\beta_{2a}$ .SH3	Ca <sub>v</sub> 1.2 $\Delta$ AID	Ca <sub>v</sub> 1.2 $\Delta$ AID + Ca <sub>v</sub> $\beta_{2a}$
Q <sub>max</sub> (pC)	132 ± 27	19 ± 4	80 ± 12	43 ± 10
$\tau$ (ms)	1.4 ± 0.1	1.3 ± 0.1	1.4 ± 0.1	1.1 ± 0.1
n	6	7	7	7

Mean ± S.E.M of parameters defining the mono-exponential function that best described the time course of Normalized Q<sub>on</sub> for Xenopus oocytes expressing Ca<sub>v</sub>1.2 (Fig. 6.1G) and Ca<sub>v</sub>1.2.AID (Fig. 6.6B, inset) with and without injection of the corresponding protein. The following equation was adjusted to the data:

$$Q_{on}(t) = Q_{max} \left(1 - \exp[-t / \tau]\right) \text{ eq. 6.S2}$$

where Q<sub>max</sub> is Q<sub>on</sub> extrapolated to steady state and  $\tau$  time constant for the development of Q<sub>on</sub>.

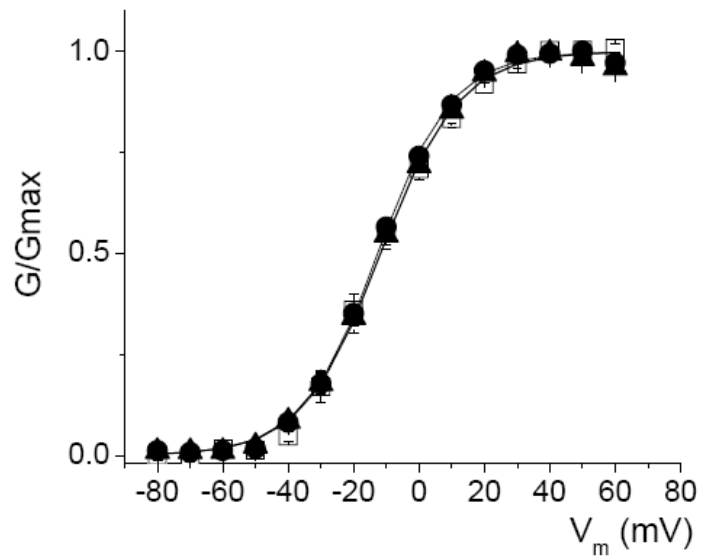


	Sh IR	Sh IR + $\beta_{2a}$ -SH3 + GST	Sh IR + $\beta_{2a}$ -SH3 + GST-Dyn <sub>829-842</sub>
$G_{\max}$ (nS)	$0.063 \pm 0.004$	$0.039 \pm 0.002$	$0.138 \pm 0.013$
$V_{1/2}$ (mV)	$-14.5 \pm 1.0$	$-14.8 \pm 0.5$	$-14.7 \pm 0.5$
Z	$2.46 \pm 0.07$	$2.51 \pm 0.05$	$2.31 \pm 0.07$
n	10	11	9

**Fig 6.S1** Normalized membrane conductance ( $G/G_{\max}$ ) as function of membrane potential ( $V_m$ ) and mean  $\pm$  S.E.M of parameters defining the Boltzmann distribution (bottom) that best fitted the data for *Xenopus* oocytes expressing Shaker IR ( $\square$ ) with different protein combinations.  $\beta_{2a}$ -SH3 was injected either together with GST ( $\bullet$ ) or with GST-Dyn<sub>829-842</sub> ( $\blacktriangle$ ). The  $G/G_{\max}$  vs  $V$  plots were obtained from the current amplitude ( $I_m$ ) evoked by 50 ms pulses from  $-80$  mV to  $+60$  mV in 10 mV increments with holding potential of  $-90$  mV. The membrane conductance ( $G$ ) was calculated as  $G = I_m / (V_m - E_{\text{rev}})$  assuming a reversal potential ( $E_{\text{rev}}$ ) of  $-90$  mV;  $V_m$  is the membrane potential during the pulse. Data was fitted according to equation:

$$G(V) = G_{\max} / 1 + \exp \left[ zF (V_{1/2} - V_m) / RT \right] \quad \text{eq. 6.S3}$$

where  $G_{\max}$  is the maximum conductance,  $V_{1/2}$  is the voltage at which the  $G$  is 50% of  $G_{\max}$ , and  $z$  the effective valence.



	Sh IR	Sh IR + GST + Ca <sub>v</sub> β <sub>2a</sub>	Sh IR + GST-Dyn <sub>829-842</sub> + Ca <sub>v</sub> β <sub>2a</sub>
G <sub>max</sub> (nS)	0.106 ± 0.034	0.086 ± 0.016	0.083 ± 0.014
V <sub>1/2</sub> (mV)	-11.7 ± 1.8	-12.7 ± 0.8	-11.5 ± 1.8
Z	2.16 ± 0.11	2.24 ± 0.13	2.20 ± 0.15
n	7	7	7

**Fig 6.S2** G/G<sub>max</sub> vs V<sub>m</sub> plot from *Xenopus* oocytes expressing Shaker IR (□) with full length Ca<sub>v</sub>β<sub>2a</sub> injected either together with GST (●) or with GST-Dyn<sub>829-842</sub> (▲). The G/V plots and statistical treatment were obtained as in Fig. 6.S1.

## **7. The guanylate kinase domain of the $\beta$ -subunit of voltage-gated calcium channels suffices to modulate gating**

Giovanni Gonzalez-Gutierrez<sup>\*</sup>, Erick Miranda-Laferte<sup>\*</sup>, Doreen Nothmann<sup>\*</sup>,  
Silke Schmidt<sup>\*</sup>, Alan Neely<sup>†‡</sup> and Patricia Hidalgo<sup>\*‡</sup>

<sup>\*</sup>Institut für Neurophysiologie, Medizinische Hochschule Hannover, 30625  
Hannover, Germany

<sup>†</sup>Centro de Neurociencia de Valparaíso, Universidad de Valparaíso 2349400  
Chile

**Proc. Natl Acad. Sci USA. 2008 vol. 105, No 37:14198-14203**

**© 2008 by The National Academy of Science of the USA**

## **7.1 Abstract**

Inactivation of voltage-gated calcium channels is crucial for the spatio-temporal coordination of calcium signals and prevention of toxic calcium build-up. Only one member of the highly conserved family of calcium channel  $\beta$ -subunits ( $\text{Ca}_v\beta$ ) inhibits inactivation and this unique feature has been attributed to short variable regions of the protein. Here we report instead, that this inhibition is conferred by a conserved guanylate kinase domain and moreover, that this domain alone recapitulates  $\text{Ca}_v\beta$ -mediated modulation of channel activation. We expressed and refolded the guanylate kinase domain of  $\text{Ca}_v\beta_{2a}$ , the unique variant that inhibits inactivation, and of  $\text{Ca}_v\beta_{1b}$ , an isoform that facilitates it. The refolded domains of both  $\text{Ca}_v\beta$ s inhibit inactivation of  $\text{Ca}_v2.3$  channels expressed in *Xenopus laevis* oocytes. These results suggest that the guanylate kinase (GK) domain endows calcium channels with a brake restraining voltage-dependent inactivation and thus, facilitation of inactivation by full-length  $\text{Ca}_v\beta$  requires additional structural determinants to antagonize GK effect. We found that  $\text{Ca}_v\beta$  can switch the inactivation phenotype conferred to  $\text{Ca}_v2.3$  from slow to fast following post-translational modifications during channel biogenesis. Our findings provide a novel framework to understand modulation of inactivation and a new functional map of  $\text{Ca}_v\beta$  in which the guanylate kinase domain regulates channel gating while the other conserved domain, namely, Src homology 3, may couple calcium channels to other signaling pathways.

*The GK domain of the  $\beta$ -subunit of VGCCs suffices to modulate gating*



## **7.2 Introduction**

Calcium signals mediate various cellular processes including neurotransmission, excitation-contraction coupling, hormone secretion, and gene expression (1). Voltage-gated calcium channels (VGCCs) activate and inactivate upon membrane depolarization allowing transient increases in cytosolic  $\text{Ca}^{2+}$  concentration. Voltage-dependent activation and inactivation of VGCCs strongly depend on association of the ancillary  $\beta$ -subunit ( $\text{Ca}_v\beta$ ) to a highly conserved sequence within the intracellular loop joining the first and second repeats (loop I-II) of the pore-forming subunit ( $\text{Ca}_v\alpha_1$ ), the so-called  $\alpha$ -interaction-domain (AID) (2).

$\text{Ca}_v\beta$  is encoded by four non-allelic genes ( $\beta_{1-4}$ ), each with multiple splice variants, and except for a few short splicing forms (3), all share a common structural arrangement. This consists of two highly conserved regions separated and flanked by shorter variable sequences (Fig 7.1A). Crystallographic studies revealed that while the first region encompasses a Src homology 3 (SH3) domain, the second a guanylate kinase (GK) domain. The AID sequence forms an  $\alpha$ -helix that fits into a hydrophobic cleft of GK module that lies on the opposite side of the SH3 domain (Fig. 7.1B) (4-6). This suggests that the isolated GK module may preserve at least some of the modulatory capabilities of the full  $\text{Ca}_v\beta$ . However, despite several attempts using different  $\text{Ca}_v\beta$  constructs and experimental approaches (7-11), the functional competence of isolated GK and its ability to mimic  $\text{Ca}_v\beta$  function remains unresolved. A contributing factor may be the reduced stability of some GK-containing constructs (11). To overcome this difficulty, we

expressed and refolded the GK domain of two  $\text{Ca}_V\beta$  isoforms,  $\text{Ca}_V\beta_{1b}$  and  $\text{Ca}_V\beta_{2a}$ . These isoforms share modulatory effects on voltage-dependent activation and exhibit opposite actions on voltage-dependent inactivation.

We studied the effect of the refolded GK modules on *Xenopus* oocytes expressing two types of  $\alpha_1$  pore-forming subunits,  $\text{Ca}_V1.2$  and  $\text{Ca}_V2.3$ , and compared it to the action of recombinant full length and the core of the  $\text{Ca}_V\beta$  protein containing both, SH3 and GK domains. While  $\text{Ca}_V\beta_{2a}$  is unique in its ability to inhibit voltage-dependent inactivation, the other  $\text{Ca}_V\beta$  isoforms facilitate it (12-17).  $\text{Ca}_V\beta_{2a}$  decelerates inactivation, increases the fraction of non-inactivating current and it shifts the steady-state inactivation curve towards more positive potentials. These distinguishing modulatory properties of  $\text{Ca}_V\beta_{2a}$  has been broadly attributed to palmitoylation of the two contiguous cysteine residues at position 3 and 4 in the N-terminus region (15;18-20).

Here we show, instead, that the GK modules derived from both  $\text{Ca}_V\beta_{2a}$  and  $\text{Ca}_V\beta_{1b}$  inhibit inactivation of  $\text{Ca}_V2.3$  channels. This finding indicates that the structural determinants of inhibition of inactivation by  $\text{Ca}_V\beta_{2a}$  are not encoded in variable regions but within the GK domain. GK appears to endow calcium channels with a brake to impair voltage-dependent inactivation and, thus, facilitation of inactivation occurs by masking the inhibitory effect of GK.

We show that  $\text{Ca}_v\beta$  acquires this capability when co-expressed with  $\text{Ca}_v\alpha_1$  but not when added later during channel biogenesis. Moreover, we found that  $\text{Ca}_v\beta_{2a}$ -GK increases peak currents and shifts the activation curve toward more negative potentials of  $\text{Ca}_v1.2$  channels. Thus, GK emerges as a functional unit that recapitulates the hallmarks of  $\text{Ca}_v\beta$  modulation.

## **7.3 Materials and Methods**

### **7.3.1 Construction of cDNA and protein expression.**

cDNA encoding the GK domain (residues 201 to 422), the SH3-GK core (residues 24 to 422) of rat  $\beta_{2a}$  (Swiss-Prot Q8VGC3-2), and GK domain (residues 209 to 413) of the rat  $\beta_{1b}$  (Swiss-Prot P54283), were subcloned by PCR methods into pRSET vector (Invitrogen). The predicted molecular masses of  $\text{Ca}_v\beta_{1b}$ -GK,  $\text{Ca}_v\beta_{2a}$ -GK and  $\text{Ca}_v\beta_{2a}$ -SH3-GK constructs, including the N-terminal His Tag, a transcript stabilizing sequence and the enterokinase cleavage recognition site, are 26.9 kDa, 28.6 kDa and 48.2 kDa, respectively.  $\text{Ca}_v\beta_{2a}$ -SH3 was prepared as in (24), full-length  $\text{Ca}_v\beta_{2a}$ , the mutant bearing two substitutions at position 3 and 4 ( $\text{Ca}_v\beta_{2a}$  C3,4S) and  $\text{Ca}_v\beta_{2a}$ -SH3-GK as in (22) while full-length  $\text{Ca}_v\beta_{1b}$  as in (30).  $\text{Ca}_v\beta_{1b}$ -GK and  $\text{Ca}_v\beta_{2a}$ -GK were expressed in bacteria and recovered from inclusion bodies as reported (30). The GK domains were refolded by batch dilution (11-fold dilution) in refolding buffer (L-arginine 400 mM, NaEDTA 2 mM, glutathione oxidized 0.5 mM, Tris base 100 mM, pH 7.0) and subsequently purified by size-exclusion chromatography onto a Superdex S-200 column (GE Healthcare Life Sciences) pre-equilibrated with non-denaturing buffer (20 mM Tris, 300 mM NaCl, 1 mM EDTA at pH 8.0). Proteins were concentrated up to 0.1 mg/ml by ultra-filtration (Amicon Ultra-4 10 kDa MWCO), fast frozen and stored at  $-80^\circ\text{C}$  until use. The identity of the purified proteins was confirmed by mass spectrometry analysis performed in the Mass spectrometry laboratory, Zentrum für Pharmakologie und Toxikologie, Medizinische Hochschule Hannover. The protein was digested by trypsin and the peptides were analyzed in Ultraflex MALDI-TOF/TOF Mass Spectrometer (Bruker Daltonics).

The loop I-II of Ca<sub>v</sub>1.2 (Swiss-Prot P15381) fused to glutathione S-transferase (GST-loop I-II) was prepared as in (30). The yellow fluorescent protein was fused to Ca<sub>v</sub> $\beta$ <sub>2a</sub>-GK at its N-terminus (YFP-Ca<sub>v</sub> $\beta$ <sub>2a</sub>-GK) and subcloned into pcDNA 3.1 vector. The cDNA encoding Ca<sub>v</sub>1.2 was fused to GK domain at the carboxyl-terminal end (Ca<sub>v</sub>1.2- Ca<sub>v</sub> $\beta$ <sub>2a</sub>-GK) by overlapping extension PCR which incorporate the sequence “MGRDLYDDDDDKD” at residue 2164 of Ca<sub>v</sub>1.2. All constructs were verified by DNA sequencing.

### **7.3.2 Binding assay.**

TsA201 cells were transfected with YFP-Ca<sub>v</sub> $\beta$ <sub>2a</sub>-GK or YFP alone encoding vector and lysed after 24-36 hours. Pre-cleared cell extracts were incubated one hour with glutathione beads coupled to either GST-loop I-II or GST alone. The beads were pelleted, washed and bound proteins were eluted with SDS/PAGE loading buffer. Proteins were then resolved on SDS/PAGE and visualized by fluorescence scanning (Typhoon imager, GE Healthcare Life Sciences).

### **7.3.3 Oocytes injection and electrophysiological recordings.**

cRNA were synthesized and *Xenopus laevis* oocytes were prepared, injected, and maintained as previously reported (30). The Ca<sub>v</sub>2.3 encoding cDNA was sequenced and when compared to the Swiss-Prot entry Q15878 the following changes were noticed: I649M, W837L, P838A and insertion of a glycine residue at position 839. The Ca<sub>v</sub>1.2-subunit used in this study bears 60 amino acids deletion at the amino terminal (31).

Electrophysiological recordings were performed with the cut-open oocyte technique four to six days after cRNA injection and one to seven hours after protein injection as described (22). For details see 7.SI Materials and Methods.

## **7.4 Results**

### **7.4.1 Refolding and binding assay of $\text{Ca}_v\beta$ -GK domain.**

The GK domain derived from  $\text{Ca}_v\beta_{1b}$  ( $\text{Ca}_v\beta_{1b}$ -GK) and  $\text{Ca}_v\beta_{2a}$  ( $\text{Ca}_v\beta_{2a}$ -GK) (Fig.7.1A) were expressed in bacteria where they accumulate in inclusion bodies and were refolded by batch dilution. The purified GK domains were concentrated up to 0.1 mg/ml since further concentration resulted in progressive protein aggregation as judged by high molecular mass peaks that appear in the void volume of the size-exclusion chromatography column. At 0.1 mg/ml,  $\text{Ca}_v\beta_{2a}$ -GK eluted from the size-exclusion chromatography in a predominant peak while  $\text{Ca}_v\beta_{1b}$ -GK shows a shoulder at this position and a main peak eluting near the albumin peak (Fig.7.1C).

Both GK constructs migrate with an apparent molecular mass larger than predicted by their amino acid sequences. This may reflect either an aberrant migration or formation of higher oligomeric states. To determine whether the refolded GK domains form multimers, we performed sucrose gradient analysis [Supporting Information (SI) Fig.7.S1-S3].  $\text{Ca}_v\beta_{2a}$ -GK distribution overlaps with a protein standard of 66 kDa, while  $\text{Ca}_v\beta_{1b}$ -GK appears over a wider range reaching a second standard of 29 kDa. Thus, our data is consistent with  $\text{Ca}_v\beta_{2a}$ -GK being essentially a dimer and  $\text{Ca}_v\beta_{1b}$ -GK existing as a mixture of dimers and monomers.

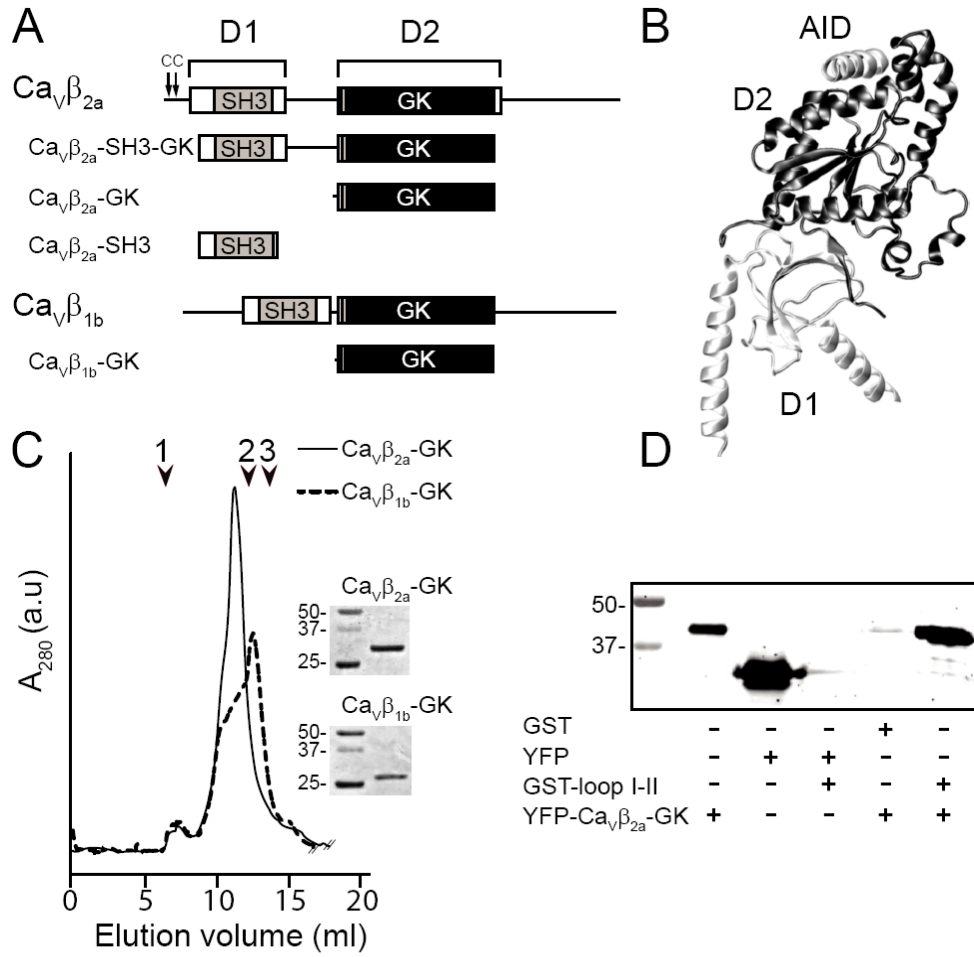




**Fig. 7.1 Domain structure, purification and binding assay of  $\text{Ca}_v\beta$  constructs.** (A), Schematic representation of  $\text{Ca}_v\beta_{2a}$ ,  $\text{Ca}_v\beta_{1b}$  and derived protein constructs used in this study.  $\text{Ca}_v\beta$  consists of two highly conserved regions, D1 and D2, (boxes) that are connected and flanked by variable regions (continuous lines). Boxed in grey is the SH3 module and in black, the GK module. The two cysteines residues at the N-terminus of  $\text{Ca}_v\beta_{2a}$  that undergo palmitoylation are indicated by arrows. (B) Ribbon diagram of the crystal structure of  $\text{Ca}_v\beta$  in complex with AID (PDB accession code 1T3L). (C) Size-exclusion chromatography elution profile on Superdex 200 10/30 column (GE Healthcare Life Sciences) of refolded  $\text{Ca}_v\beta_{2a}$ -GK and  $\text{Ca}_v\beta_{1b}$ -GK. Number 1 indicates void volume; 2, elution volume of albumin (67 kDa) and 3, of ovalbumin (43 kDa). The inset shows Coomassie-stained SDS/PAGE gels of the indicated proteins. Numbers indicate the molecular mass of standards in kDa. (D) SDS/PAGE gel of the binding reaction with the indicated proteins. YFP- $\text{Ca}_v\beta_{2a}$ -GK binds specifically to GST-loop I-II (last lane). The binding assay was repeated 3 times.

To assess binding ability of  $\text{Ca}_v\beta_{2a}$ -GK to the loop I-II, we fused the former to the yellow fluorescence protein (YFP- $\text{Ca}_v\beta_{2a}$ -GK) and the latter to GST (GST-loop I-II).  $\text{Ca}_v\beta_{2a}$ -GK binds specifically to loop I-II, since no association between GST and YFP- $\text{Ca}_v\beta_{2a}$ -GK or between YFP and the GST-loop I-II was detected (Fig. 7.1D).

#### **7.4.2 $\text{Ca}_v\beta_{2a}$ -GK increases peak current amplitude and shifts the current-voltage relationship of $\text{Ca}_v1.2$ channels.**

To investigate modulation of voltage-dependent activation by  $\text{Ca}_v\beta_{2a}$ -GK, we used the  $\text{Ca}_v1.2$   $\alpha_1$ -subunit because it exhibits little inactivation and the coupling between voltage sensor and channel opening is extremely sensitive to the presence of  $\text{Ca}_v\beta$ . This  $\text{Ca}_v\alpha_1$  isoform is also more amenable to monitor channel expression through gating currents measurements (21).

Injection of recombinant full-length  $\text{Ca}_v\beta_{2a}$  into oocytes expressing  $\text{Ca}_v1.2$  channels results in an increase in the ionic-current to charge-movement ratio (I/Q) and a leftward shift in the current-voltage relationship (22).  $\text{Ca}_v\beta_{2a}$ -SH3-GK is equally robust in modulating activation of  $\text{Ca}_v1.2$  channels (Fig. 7.2A and SI Fig. 7.S4 and Table 7.S1). Here, as in a previous report (22), we measured charge movement by integrating outward transient currents at the onset of depolarizing pulses to the ionic current reversal potential. Injection of  $\text{Ca}_v\beta_{2a}$ -SH3-GK into  $\text{Ca}_v1.2$ -expressing oocytes, increases I/Q from  $0.3\pm 0.6$  nA/pC (n=15) to  $4.6\pm 0.7$  nA/pC (n=17) which is comparable to values obtained following injection of  $\text{Ca}_v\beta_{2a}$  ( $4.6\pm 0.9$  nA/pC, n=18). The effect of  $\text{Ca}_v\beta_{2a}$ -GK was seen more

clearly at reduced channel expression levels where gating currents are barely visible and thus I/Q plots were not readily measurable. Nevertheless, the normal current-voltage relationship was shifted to more negative potentials and to similar extent with  $\text{Ca}_v\beta_{2a}$  (as protein or cRNA),  $\text{Ca}_v\beta_{2a}$ -SH3-GK or  $\text{Ca}_v\beta_{2a}$ -GK (Fig. 7.2B).

We attributed the limited activity of refolded  $\text{Ca}_v\beta_{2a}$ -GK to the low concentration of this protein, calculated to be 0.3  $\mu\text{M}$  for a 525 nl oocyte. In addition, at high expression levels, a large amount of  $\text{Ca}_v1.2$  subunit remains in the cytoplasm and may be acting as a sink. Another contributing factor could be the protein's reduced stability (see below). To overcome this potential problem, and inspired by the experiment showing that  $\text{Ca}_v\beta_{2a}$  recapitulates channel modulation when attached to the C-termini of  $\text{Ca}_v\alpha_1$  (23), we covalently linked  $\text{Ca}_v\beta$ -GK to  $\text{Ca}_v1.2$  ( $\text{Ca}_v1.2$ - $\text{Ca}_v\beta_{2a}$ -GK) and compared to  $\text{Ca}_v1.2$  linked to  $\text{Ca}_v\beta_{2a}$  ( $\text{Ca}_v1.2$ - $\text{Ca}_v\beta_{2a}$ ). Fig. 7.3 shows gating and ionic currents from oocytes expressing  $\text{Ca}_v1.2$ - $\text{Ca}_v\beta_{2a}$  or  $\text{Ca}_v1.2$ - $\text{Ca}_v\beta_{2a}$ -GK. When covalently linked to  $\text{Ca}_v1.2$ ,  $\text{Ca}_v\beta_{2a}$ -GK appears as efficient as full-length  $\text{Ca}_v\beta_{2a}$  in increasing I/Q and shifting the voltage dependence of activation. This effect was abolished by a mutation in the conserved tryptophan within the AID (W470S) shown to prevent binding to  $\text{Ca}_v\beta$  (22), indicating that the changes in gating properties come about through specific association of the fused GK moiety to the AID site and not from alterations of channel activity generated by the GK linkage.

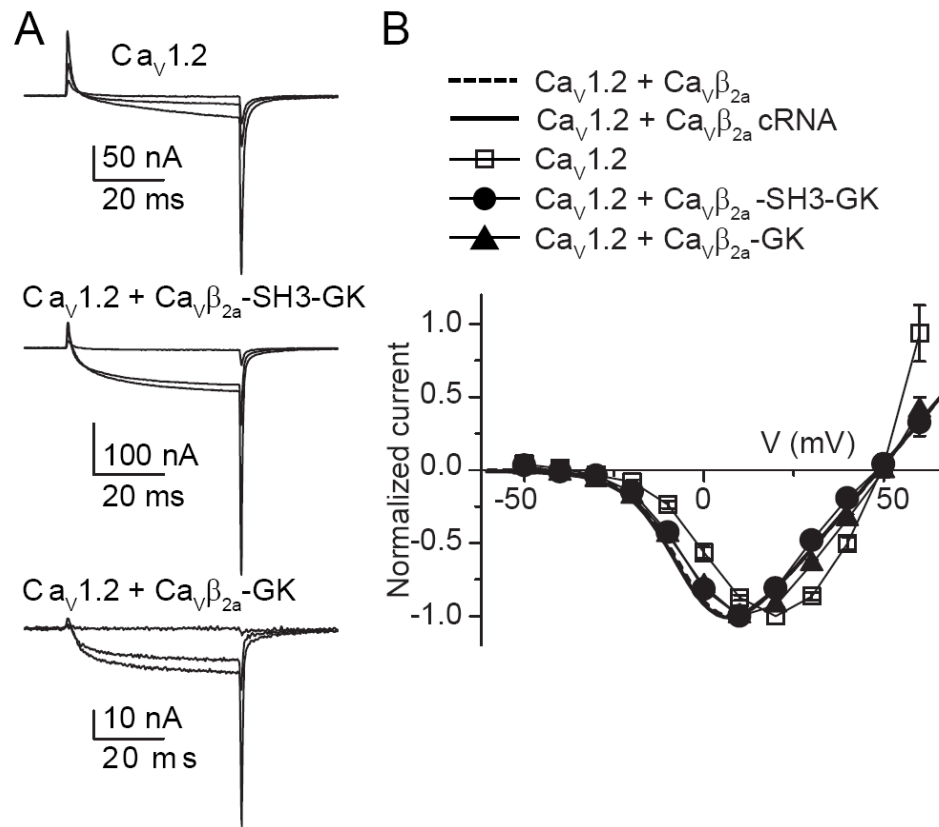


**Fig.7.2 Refolded Ca<sub>v</sub>β<sub>2a</sub>-GK and Ca<sub>v</sub>β<sub>2a</sub>-SH3-GK shift the current-voltage relationship of Ca<sub>v</sub>1.2-mediated currents.** (A) Representative gating and ionic currents traces from oocytes expressing Ca<sub>v</sub>1.2 cRNA alone and following injection of either Ca<sub>v</sub>β<sub>2a</sub>-SH3-GK or Ca<sub>v</sub>β<sub>2a</sub>-GK. Currents were evoked by 50 ms pulses to -30, 0 and +30 mV from a holding potential of -80 mV. (B) Normalized current-voltage plot from oocytes expressing the different subunit combinations. Ca<sub>v</sub>1.2 cRNA (n=11), Ca<sub>v</sub>1.2 + Ca<sub>v</sub>β<sub>2a</sub>-SH3-GK (n=14) and Ca<sub>v</sub>1.2 + Ca<sub>v</sub>β<sub>2a</sub>-GK (n=16). For comparison, normalized current-voltage curve for Ca<sub>v</sub>1.2 + Ca<sub>v</sub>β<sub>2a</sub>, either injected as a protein (dashed line) or co-injected as cRNA (continuous line) are shown (see SI Table 7.S1 for details).

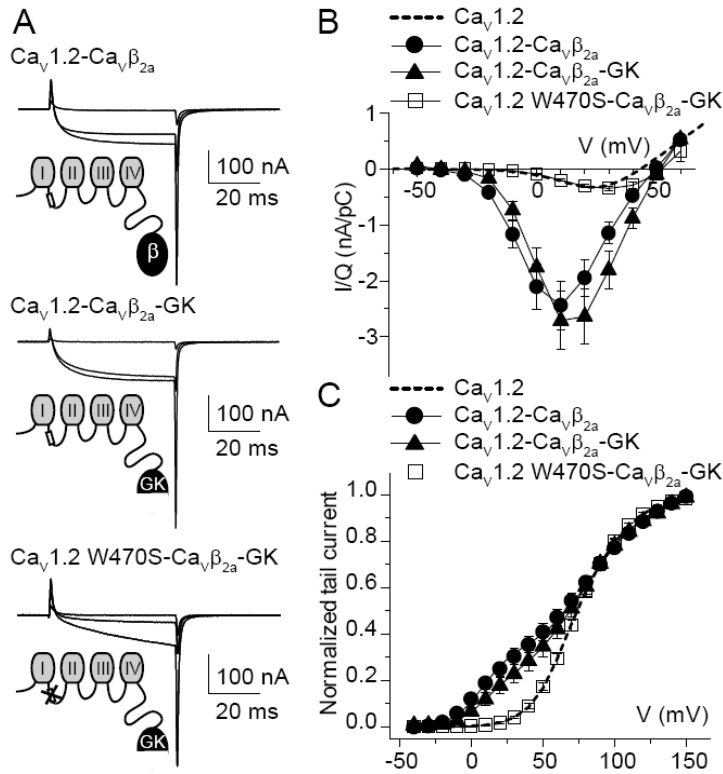


**Fig.7.3  $\text{Ca}_v\beta_{2a}$ -GK covalently linked to  $\text{Ca}_v1.2$  WT, but not to  $\text{Ca}_v1.2$  W470S, increases peak current amplitudes and shifts the current-voltage relationship.** (A) Representative gating and ionic currents traces from oocytes expressing  $\text{Ca}_v1.2$  WT covalently linked to either  $\text{Ca}_v\beta_{2a}$  ( $\text{Ca}_v1.2\text{-Ca}_v\beta_{2a}$ ) or  $\text{Ca}_v\beta_{2a}\text{-GK}$  ( $\text{Ca}_v1.2\text{-Ca}_v\beta_{2a}\text{-GK}$ ) and,  $\text{Ca}_v1.2$  W470S covalently linked to  $\text{Ca}_v\beta_{2a}\text{-GK}$  ( $\text{Ca}_v1.2\text{ W470S-Ca}_v\beta_{2a}\text{-GK}$ ). Currents were evoked by 50 ms pulses to -30, 0 and +30 mV from a holding potential of -80 mV. (B) Ionic current from oocytes expressing the different constructs were normalized by charge movement ( $I/Q$ ) and plotted versus voltage. For  $\text{Ca}_v1.2\text{-Ca}_v\beta_{2a}$  peak  $I/Q$  was  $2.44\pm 0.44$  nA/pC ( $n=17$ ), for  $\text{Ca}_v1.2\text{-Ca}_v\beta_{2a}\text{-GK}$  it was  $2.71\pm 0.52$  nA/pC ( $n=17$ ) and for  $\text{Ca}_v1.2\text{ W470S-Ca}_v\beta_{2a}\text{-GK}$   $0.35\pm 0.03$  nA/pC ( $n=17$ ). For comparison, average  $I/Q$  from 15 oocytes expressing  $\text{Ca}_v1.2$  alone are shown as dashed line ( $0.30\pm 0.06$  nA/pC). (C) Normalized tail currents from oocytes expressing the different constructs. Continuous lines correspond to the fit of the sum of two Boltzmann distributions and the dashed line to the fit obtained from  $\text{Ca}_v1.2$  expressing oocytes (see SI Fig. 7.S4 and Table 7.S1 for details). The fit to  $\text{Ca}_v1.2\text{ W470S-Ca}_v\beta_{2a}\text{-GK}$  was excluded from the plot for clarity.

### **7.4.3 $\text{Ca}_v\beta_{2a}$ -GK inhibits inactivation of $\text{Ca}_v2.3$ WT channels.**

Next, we investigated the ability of  $\text{Ca}_v\beta_{2a}$ -GK to regulate inactivation kinetics, using the fast inactivating  $\text{Ca}_v2.3$  channels (Fig. 7.4). Injection of refolded  $\text{Ca}_v\beta_{2a}$ -GK into  $\text{Ca}_v2.3$  expressing oocytes results in a six-fold increase in the decay time to half peak current amplitude ( $t_{1/2}$ , Fig. 7. 4A, B). However, when  $\text{Ca}_v\beta_{2a}$ -GK is co-injected as cRNA fails to modulate  $\text{Ca}_v2.3$ -mediated currents. A larger increase in  $t_{1/2}$  was observed upon injection of full-length  $\text{Ca}_v\beta_{2a}$ , either injected as protein or co-injected as cRNA, and  $\text{Ca}_v\beta_{2a}$ -SH3-GK. Consistently with our previous report,  $\text{Ca}_v\beta_{2a}$ -SH3 decreased ionic currents without changing its time course (24). The effect of refolded  $\text{Ca}_v\beta_{2a}$ -GK vanishes five hours after being injected, indicative of some degree of protein instability (Fig. 7.4C). The latter may also explain the lack of effect of  $\text{Ca}_v\beta_{2a}$ -GK cRNA.

Both  $\text{Ca}_v\beta_{2a}$ -GK and  $\text{Ca}_v\beta_{2a}$ -SH3-GK shifted the steady-state inactivation curve of  $\text{Ca}_v2.3$ -mediated currents to more positive potentials. A residual current at the end of the pulse also emerges, but it is only a fraction of what is observed with full-length  $\text{Ca}_v\beta_{2a}$  (Fig. 7.5). Half-inactivation voltages ( $V_{1/2}$ ), derived from the fit to a Boltzmann distribution plus the residual component, were similar with  $\text{Ca}_v\beta_{2a}$ -GK,  $\text{Ca}_v\beta_{2a}$ -SH3-GK and full-length  $\text{Ca}_v\beta_{2a}$ , but were significantly more positive than  $\text{Ca}_v2.3$  alone (Fig. 7.5B and Table 7.SII). Overall,  $\text{Ca}_v\beta_{2a}$  derivatives appear less effective than full-length  $\text{Ca}_v\beta_{2a}$  in inhibiting inactivation and may reflect contribution of unoccupied  $\text{Ca}_v2.3$  subunits. Nevertheless, inactivation of  $\text{Ca}_v2.3$  channels bearing the W386S mutation that disrupt binding to  $\text{Ca}_v\beta$  (25), were not modulated by  $\text{Ca}_v\beta_{2a}$  or  $\text{Ca}_v\beta_{2a}$ -GK (SI Fig. 7.S5),

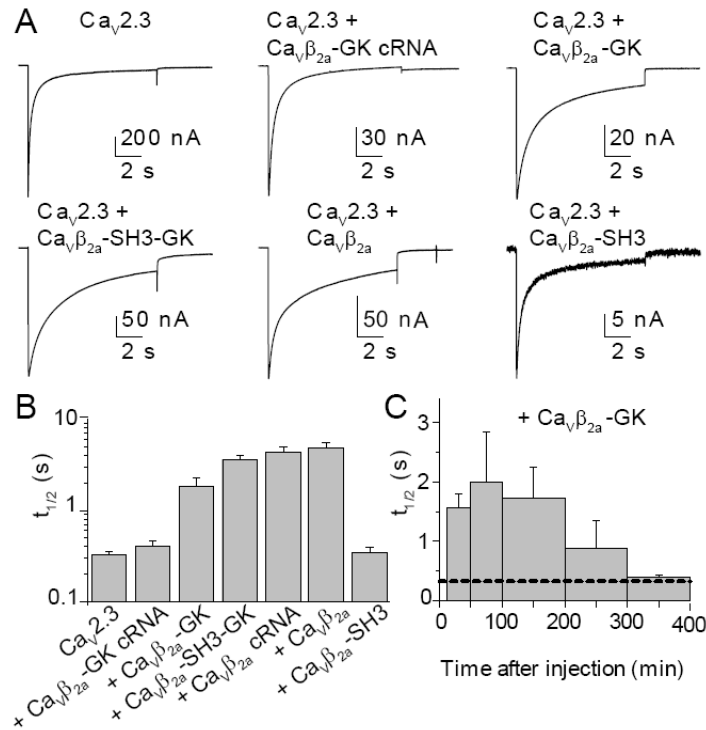


**Fig. 7.4**  $Ca_v\beta$ -GK slows down inactivation of  $Ca_v2.3$ -mediated currents. (A) Representative current traces from oocytes expressing  $Ca_v2.3$  cRNA alone or following injection of the indicated protein during a 10 s pulse to 0 mV from a holding potential of -90 mV. (B) Average decay times to half peak current amplitude ( $t_{1/2}$ ) for the different subunit combinations. For  $Ca_v2.3$  cRNA  $t_{1/2} = 0.33 \pm 0.03$  s (n=26), for  $Ca_v2.3 + Ca_v\beta_{2a}\text{-GK cRNA}$   $t_{1/2} = 0.41 \pm 0.05$  s (n=13), for  $Ca_v2.3 + Ca_v\beta_{2a}\text{-GK}$   $t_{1/2} = 1.85 \pm 0.44$  s (n=13), for  $Ca_v2.3 + Ca_v\beta_{2a}\text{-SH3-GK}$   $t_{1/2} = 3.57 \pm 0.42$  s (n=21), for  $Ca_v2.3 + Ca_v\beta_{2a}$  cRNA  $t_{1/2} = 4.11 \pm 0.65$  s (n=12), for  $Ca_v2.3 + Ca_v\beta_{2a}$   $t_{1/2} = 4.76 \pm 0.70$  s (n=16), and for  $Ca_v2.3 + Ca_v\beta_{2a}\text{-SH3}$   $t_{1/2} = 0.35 \pm 0.04$  s (n=13).  $t_{1/2}$  from  $Ca_v2.3 + Ca_v\beta_{2a}\text{-GK}$ ,  $Ca_v2.3 + Ca_v\beta_{2a}\text{-SH3-GK}$ , and  $Ca_v2.3 + Ca_v\beta_{2a}$  were significantly different from  $t_{1/2}$  measured in oocytes expressing  $Ca_v2.3$  alone (t-test,  $p < 0.01$ ). (C) Time course of inhibition of inactivation by  $Ca_v\beta_{2a}\text{-GK}$ . Each bar corresponds to the average  $t_{1/2}$  measured at different time intervals following protein injection. The first bar includes recordings from 12 to 50 min (n=4), the second from 51 to 100 min (n=6) and every 100 min thereafter (n=7, 2 and 4, respectively). The dashed line corresponds to  $t_{1/2}$  for  $Ca_v2.3$  alone.

indicating that  $\text{Ca}_v\beta_{2a}$ -GK action is AID-dependent and does not involve non-specific binding. As in previous work (25), we also observed that this substitution results in  $\text{Ca}_v2.3$  channels that inactivates more slowly than wild-type channels. Taken together, these findings reveal that the N-terminus of  $\text{Ca}_v\beta_{2a}$  is not mandatory for inhibiting inactivation and predict, due to the highly conserved nature of GK domain, that inhibition of inactivation is a property shared by all GKs in the different  $\text{Ca}_v\beta$  isoforms.

#### **7.4.4 $\text{Ca}_v\beta_{1b}$ -GK resembles $\text{Ca}_v\beta_{2a}$ in inhibiting inactivation of $\text{Ca}_v2.3$ WT channels.**

We studied the effect of a GK module derived from  $\text{Ca}_v\beta_{1b}$ , an isoform that accelerates inactivation and shifts the steady state inactivation curve to more negative potentials when co-expressed as cRNA (12). Refolded  $\text{Ca}_v\beta_{1b}$ -GK injected into oocytes expressing  $\text{Ca}_v2.3$  channels yields currents that inactivate slowly ( $t_{1/2}=4.20\pm 0.87$  s,  $n=16$ , Fig. 7.6A).  $\text{Ca}_v\beta_{1b}$ -GK also shifts the steady-state inactivation curves toward more depolarizing potentials and, like  $\text{Ca}_v\beta_{2a}$ -GK, it induces a residual current (Fig. 7.6B, C). We conclude then that the GK module encompasses the minimal structural requirements to inhibit voltage-dependent inactivation. A question that naturally arises is what determines facilitation of inactivation by full length  $\text{Ca}_v\beta$  proteins.

#### **7.4.5 Full-length $\text{Ca}_v\beta$ proteins switch $\text{Ca}_v2.3$ -inactivation phenotype depending on the time of injection.**

Our finding that the GK module inhibits inactivation implies that full-length proteins that facilitate inactivation must be able to counteract the GK effect. This facilitation has been



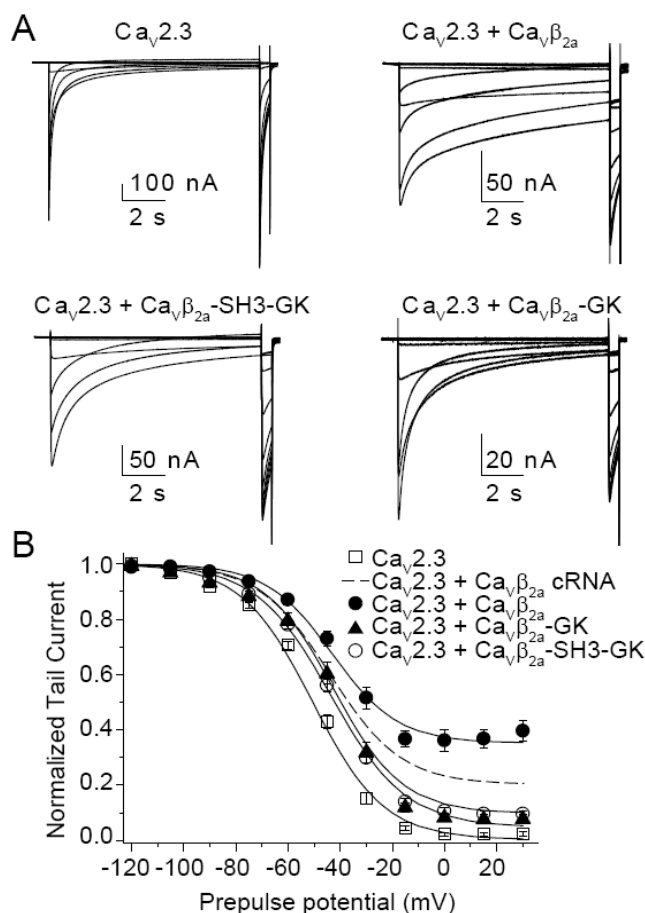


**Fig.7.5  $Ca_v\beta$ -GK shifts mid-point voltage for the steady-state inactivation of  $Ca_v2.3$ -mediated currents.** (A) Representative traces of  $Ca_v2.3$ -mediated currents in the presence of the indicated protein during a steady-state inactivation pulse protocol. This consisted of a 10 s conditioning period to voltages of increasing amplitude, from -120 mV to +30 mV in 15 mV increments, followed by a 0.4 s test pulse to 0 mV. Pulses were delivered once every 50 s from a holding potential of -90 mV. (B) Average steady-state inactivation curves from oocytes expressing  $Ca_v2.3$  alone (n=22) or following injection of full-length  $Ca_v\beta_{2a}$  (n=13),  $Ca_v\beta_{2a}$ -SH3-GK (n=23) or  $Ca_v\beta_{2a}$ -GK (n=15). Continuous lines correspond to Boltzmann distributions plus a non-inactivating current component that best described each set of data. For comparison, the Boltzmann distributions that best described  $Ca_v2.3 + Ca_v\beta_{2a}$  cRNA data (dashed line) are shown.  $V_{1/2}$  from  $Ca_v2.3 + Ca_v\beta_{2a}$ -GK and  $Ca_v2.3 + Ca_v\beta_{2a}$ -SH3-GK were significantly different from  $V_{1/2}$  measured in oocytes expressing  $Ca_v2.3$  alone (t-test,  $p < 0.01$ ) (see SI Table 7.S2 for details).

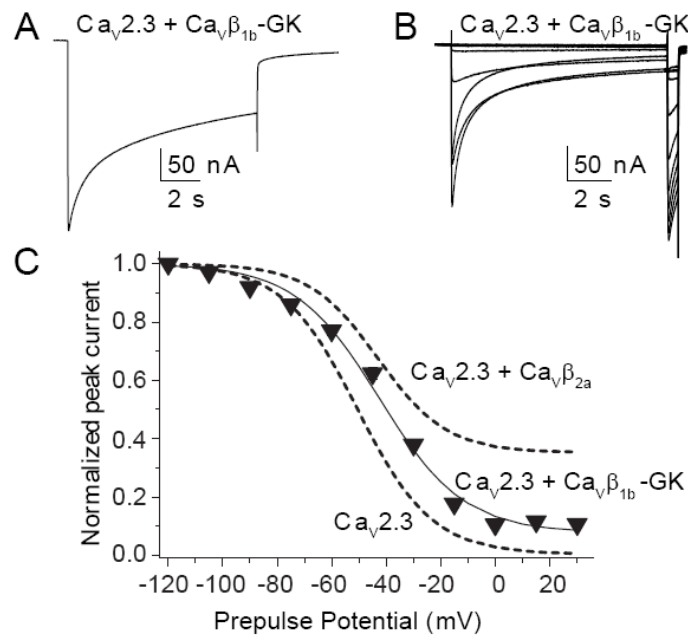


**Fig. 7.6.  $\text{Ca}_v\beta_{1b}\text{-GK}$  slows down inactivation of  $\text{Ca}_v2.3$ -mediated currents and shifts the steady-state inactivation toward more depolarized potentials.** (A) Representative currents traces from a  $\text{Ca}_v2.3$  expressing oocytes injected with  $\text{Ca}_v\beta_{1b}\text{-GK}$  during a 10 s pulse to 0 mV from a holding potential of -90 mV. (B) Current traces evoked with the steady-state inactivation pulse protocol from the same oocytes shown in A. (C) Average steady-state inactivation curve from oocytes expressing  $\text{Ca}_v2.3$  and injected with  $\text{Ca}_v\beta_{1b}\text{-GK}$ -protein ( $n=14$ ). For comparison, the Boltzmann distributions that best described  $\text{Ca}_v2.3$  and  $\text{Ca}_v2.3 + \text{Ca}_v\beta_{2a}$  data from Fig. 5 are shown (dashed lines).  $V_{1/2}$  from  $\text{Ca}_v2.3 + \text{Ca}_v\beta_{1b}\text{-GK}$  was significantly different from  $V_{1/2}$  measured in oocytes expressing  $\text{Ca}_v2.3$  alone (t-test,  $p < 0.01$ ) (see SI Table 7.S2 for details).

documented for  $\text{Ca}_v2.3$  channels co-expressed with cRNA encoding full-length  $\text{Ca}_v\beta_{1b}$  or a palmitoylation deficient mutant of  $\text{Ca}_v\beta_{2a}$  bearing two cysteine-to-serine substitutions at position 3 and 4 ( $\text{Ca}_v\beta_{2a}$ , C3,4S) (12;18).

Here we report that these  $\text{Ca}_v\beta$  constructs injected as proteins into oocytes already expressing  $\text{Ca}_v2.3$  channels (late-injection) slowed the time course of inactivation compared to  $\text{Ca}_v2.3$  alone (Fig. 7.7A, B). Furthermore,  $\text{Ca}_v\beta$  C3,4S shifted the steady-state inactivation curve toward more positive potentials (Fig. 7.7C, D and Table 7.S2). Assuming that these full-length proteins are correctly folded, we reasoned that post-translational modifications requiring longer times than allowed by the experiment are necessary to confer their native phenotype. Therefore, we co-injected these proteins together with the cRNA encoding  $\text{Ca}_v2.3$  subunit (co-injection), and indeed found that inactivation was accelerated (Fig. 7.7A, B) and the steady-state inactivation curve shifted toward more negative potentials (Fig. 7.7C, D and Table 7.S2). These findings indicate that the recombinant proteins are properly folded and that, following post-translational modifications during biogenesis of the channel complex,  $\text{Ca}_v\beta$  can switch the phenotype conferred to  $\text{Ca}_v2.3$  from slow to fast inactivating.

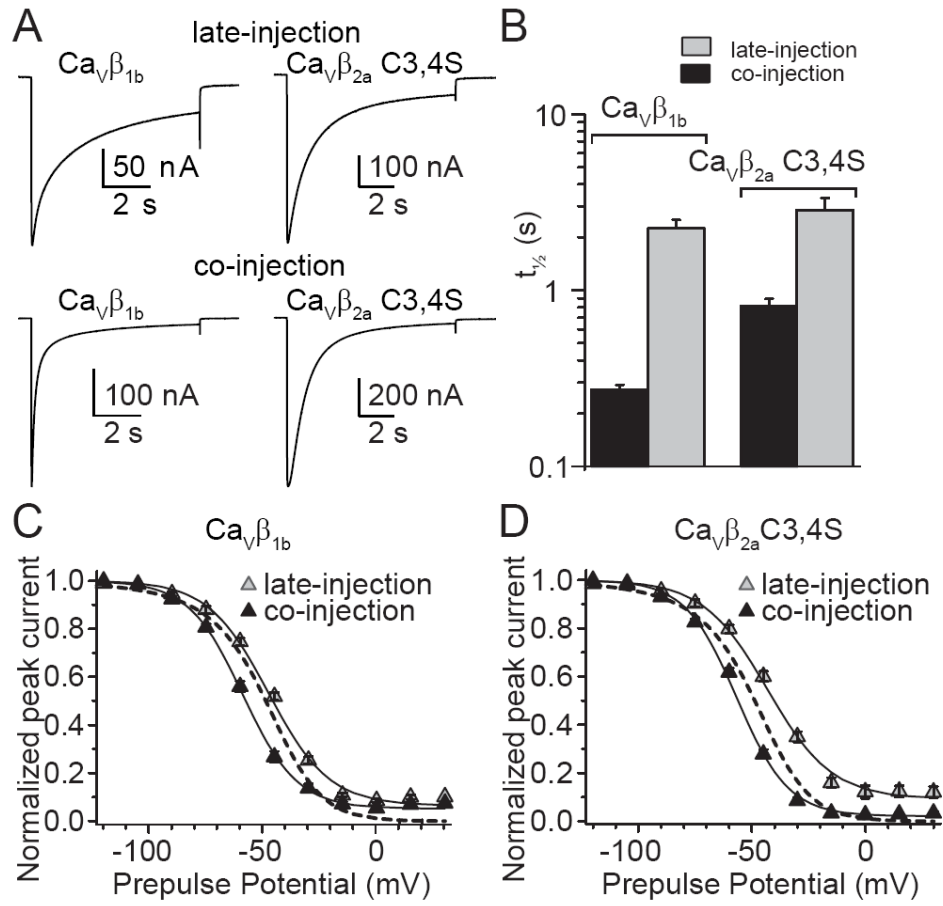


**Fig.7.7.  $\text{Ca}_v2.3$ -inactivation phenotype induced by full-length  $\text{Ca}_v\beta_{1b}$  and  $\text{Ca}_v\beta_{2a}\text{C3,4S}$  depends on the time of injection.** (A) Representative current traces from oocytes expressing  $\text{Ca}_v2.3$  channels with  $\text{Ca}_v\beta_{1b}$  or  $\text{Ca}_v\beta_{2a}\text{C3,4S}$  either injected 2 to 7 hours before recording (late-injection) or co-injected with  $\text{Ca}_v2.3$ -encoding cRNA (co-injection). Currents were evoked by a 10 s pulse to 0 mV from a holding potential of -90 mV. (B) Average  $t_{1/2}$  for both subunit combinations shown in A. Using  $\text{Ca}_v\beta_{1b}$ ,  $t_{1/2}$  for co-injection ( $0.29\pm 0.02$  s,  $n=11$ ) and late-injection ( $2.19\pm 0.25$  s,  $n=14$ ) experiments were significantly different. With  $\text{Ca}_v\beta_{2a}\text{C3,4S}$ ,  $t_{1/2}$  was also significantly different between co-injected ( $0.82\pm 0.08$  s,  $n=13$ ) and late-injection ( $2.86\pm 0.48$  s,  $n=16$ ) experiments (t-test,  $p<0.01$ ). (C) Steady-state inactivation curves from oocytes either co-injected or late injected with  $\text{Ca}_v\beta_{1b}$ . Continuous lines correspond to the Boltzmann distributions that best describe each set of data. For comparison, the Boltzmann distributions that best described  $\text{Ca}_v2.3$  data from Fig. 7.5 are shown (dashed lines). (D) As in C but for  $\text{Ca}_v\beta_{2a}\text{C3,4S}$ . With both proteins, co-injection experiments yield  $V_{1/2}$  significantly more negative than late injection (t-test,  $p<0.01$ ). With  $\text{Ca}_v\beta_{2a}\text{C3,4S}$ ,  $V_{1/2}$  from late and co-injection experiments were significantly different to  $\text{Ca}_v2.3$  alone (t-test,  $p<0.01$ ). With  $\text{Ca}_v\beta_{1b}$ ,  $V_{1/2}$  differs from  $\text{Ca}_v2.3$  alone only in co-injection experiments. With both proteins,  $t_{1/2}$  in late and co-injection experiments were significantly different from each other and from  $\text{Ca}_v2.3$  alone (t-test,  $p<0.01$ ) (see SI Table 7.S2 for details).

## **7.5 Discussion**

Here we demonstrate that the GK module of the voltage-gated calcium channel  $\beta$ -subunit recapitulates key modulatory properties of the full length protein and thus,  $\text{Ca}_v\beta$ -GK emerges as a functional competent domain. This implies that  $\text{Ca}_v\alpha_1$ /GK interaction suffices for channel gating regulation. Moreover, we show that regulation by GK is abolished by mutating the AID sequence consistent with the idea that the AID/GK binding surface is critical for channel modulation (26).

Although, our size-exclusion chromatography and sucrose gradient analysis reveals that purified GK domains forms dimers in solution, the fact that a  $\text{Ca}_v\beta_{2a}$ -GK covalently linked to  $\text{Ca}_v1.2$  pore-forming subunit fully recapitulates activation properties of the channel (Fig. 7.3) proves that the functional unit is a single GK molecule.

Our experiments also demonstrate that  $\text{Ca}_v\beta$ -GK can sustain inhibition of voltage-dependent inactivation of  $\text{Ca}_v2.3$  channels. The prevailing view is that this phenotype is conferred uniquely by  $\text{Ca}_v\beta_{2a}$  because it is anchored to the membrane and constrains the movement of the inactivating particle encoded by loop I-II (15;27). Our results reveal instead that inhibition of inactivation is not a unique feature of  $\text{Ca}_v\beta_{2a}$  but rather an inherent property of the GK module that appears to act as a brake that impairs voltage-dependent inactivation.

A corollary of this conclusion is that facilitation of inactivation by full-length  $\text{Ca}_v\beta$  requires additional structural determinants to antagonize GK brake-like effect. Full length proteins,  $\text{Ca}_v\beta_{1b}$  and  $\text{Ca}_v\beta_{2a}$  C3,4S, were able to counteract GK action only when co-injected with the  $\text{Ca}_v2.3$  encoding cRNA as if these determinants were acquired within a restricted time window during channel biogenesis.

We envision that in cRNA or protein co-injection experiments, the formation the  $\text{Ca}_v\alpha_1$ - $\text{Ca}_v\beta$  complex in early compartments, such as the endoplasmic reticulum, allows chemical or structural modifications necessary for counteracting the brake-like effect of GK. Within this framework, palmitoylation may sequester  $\text{Ca}_v\beta_{2a}$  to other membranous compartments early during biogenesis, hindering the formation of  $\text{Ca}_v\alpha_1$ - $\text{Ca}_v\beta$  complexes in the compartment that is permissive for these structural modifications. Alternatively,  $\text{Ca}_v\beta$  protein may gradually switch to fast inactivation-conferring phenotype over a period of several days independently of its location or association state. In any case, the conclusion is that fast inactivation relies on further post-translational modifications of  $\text{Ca}_v\beta$ , although the precise molecular mechanism remains to be solved.

In clear contrast to the protein injection experiments, we did not observe any modulation when  $\text{Ca}_v\beta$ -SH3-GK or  $\text{Ca}_v\beta$ -GK was co-injected as cRNA. Most likely, variable parts of  $\text{Ca}_v\beta$  are important for either efficient translation or stability of the protein in the oocyte cytoplasm. Indeed, modulation of inactivation by  $\text{Ca}_v\beta_{2a}$ -GK, injected as protein, is rather transient compared to the full-length protein, indicating a reduced lifetime. This may

explain why previous attempts, either by co-expressing or co-injecting the protein more than 24 hours prior to the recordings, yield seemingly contradictory results (7-11). Although, the time course of  $\text{Ca}_v\beta_{2a}$ -GK effect on  $\text{Ca}_v1.2$  activation could not be determined, linking GK to  $\text{Ca}_v1.2$  proved to be an effective strategy to stabilize this module and increase its potency. So far, we have been unable to express a concatamer of  $\text{Ca}_v2.3$  with either the full-length  $\text{Ca}_v\beta$  or the GK domain.

As new protein partners are being discovered, the functional role of  $\text{Ca}_v\beta$  is expanding rapidly (28;29). We recently found that the SH3 module of  $\text{Ca}_v\beta$  binds to the endocytotic protein dynamin (24) and now we report that the GK module regulates calcium channel function. Together these findings introduce a new perspective of  $\text{Ca}_v\beta$ . Calcium entry through VGCCs upon membrane depolarization ensues a transient change in intracellular calcium concentration that regulates diverse cellular functions.

Integration of these different cellular processes must be tightly coordinated in living cells and the domain architecture of  $\text{Ca}_v\beta$  with two functionally independent modules appears particularly well suited to orchestrate calcium signaling. We suggest that while GK regulates calcium entrance, the SH3 domain links channel activity to other cellular processes by binding to additional proteins.



## **ACKNOWLEDGMENTS**

We thank Christoph Fahlke and David Naranjo for insightful discussion and Andreas Pich for the mass spectrometry. This work was supported by grants from the Deutsche Forschung Gemeinschaft (DFG) (FOR 450) to PH, Anillo de Ciencia y Tecnologia (ACT-46) to AN and the German-Chilean Scientific Cooperation Program DFG-CONICYT 2008 to PH and AN.

## **7.6 References**

1. Catterall, W. A. (2000) Structure and regulation of voltage-gated  $\text{Ca}^{2+}$  channels, *Annu. Rev. Cell Dev. Biol.* 16, 521-555.
2. Pragnell, M., De Waard, M., Mori, M., Tanabe, T., Snutch, T. P., and Campbell, K. P. (1994) Calcium channel  $\beta$ -subunit binds to a conserved motif in the I-II cytoplasmic linker of the  $\alpha_1$ -subunit., *Nature* 368, 67-70.
3. Harry, J. B., Kobrinsky, E., Abernethy, D. R., and Soldatov, N. M. (2004) New short splice variants of the human cardiac Cavbeta2 subunit: redefining the major functional motifs implemented in modulation of the Cav1.2 channel, *J Biol Chem* 279, 46367-46372.
4. Opatowsky, Y., Chen, C. C., Campbell, K. P., and Hirsch, J. A. (2004) Structural analysis of the voltage-dependent calcium channel beta subunit functional core and its complex with the alpha 1 interaction domain, *Neuron* 42, 387-399.
5. Chen, Y. H., Li, M. H., Zhang, Y., He, L. L., Yamada, Y., Fitzmaurice, A., Shen, Y., Zhang, H., Tong, L., and Yang, J. (2004) Structural basis of the alpha1-beta subunit interaction of voltage-gated  $\text{Ca}^{2+}$  channels, *Nature* 429, 675-680.
6. Van Petegem F., Clark, K. A., Chatelain, F. C., and Minor, D. L., Jr. (2004) Structure of a complex between a voltage-gated calcium channel beta-subunit and an alpha-subunit domain, *Nature* 429, 671-675.

7. Maltez, J. M., Nunziato, D. A., Kim, J., and Pitt, G. S. (2005) Essential Ca(V) $\beta$  modulatory properties are AID-independent, *Nat. Struct. Mol. Biol.* 12, 372-377.
8. Takahashi, S. X., Miriyala, J., and Colecraft, H. M. (2004) Membrane-associated guanylate kinase-like properties of beta-subunits required for modulation of voltage-dependent Ca<sup>2+</sup> channels, *Proc. Natl. Acad. Sci. U. S. A* 101, 7193-7198.
9. He, L. L., Zhang, Y., Chen, Y. H., Yamada, Y., and Yang, J. (2007) Functional modularity of the beta-subunit of voltage-gated Ca<sup>2+</sup> channels, *Biophys. J* 93, 834-845.
10. McGee, A. W., Nunziato, D. A., Maltez, J. M., Prehoda, K. E., Pitt, G. S., and Bredt, D. S. (2004) Calcium channel function regulated by the SH3-GK module in beta subunits, *Neuron* 42, 89-99.
11. Richards, M. W., Leroy, J., Pratt, W. S., and Dolphin, A. C. (2007) The HOOK-Domain Between the SH3- and the GK-Domains of Ca<sub>v</sub> $\beta$  Subunits Contains Key Determinants Controlling Calcium Channel Inactivation, *Channels* 1, 92-101.
12. Olcese, R., Qin, N., Schneider, T., Neely, A., Wei, X., Stefani, E., and Birnbaumer, L. (1994) The amino termini of calcium channel  $\beta$  subunits set rates of inactivation independently of their effect on activation., *Neuron* 13, 1433-1438.
13. Qin, N., Olcese, R., Zhou, J., Cabello, O. A., Birnbaumer, L., and Stefani, E. (1996) Identification of a second region of the beta-subunit involved in regulation of calcium channel inactivation, *Am. J Physiol* 271, C1539-C1545.

14. Sokolov, S., Weiss, R. G., Timin, E. N., and Hering, S. (2000) Modulation of slow inactivation in class A Ca<sup>2+</sup> channels by beta- subunits, *J. Physiol. (Lond. )* 527 Pt 3, 445-454.
15. Restituito, S., Cens, T., Barrere, C., Geib, S., Galas, S., De Waard, M., and Charnet, P. (2000) The [beta]2a subunit is a molecular groom for the Ca<sup>2+</sup> channel inactivation gate, *J. Neurosci.* 20, 9046-9052.
16. Hering, S., Berjukow, S., Sokolov, S., Marksteiner, R., Weiss, R. G., Kraus, R., and Timin, E. N. (2000) Molecular determinants of inactivation in voltage-gated Ca<sup>2+</sup> channels, *J Physiol* 528 Pt 2, 237-249.
17. Jones, L. P., Wei, S. K., and Yue, D. T. (1998) Mechanism of auxiliary subunit modulation of neuronal alpha1E calcium channels, *J Gen. Physiol* 112, 125-143.
18. Qin, N., Platano, D., Olcese, R., Costantin, J. L., Stefani, E., and Birnbaumer, L. (1998) Unique regulatory properties of the type 2a Ca<sup>2+</sup> channel beta subunit caused by palmitoylation, *Proc. Natl. Acad. Sci. USA* 95, 4690-4695.
19. Chien, A. J., Carr, K. M., Shirokov, R. E., Rios, E., and Hosey, M. M. (1996) Identification of palmitoylation sites within the L-type calcium channel beta2a subunit and effects on channel function, *J. Biol. Chem.* 271, 26465-26468.
20. Hurley, J. H., Cahill, A. L., Currie, K. P., and Fox, A. P. (2000) The role of dynamic palmitoylation in Ca<sup>2+</sup> channel inactivation, *Proc. Natl. Acad. Sci. USA* 97, 9293-9298.

21. Neely, A., Wei, X., Olcese, R., Birnbaumer, L., and Stefani, E. (1993) Potentiation by the  $\beta$  subunit of the ratio of the ionic current to the charge movement in the cardiac calcium channel, *Science* 262, 575-578.
22. Hidalgo, P., Gonzalez-Gutierrez, G., Garcia-Olivares, J., and Neely, A. (2006) The alpha 1-beta subunit interaction that modulates calcium channel activity is reversible and requires a competent alpha -interaction domain, *J. Biol. Chem.* 281, 24104-24110.
23. Dalton, S., Takahashi, S. X., Miriyala, J., and Colecraft, H. M. (2005) A single  $\text{Ca}_v\beta$  can reconstitute both trafficking and macroscopic conductance of voltage-dependent calcium channels, *J. Physiol* 567, 757-769.
24. Gonzalez-Gutierrez, G., Miranda-Laferte, E., Neely, A., and Hidalgo, P. (2007) The Src Homology 3 Domain of the beta-Subunit of Voltage-gated Calcium Channels Promotes Endocytosis via Dynamin Interaction, *J Biol Chem* 282, 2156-2162.
25. Berrou, L., Klein, H., Bernatchez, G., and Parent, L. (2002) A specific tryptophan in the I-II linker is a key determinant of beta-subunit binding and modulation in  $\text{Ca}_v2.3$  calcium channels, *Biophys. J.* 2002. Sep. ;83. (3):1429. -42. 83, 1429-1442.
26. Van Petegem F., Duderstadt, K. E., Clark, K. A., Wang, M., and Minor, D. L., Jr. (2008) Alanine-scanning mutagenesis defines a conserved energetic hotspot in the

- Ca<sub>v</sub> $\alpha_1$  AID-CaV $\beta$  interaction site that is critical for channel modulation, *Structure*. 16, 280-294.
27. Berrou, L., Bernatchez, G., and Parent, L. (2001) Molecular determinants of inactivation within the I-II linker of  $\alpha_1E$  (CaV2.3) calcium channels, *Biophys. J.* 80, 215-228.
  28. Hidalgo, P. and Neely, A. (2007) Multiplicity of protein interactions and functions of the voltage-gated calcium channel  $\beta$ -subunit, *Cell Calcium* 42, 389-396.
  29. Zou, S., Jha, S., Kim, E. Y., and Dryer, S. E. (2008) The  $\beta_1$  subunit of L-type voltage-gated Ca<sup>2+</sup> channels independently binds to and inhibits the gating of large-conductance Ca<sup>2+</sup>-activated K<sup>+</sup> channels, *Mol. Pharmacol.* 73, 369-378.
  30. Neely, A., Garcia-Olivares, J., Voswinkel, S., Horstkott, H., and Hidalgo, P. (2004) Folding of active calcium channel  $\beta(1b)$  -subunit by size-exclusion chromatography and its role on channel function, *J. Biol. Chem.* 279, 21689-21694.
  31. Wei, X., Neely, A., Olcese, R., Lang, W., Stefani, E., and Birnbaumer, L. (1996) Increase in Ca<sup>2+</sup> channel expression by deletions at the amino terminus of the cardiac  $\alpha_1C$  subunit, *Receptors Channels*. 4, 205-215.

## **7.7 Supplemental Data**

### **7.SI Materials and Methods**

**Sucrose Density Gradient Centrifugation.** Sucrose gradient analysis on purified proteins was performed as previously described (1). Purified  $\text{Ca}_v\beta_{2a}$ -GK and  $\text{Ca}_v\beta_{1b}$ -GK alone or together with a protein marker were fractionated on a linear sucrose gradient (0-15% in Buffer A). Gradients were generated by a gradient mixer to a final volume of 4 ml, the proteins were layered on top of separate gradients and centrifuged in a Beckman SW-41Ti rotor at 100,000 g for 16 h at 4°C. After sedimentation, individual gradients were fractionated bottom-to-top by drop-wise collection into 14 to 16 tubes and all fractions were analyzed by SDS-PAGE and western blot. All sucrose gradients were repeated at least twice.

**Western Blot Analysis.** Aliquots from the different sucrose gradient fractions were resolved on a reducing SDS-PAGE and the gels were electroblotted onto nitrocellulose membrane Hybond-ECL<sup>TM</sup>, GE Healthcare Life Science) using sodium carbonate buffer, pH 9.9. After blocking with 3% BSA, the membrane was incubated with either anti-Penta-His antibody (Qiagen). Secondary horseradish peroxidase (HRP)-coupled rabbit anti-mouse IgG antibody (Pierce) was used for detection of immune complex by enhanced chemiluminescence (Super ELISA femto maximum sensitivity substrate, Pierce) using a GeneGnome Syngene Bioimaging System.

**Electrophysiological Recording.** Electrophysiological Recordings were performed four to six days after cRNA injection and two to seven hours after protein injection (50 nl of the protein stock solution) using the cut-open oocytes technique (2) with a CA-1B amplifier (Dagan Corp., Minneapolis MN USA) as described (3). The external solution contained in mM, 10  $Ba^{2+}$ , 96 n-Methylglucamine and 10 HEPES, pH 7.0 and the internal solution 120 n-Methylglucamine, 10 EGTA and 10 HEPES, pH 7.0. For a better control of calcium-activated chloride currents EGTA was replaced by BAPTA in the internal solution when recording oocytes expressing the  $Ca_v2.3$  subunit. Data acquisition and analysis were performed using the pCLAMP system and software (Axon Instruments Inc., Foster City CA USA). Currents were filtered at 2 kHz and digitized at 10 kHz. Linear components were eliminated by P/-4 prepulse protocol (4).



Coomassie blue

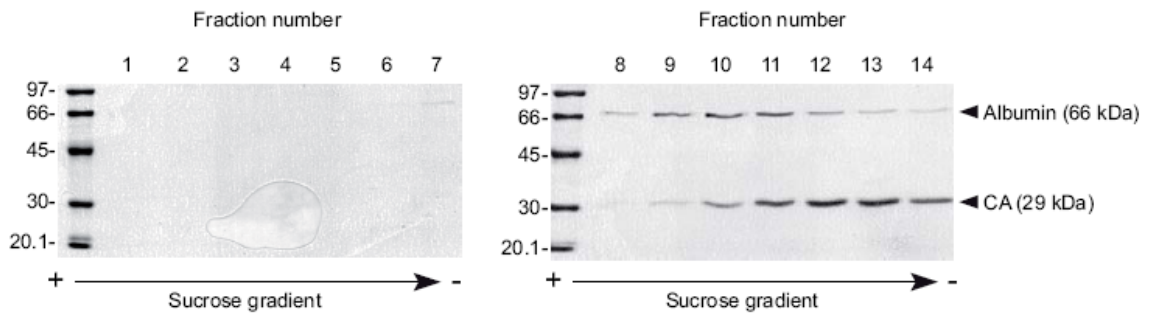


**Fig 7.S1 Sucrose Gradient analysis of molecular standards.** Two molecular mass standards, albumin (66 kDa, Sigma) and carbonic anhydrase, CA; (29 kDa, Sigma) were loaded onto a 0-15% linear sucrose gradient. After sedimentation, the gradient was fractionated bottom-to-top into 14 fractions and each fraction was resolved onto SDS-PAGE to monitor the protein distribution profile. Albumin and CA distributed throughout the second half of the gradient, with CA appearing at later fractions as expected from its reduced molecular mass

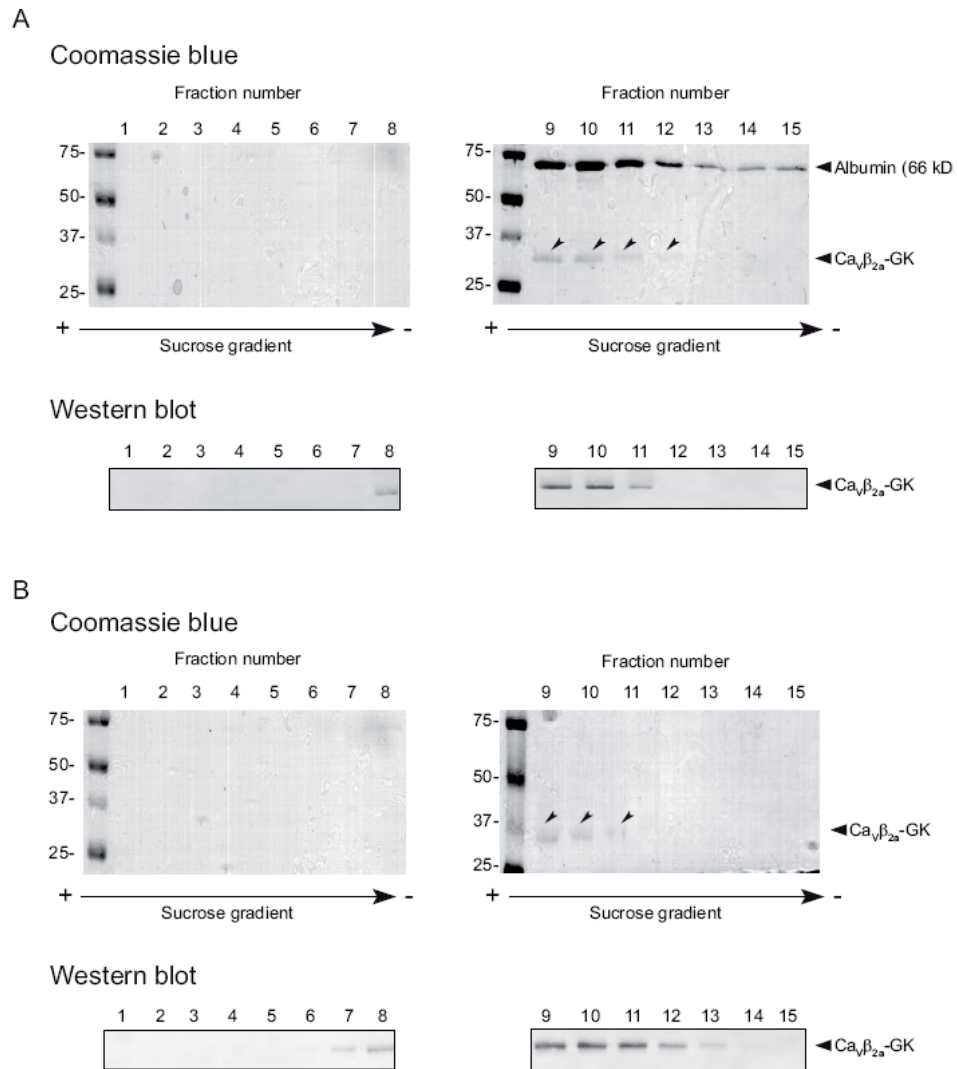


**Fig 7.S2 Sucrose Gradient analysis of  $\text{Ca}_v\beta_{2a}$ -GK.** Two separated 0-15% linear sucrose gradients were loaded with  $\text{Ca}_v\beta_{2a}$ -GK either together with albumin (A) or alone (B). After sedimentation, the gradient was fractionated bottom-to-top into 15 fractions and each fraction resolved onto SDS-PAGE. The presence of albumin did not alter the sedimentation profile of  $\text{Ca}_v\beta_{2a}$ -GK.  $\text{Ca}_v\beta_{2a}$ -GK with a predicted molecular mass of 28.6 kDa, co-distributes with albumin, indicating the presence of dimers.

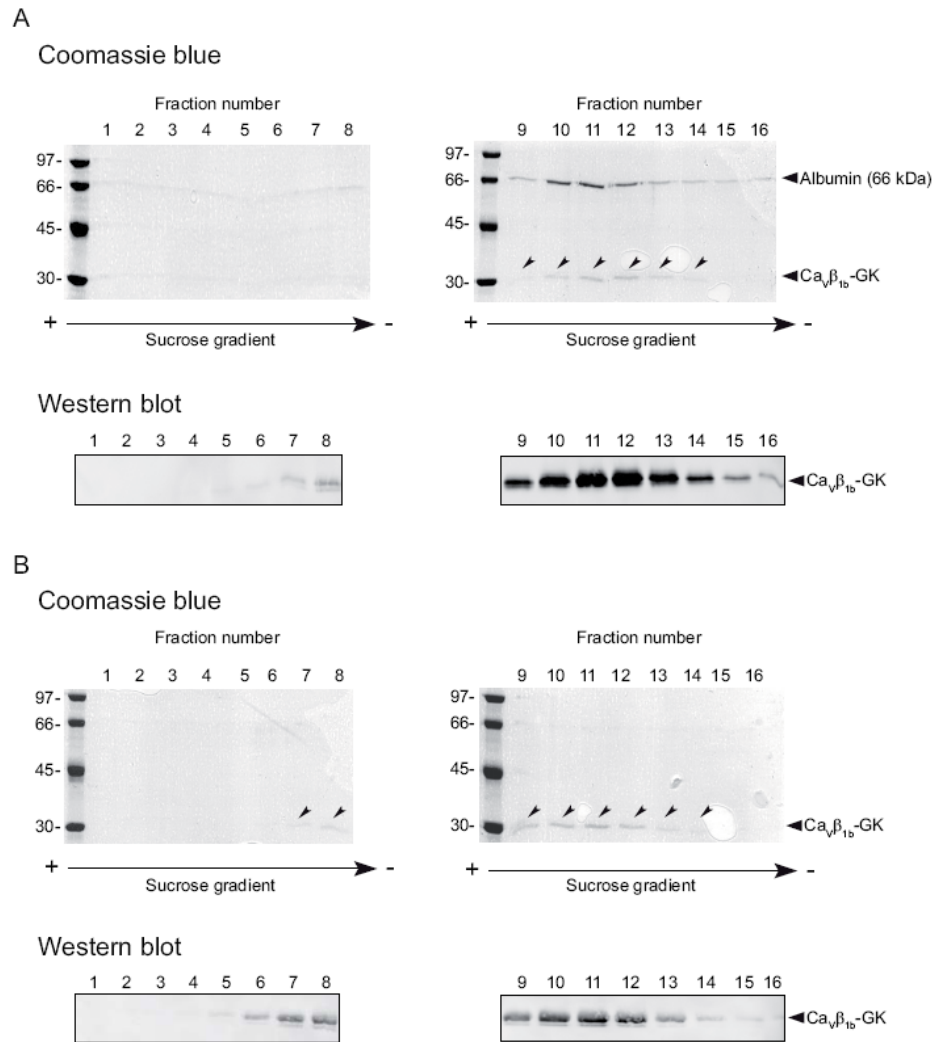


**Fig 7.S3 Sucrose Gradient analysis of Ca<sub>v</sub>β<sub>1b</sub>-GK.** Two separated 0-15% linear sucrose gradients were loaded with Ca<sub>v</sub>β<sub>1b</sub>-GK either together with albumin (A) or alone (B). After sedimentation, the gradient was fractionated bottom-to-top into 16 fractions and each fraction resolved onto SDS-PAGE. The presence of albumin did not alter the sedimentation profile of Ca<sub>v</sub>β<sub>1b</sub>-GK. Ca<sub>v</sub>β<sub>1b</sub>-GK distributes along with albumin and CA (see Fig 7.S1), indicating the presence of dimers and monomers.

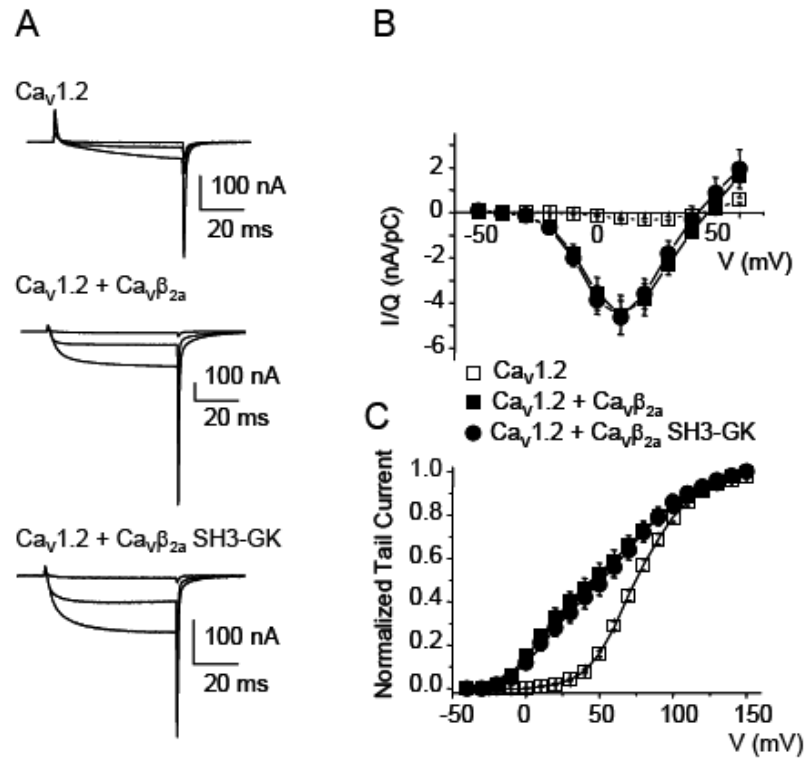


**Fig 7.S4** Ca<sub>v</sub>β<sub>2a</sub>-SH3-GK is as effective as full length Ca<sub>v</sub>β<sub>2a</sub> in modulating activation of Ca<sub>v</sub>1.2-mediated currents. (A) Representative gating and ionic currents traces from oocytes expressing Ca<sub>v</sub>1.2 cRNA alone and following injection of Ca<sub>v</sub>β<sub>2a</sub> or Cavβ<sub>2a</sub>-SH3-GK during a 60 ms pulse to -30,0 and +30mV from a holding potential of -80mV. (B) Current-voltage plot normalized by charge movement (I/Q) from oocytes expressing the different subunit combination shown in A. Peak I/Q for oocytes expressing Ca<sub>v</sub>1.2 alone was  $0.30 \pm 0.06$  nA/pC (n=15), for Ca<sub>v</sub>1.2 + Cavβ<sub>2a</sub>-SH3-GK  $4.6 \pm 0.7$  nA/pC (n=17) and for Ca<sub>v</sub>1.2 + Cavβ<sub>2a</sub>  $4.5 \pm 0.9$  nA/pC (n=18). (C) Normalized tail currents from oocytes expressing the different subunit combinations shown in B. Continuous lines correspond to the fit of the sum of the two Boltzmann distributions that best described each set of data (for details, see SI Table 7.S1).

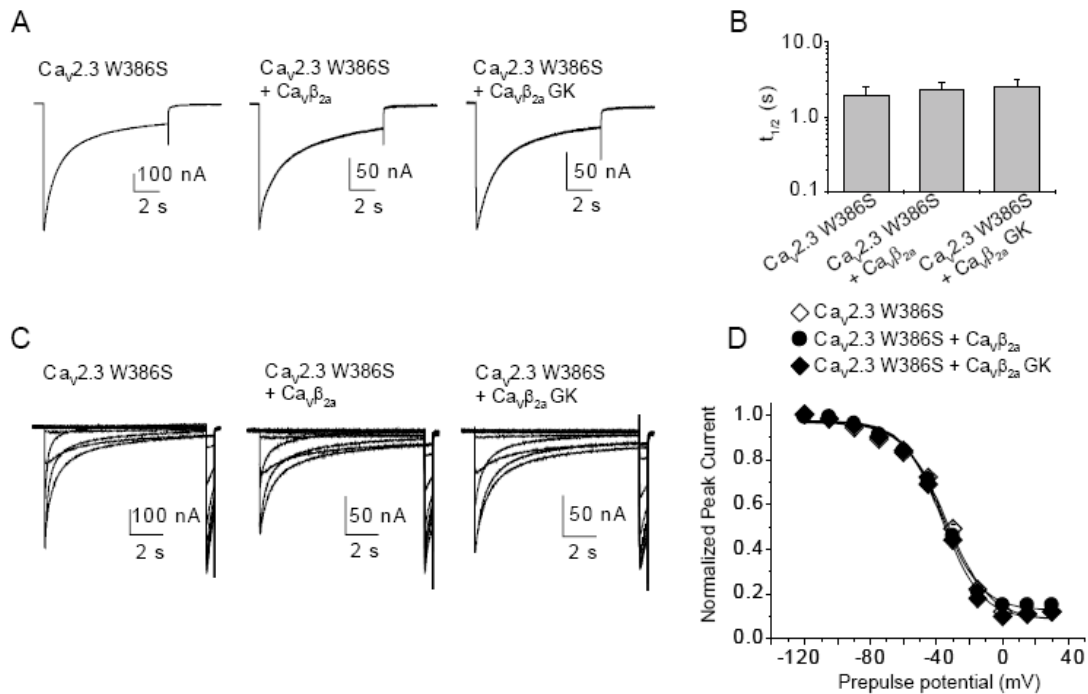


**Fig 7.S5 Mutation of a fully conserved tryptophan within the AID sequence yields Ca<sub>v</sub>2.3 channels insensitive to full length Ca<sub>v</sub>β<sub>2a</sub> and refolded Ca<sub>v</sub>β<sub>2a</sub>-GK.** (A) Representative current traces from oocytes expressing Ca<sub>v</sub>2.3 W386S cRNA alone or following injection of either full length Ca<sub>v</sub>β<sub>2a</sub> or Ca<sub>v</sub>β<sub>2a</sub>-GK during a 10 s pulse to 0 mV from a holding potential of -90 mV. (B) Average decay times to half peak current amplitude (t<sub>1/2</sub>) for the different subunit combinations shown in A. (C) Representative current traces evoked with the steady-state inactivation pulse protocol consisting of a 10 s conditioning period to voltages of increasing amplitude, from -120 mV to +30 mV in 15 mV increment, followed by a 0.4 s test pulse to 0 mV. (D) Average steady state inactivation curves from oocytes expressing Ca<sub>v</sub>2.3 W386S cRNA alone or following injection of either full length Ca<sub>v</sub>β<sub>2a</sub> or Ca<sub>v</sub>β<sub>2a</sub>-GK. Continuous lines correspond the fit to Boltzmann distributions plus a non-inactivating current component that best describes each set of data (for details, see SI Table 7.S2).

	Max I/Q (nA/pC)		G <sub>1</sub> fraction	V <sub>1</sub> (mV)	Z <sub>1</sub>	V <sub>2</sub> (mV)	Z <sub>2</sub>	N
	Mean ± SEM	N						
Ca <sub>v</sub> 1.2	0.30 ± 0.06	15	0.64 ± 0.02	68.5 ± 2.9	2.0 ± 0.1	97.3 ± 2.6	1.5 ± 0.1	16
Ca <sub>v</sub> 1.2 + Ca <sub>v</sub> β <sub>2a</sub>	4.51 ± 0.85*	18	0.47 ± 0.04*	15.9 ± 3.5*	2.1 ± 0.2	77.5 ± 4.8*	1.4 ± 0.1	11
Ca <sub>v</sub> 1.2 + Ca <sub>v</sub> β <sub>2a</sub> -SH3-GK	4.63 ± 0.75*	17	0.47 ± 0.08*	19.0 ± 5.8*	2.1 ± 0.4	80.4 ± 6.3*	1.5 ± 0.1	6
Ca <sub>v</sub> 1.2 - Ca <sub>v</sub> β <sub>2a</sub> concatamer	2.44 ± 0.44*	17	0.58 ± 0.02	38.4 ± 4.8*	1.3 ± 0.1*	97.1 ± 2.9	1.5 ± 0.1	17
Ca <sub>v</sub> 1.2 - Ca <sub>v</sub> β <sub>2a</sub> -GK concatamer	2.71 ± 0.52*	17	0.58 ± 0.01	48.6 ± 5.8*	1.3 ± 0.1*	90.1 ± 4.5	1.5 ± 0.0	15
Ca <sub>v</sub> 1.2 W470S - Ca <sub>v</sub> β <sub>2a</sub> -GK concatamer	0.35 ± 0.03†	17	0.60 ± 0.01	65.9 ± 1.1†	2.1 ± 0.1†	95.8 ± 1.6	1.5 ± 0.0	17

**Table 7.S1. Parameters defining the sum of two Boltzmann distributions that best fitted normalized tail currents for the indicated Ca<sub>v</sub>1.2 subunit combinations.** Mean ± SEM of maximal current normalized by total charge movement (I/Q) and parameters defining the best fit to the sum of the two Boltzmann's distributions that describe the activation curve. Peak tail currents (I<sub>tail</sub>) were measured during deactivation at -40 mV following a 65 ms pulse of increasing voltage, normalized and plotted versus to pre-pulse potential to yield the GV curve that was then fitted to:

$$I_{\text{tail}}(V) = \left( \frac{I_{\text{MAX1}}}{1 + \exp\left[\frac{(V_1 - V) \cdot z_1 F}{RT}\right]} + \frac{I_{\text{MAX2}}}{1 + \exp\left[\frac{(V_2 - V) \cdot z_2 F}{RT}\right]} \right)$$

Where R is Universal Gas Constant, F the Faraday's Constant, T is temperature, V is the voltage preceding repolarization to -40mV, I<sub>MAX1</sub> and I<sub>MAX2</sub> the contribution of each Boltzmann distribution, characterized by slope factors z<sub>1</sub> and z<sub>2</sub> and half activation potential V<sub>1</sub> and V<sub>2</sub>. Normalized conductances were obtained by I<sub>tail</sub> / ( I<sub>MAX1</sub> + I<sub>MAX2</sub>) yielding G<sub>1</sub> and G<sub>2</sub> fractions. \* denotes t-test p< 0.01 compared to values measured in oocytes expressing Ca<sub>v</sub>1.2 alone. † denotes t-test p< 0.01 compared to values measured in oocytes expressing Ca<sub>v</sub>1.2-Ca<sub>v</sub>β<sub>2a</sub> concatamer.

*The GK domain of the  $\beta$ -subunit of VGCCs suffices to modulate gating*

	Inactivation Rates		Steady State Inactivation Parameters					
	$t_{1/2}$ (s)		$V_{1/2}$ (mV)		Z		% $I_{res}$	
	Mean $\pm$ SEM	N	Mean $\pm$ SEM	Mean $\pm$ SEM	Mean $\pm$ SEM	Mean $\pm$ SEM	N	
Ca <sub>v</sub> 2.3	0.33 $\pm$ 0.03	26	-48.7 $\pm$ 1.0	-2.2 $\pm$ 0.1	0.6 $\pm$ 0.5		22	
Ca <sub>v</sub> 2.3 + Ca <sub>v</sub> $\beta$ <sub>2a</sub>	4.76 $\pm$ 0.70*	16	-41.3 $\pm$ 1.4*	-2.6 $\pm$ 0.2	35.2 $\pm$ 4.2*		13	
Ca <sub>v</sub> 2.3 + Ca <sub>v</sub> $\beta$ <sub>2a</sub> cRNA	4.11 $\pm$ 0.65*	12	-42.4 $\pm$ 2.2	-2.2 $\pm$ 0.1	19.5 $\pm$ 2.2*,†		12	
Ca <sub>v</sub> 2.3 + Ca <sub>v</sub> $\beta$ <sub>2a</sub> -SH3-GK	3.57 $\pm$ 0.42*	21	-44.3 $\pm$ 1.1*	-2.1 $\pm$ 0.0	8.4 $\pm$ 1.2*,†		23	
Ca <sub>v</sub> 2.3 + Ca <sub>v</sub> $\beta$ <sub>2a</sub> -SH3	0.35 $\pm$ 0.04	13	N/A	N/A	N/A		N/A	
Ca <sub>v</sub> 2.3 + Ca <sub>v</sub> $\beta$ <sub>2a</sub> GK cRNA	0.41 $\pm$ 0.05	13	-45.9 $\pm$ 1.6	-2.6 $\pm$ 0.1	1.4 $\pm$ 1.8†		12	
Ca <sub>v</sub> 2.3 + Ca <sub>v</sub> $\beta$ <sub>2a</sub> -GK	1.85 $\pm$ 0.44*,†	13	-41.5 $\pm$ 1.8*	-2.3 $\pm$ 0.1	6.3 $\pm$ 1.6*,†		15	
Ca <sub>v</sub> 2.3 + Ca <sub>v</sub> $\beta$ <sub>1b</sub> -GK	4.20 $\pm$ 0.87*	16	-40.9 $\pm$ 1.4*	-1.8 $\pm$ 0.1*,†	8.1 $\pm$ 1.2*,†		14	
Ca <sub>v</sub> 2.3 + Ca <sub>v</sub> $\beta$ <sub>1b</sub> cRNA	0.29 $\pm$ 0.02	11	-59.1 $\pm$ 1.2*	-2.7 $\pm$ 0.1*	0.7 $\pm$ 0.4		11	
Ca <sub>v</sub> 2.3 + Ca <sub>v</sub> $\beta$ <sub>1b</sub> late-injection	2.19 $\pm$ 0.25*,#	18	-46.8 $\pm$ 0.9#	-2.1 $\pm$ 0.1#	7.0 $\pm$ 0.8*,#		18	
Ca <sub>v</sub> 2.3 + Ca <sub>v</sub> $\beta$ <sub>1b</sub> co-injection	0.27 $\pm$ 0.02*	14	-59.3 $\pm$ 0.8*	-2.2 $\pm$ 0.1#	5.1 $\pm$ 0.7*,#		14	
Ca <sub>v</sub> 2.3 + Ca <sub>v</sub> $\beta$ <sub>2a</sub> C3,4S late-injection	2.86 $\pm$ 0.48*,#	16	-42.9 $\pm$ 1.6*,#	-2.1 $\pm$ 0.1#	10.5 $\pm$ 2.4*,#		12	
Ca <sub>v</sub> 2.3 + Ca <sub>v</sub> $\beta$ <sub>2a</sub> C3,4S co-injection	0.80 $\pm$ 0.08*,#	13	-55.7 $\pm$ 0.8*	-2.4 $\pm$ 0.1#	2.1 $\pm$ 0.7		14	
Ca <sub>v</sub> 2.3 W386S	1.92 $\pm$ 0.54*	19	-34.3 $\pm$ 1.1*	-2.0 $\pm$ 0.1	8.5 $\pm$ 1.5		17	
Ca <sub>v</sub> 2.3 W386S + Ca <sub>v</sub> $\beta$ <sub>2a</sub>	2.35 $\pm$ 0.50*	17	-36.8 $\pm$ 1.0*	-2.1 $\pm$ 0.1	7.1 $\pm$ 2.1		15	
Ca <sub>v</sub> 2.3 W386S + Ca <sub>v</sub> $\beta$ <sub>2a</sub> -GK	2.48 $\pm$ 0.66*	15	-36.8 $\pm$ 1.5*	-2.2 $\pm$ 0.1	13.2 $\pm$ 3.4		14	

**Table 7.S2 Average  $t_{1/2}$  and parameters defining the Boltzmann distribution and the percentage of non-inactivating current component that best fitted steady-state inactivation for the indicated Ca<sub>v</sub>2.3 subunit combinations.** Steady state parameters were obtained by plotting the peak currents in a test pulse to 0 mV after a pre-pulse to different voltages and fitting to the follow equation:

$$I = I_{res} + \frac{(I_{max} - I_{res})}{1 + e^{-\frac{zF}{RT}(V - V_{1/2})}}$$

Where  $I_{max}$  is the current at peak,  $I_{res}$  is the non inactivating current, F is the Faraday's constant, R the Universal constant of gases, T is temperature (298 K), V is the membrane voltage and  $V_{1/2}$  is the voltage where the fraction of channels inactivated and non-inactivated is equal. N/A, not applicable. \* denotes t-test  $p < 0.01$  compared to values measured in oocytes expressing Ca<sub>v</sub>2.3 alone. † denotes t-test  $p < 0.01$  compared to values measured in oocytes expressing Ca<sub>v</sub>1.2 + Ca<sub>v</sub> $\beta$ <sub>2a</sub>. # denotes t-test  $p < 0.01$  compared to values measured in oocytes expressing Ca<sub>v</sub>1.2 + Ca<sub>v</sub> $\beta$ <sub>1b</sub> cRNA.

## **7.SI References**

1. Neely A, Garcia-Olivares J, Voswinkel S, Horstkott H, and Hidalgo P (2004) Folding of active calcium channel beta(1b)-subunit by size exclusion chromatography and its role on channel function. *J. Biol. Chem.* 279:575-578.
2. Tagliatela M, Toro L, Stefani E (1992) Novel voltage clamp to record small fast currents from ion channels expressed in *Xenopus* oocytes. *Biophys J.* 61, 78-82.
3. Hidalgo P, Gonzalez-Gutierrez G, Garcia-Olivares J, Neely A (2006) The  $\alpha_1$ - $\beta$  subunit interaction that modulates calcium channel activity is reversible and requires a competent  $\alpha$ -interaction domain. *J. Biol. Chem.* 281: 24104-24110.
4. Neely A, Wei X, Olcese R, Birnbaumer L, Stefani E (1993) Potentiation by the  $\beta$  subunit of the ratio of the ionic current to the charge movement in the cardiac calcium channel. *Science* 262:575-578.



**8. Dimerization of the Src homology 3 domain of the voltage-gated calcium channel  $\beta$ -subunit regulates endocytosis**

Erick Miranda-Laferte<sup>1</sup>, Giovanni Gonzalez-Gutierrez<sup>1</sup>, Silke Schmidt<sup>1</sup>, Alan Neely<sup>2</sup> and Patricia Hidalgo<sup>1</sup>

<sup>1</sup>Institut für Neurophysiologie, Medizinische Hochschule Hannover, 30625 Hannover, Germany

<sup>2</sup>Centro de Neurociencia de Valparaíso, Universidad de Valparaíso 2349400 Chile

Manuscript to be submitted to *EMBO Reports*

## **8.1 Abstract**

The auxiliary  $\beta$ -subunit of voltage-gated calcium channels ( $\text{Ca}_v\beta$ ) is traditionally known as a potent regulator of channel function. However it also participates in other cellular functions including endocytosis.  $\text{Ca}_v\beta$  encompasses an Src homology 3 ( $\text{Ca}_v\beta$ -SH3) and a guanylate kinase ( $\text{Ca}_v\beta$ -GK) domain. While  $\text{Ca}_v\beta$ -GK associates to the  $\alpha_1$  pore-forming subunit and modulates channel function,  $\text{Ca}_v\beta$ -SH3 interacts with dynamin and promotes endocytosis. The molecular mechanism by which  $\text{Ca}_v\beta$ -SH3 supports endocytosis is completely unknown. Here, we show that substitution of the single cysteine residue in  $\text{Ca}_v\beta_{2a}$ -SH3 by alanine ( $\text{Ca}_v\beta_{2a}$ -SH3 C113A) abolishes dimerization indicating that formation of dimers occurs through a single cysteine bridge.  $\text{Ca}_v\beta_{2a}$ -SH3 C113A still binds to dynamin but does not internalize  $\text{Ca}_v1.2$  channels expressed in *Xenopus* oocytes. Endocytosis is restored when two  $\text{Ca}_v\beta_{2a}$ -SH3 C113A molecules are covalently linked to form a concatamer. Thus, dimerization appears essential for the endocytic function exhibited by  $\text{Ca}_v\beta_{2a}$ -SH3. Moreover we found that full-length  $\text{Ca}_v\beta$  also dimerizes. We propose that dimerization enables this modular protein to switch from channel regulator to endocytosis activator.

## **8.2 Introduction**

The auxiliary  $\beta$ -subunit of voltage-gated calcium channels ( $\text{Ca}_v\beta$ ) has traditionally been recognized for its role in modulation of high-voltage gated calcium channels (Arikkath and Campbell, 2003; Catterall, 2000; Dolphin, 2003). More recently it has been shown that the same subunit mediates several other cellular processes (for review see, Hidalgo and Neely, 2007), including regulation of insulin secretion (Berggren *et al.*, 2004), gene transcription (Hibino *et al.*, 2003) and endocytosis (Gonzalez-Gutierrez *et al.*, 2007). Crystallographic studies provided the molecular basis for such functional versatility. They identified  $\text{Ca}_v\beta$  as a member of the membrane associated guanylate kinase (MAGUK) family of scaffolding proteins containing two protein-protein interactions modules: an Src homology 3 (SH3) and a guanylate kinase (GK) domain, (Chen *et al.*, 2004; Opatowsky *et al.*, 2004; Van Petegem F. *et al.*, 2004). While modulation of channel activity is achieved by association of the GK domain with the  $\alpha_1$ -interacton domain (AID), a highly conserved site in the  $\alpha_1$  pore-forming subunit ( $\text{Ca}_v\alpha_1$ ), interaction between the SH3 domain and dynamin mediates endocytosis (Gonzalez-Gutierrez *et al.*, 2007; Gonzalez-Gutierrez *et al.*, 2008; Pragnell *et al.*, 1994). Dynamin is a major endocytic protein belonging to the family of large GTPases that besides the GTPase domain encompasses a proline-rich domain that interacts with SH3 domains of various proteins (Gout *et al.*, 1993).  $\text{Ca}_v\beta$ -SH3 appears also to interact within the proline rich domain of dynamin, but the molecular events leading to activation of endocytosis by  $\text{Ca}_v\beta$ -SH3 are completely unexplored (Gonzalez-Gutierrez *et al.*, 2007). It has been proposed that the recruitment of dynamin to clathrin-coated pits in nerve terminals is driven by heterodimerization of amphiphysin (Wigge *et al.*, 1997). Amphiphysin is an SH3-containing protein that expresses at high levels in mammalian brain and binds dynamin through its SH3 domain (Owen *et al.*, 1998; Wigge and

McMahon, 1998). Here we investigate a potential role of  $\text{Ca}_v\beta$ -SH3 dimerization in promoting endocytosis. Using blue-native polyacrylamide gel electrophoresis (BN-PAGE) we found that  $\text{Ca}_v\beta$ -SH3 forms dimers *in vitro* through a single disulfide bond. Substitution of the unique cysteine residue by alanine not only abolishes dimerization but also endocytosis promoted by  $\text{Ca}_v\beta$ -SH3 though interaction with dynamin is preserved. The endocytic function of this domain is rescued by covalently linking two molecules of  $\text{Ca}_v\beta$ -SH3 dimerization-deficient mutant. Our findings demonstrate that dimerization of  $\text{Ca}_v\beta$ -SH3 is a crucial step to mediate endocytosis.

## **8.3 Materials and Methods**

### **8.3.1 cDNA constructs and recombinant proteins.**

Ca<sub>v</sub>1.2 channel construct and dynamin fused to the hematoagglutinin tag (HA) has been described elsewhere (Gonzalez-Gutierrez *et al.*, 2007). Full length Ca<sub>v</sub> $\beta$ <sub>2a</sub> wild type (Swiss-Prot entry:Q8VGC3), wild-type Ca<sub>v</sub> $\beta$ <sub>2a</sub>-SH3 and Ca<sub>v</sub> $\beta$ <sub>2a</sub>-SH3 C113A monomers and concatamers were prepared as described (Gonzalez-Gutierrez *et al.*, 2007;Hidalgo *et al.*, 2006). All protein constructs bear a six histidine tag (His<sub>6</sub>) fused at the N-terminal end of the protein. GST alone and GST fused to Ca<sub>v</sub>1.2 loop I-II (GST- Ca<sub>v</sub>1.2 loop I-II) were expressed in bacteria and purified as described (Hidalgo *et al.*, 2006).

### **8.3.2 Immunoprecipitation.**

Cells (tsA201) were transfected with HA-dynamin expression plasmid and lysed after 24-30 hours transfection. The cell lysate was incubated with anti HA antibody (Roche Applied Sciences) and recombinant Ca<sub>v</sub> $\beta$ <sub>2a</sub>-SH3 protein derivatives for one hour on ice. Protein G beads were added (GE Healthcare Life Sciences) and the mix incubated one additional hour at 4°C. After extensive washes the bound proteins were eluted with SDS-loading buffer, resolved in SDS-PAGE and detected by western blot using anti-His antibody (Qiagen) and chemiluminescence.

### **8.3.3 Pull-down assays.**

Pull down assays using Ca<sub>v</sub> $\beta$ <sub>2a</sub> fused to Strep-tag II<sup>TM</sup> tag (IBA GmbH) as bait and Ca<sub>v</sub> $\beta$ <sub>2a</sub> fused to yellow fluorescence protein (YFP-Ca<sub>v</sub> $\beta$ <sub>2a</sub>) as prey were performed as described (Neely *et al.*, 2004). Strep-Ca<sub>v</sub> $\beta$ <sub>2a</sub> and YFP-Ca<sub>v</sub> $\beta$ <sub>2a</sub> were expressed in

tsA201 cells and the cell extract obtained 24-48 hours after transfection was incubated with Strep-tactin™ (IBA GmbH) beads for one hour at 4°C. The beads were pelleted, washed and bound proteins were eluted with SDS loading buffer and resolved on SDS-PAGE which was later visualized by fluorescence scanning using a Typhoon imager (GE Healthcare Life Sciences).

#### **8.3.4 *Xenopus* Oocytes preparation, injection and electrophysiological recordings.**

*Xenopus laevis* oocytes were prepared, injected and maintained as in previous report (Neely *et al.*, 2004). All capped cRNA were synthesized using the MESSAGE-machine (Ambion, Austin TX, USA), resuspended in 10  $\mu$ l water and stored in 2  $\mu$ l aliquots at  $-80$  °C until use. Electrophysiological recordings on  $Ca_v1.2$  expressing oocytes were performed using the cut-open oocyte technique with a CA-1B amplifier (Dagan Corp., Minneapolis MN USA) as described (Hidalgo *et al.*, 2006). Briefly, recordings were done two to five hours after protein injection (50 nl of the protein stock solution, 1 mg/ml, per oocyte) and five to seven days after cRNA injection. The external solution contained in mM, 10  $Ba^{2+}$ , 96 n-Methylglucamine, and 10 pH 7.0 and the internal solution 120 n-Methylglucamine, 10 EGTA, and 10 HEPES, pH 7.0. Charge movement  $Q_{on}$  was measured by integrating gating current during a step near the reversal potential for the permeant ion (Barium) determined empirically by stepping to several potentials in 2-mV increments (Gonzalez-Gutierrez *et al.*, 2007).

Data acquisition and analysis were performed using the pCLAMP system and software (Axon Instruments Inc., Foster City CA USA). Currents were filtered at 2 kHz and digitized at 10 kHz. Linear components were eliminated by P/-4 prepulse protocol. Currents were filtered at 1 kHz and digitized at 20 kHz.

### **8.3.5 Blue native polyacrylamide gel electrophoresis (BN-PAGE).**

BN-PAGE were done as described (Niepmann and Zheng, 2006). Briefly, proteins were incubated with loading buffer alone or either supplemented with DTT or SDS for 30 minutes at room temperature and resolved in a gradient gel (4-20% of acrylamide) overnight at 4 °C.

## **8.4 Results and Discussion**

### **8.4.1 $\text{Ca}_v\beta_{2a}$ -SH3 dimerizes through a single disulfide bond**

Here, we used BN-PAGE analysis to investigate the oligomeric structure of  $\text{Ca}_v\beta$ -SH3. Purified  $\text{Ca}_v\beta$ -SH3 migrates in BN-PAGE as two bands suggesting the co-existence of two populations with different number of subunits (Fig. 8.1A). Incubation with denaturing agent (SDS) produces no changes in the mobility of both forms. However, dithiothreitol (DTT) leads to the disappearance of the slower migrating band while migration of the faster one remains unchanged. The mobility of the protein in non-denaturing electrophoresis depends on the shape and hence, estimation of the numbers of monomers assembled per complex is not readily calculated from molecular mass standards. To assess the number of monomeric units assembled in each population we engineered a concatameric construct consisting in two  $\text{Ca}_v\beta$ -SH3 molecules covalently linked. This concatamer migrates at approximately the same position as the higher molecular weight band observed in native conditions indicating that this form corresponds to a homodimer and hence the faster migrating band to a monomer. All together, these results show that  $\text{Ca}_v\beta$ -SH3 dimerizes via disulfide bonding. Accordingly, we expressed in bacteria and purified a mutant of  $\text{Ca}_v\beta$ -SH3 carrying a substitution of the single cysteine residue in at position 113 by alanine ( $\text{Ca}_v\beta_{2a}$ -SH3 C113A). This mutant elutes as a monodisperse peak from a size exclusion chromatography indicating a homogenous protein population and migrates as a single band in a blue native gel (Fig. 1B-C). When compared to  $\text{Ca}_v\beta_{2a}$ -SH3 concatamer this single band migrates faster indicating that it corresponds to the monomeric form. Thus, substitution of the single cysteine residue in  $\text{Ca}_v\beta_{2a}$ -SH3 C113A abolishes dimer formation.



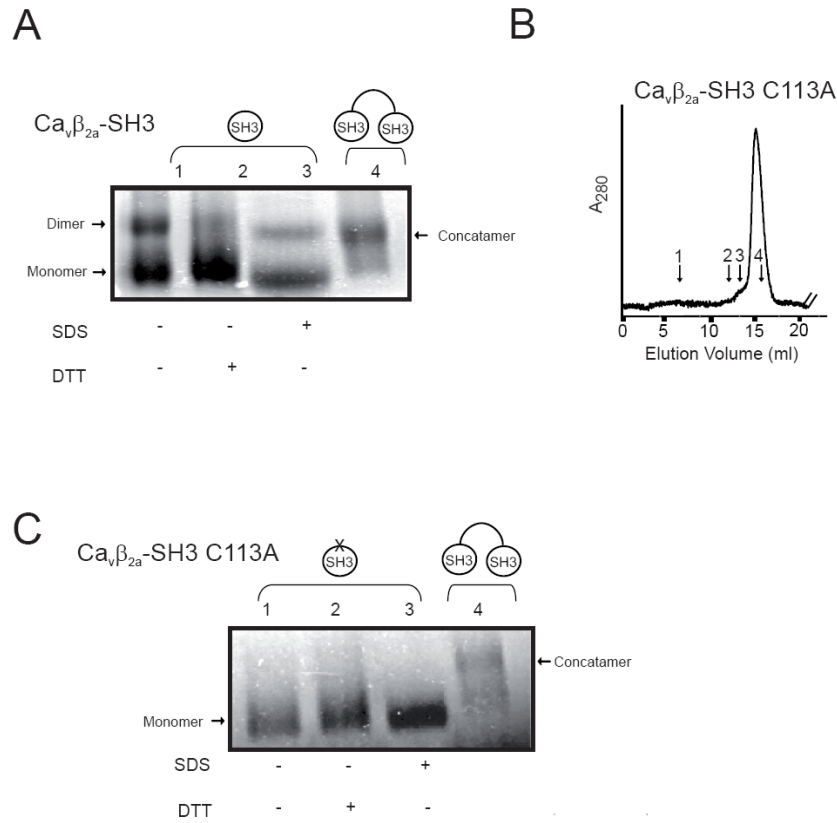


**Fig. 8.1. BN-PAGE analysis of wild type Ca<sub>v</sub>β<sub>2a</sub>-SH3 and Ca<sub>v</sub>β<sub>2a</sub>-SH3 C113A.** *A*, Ca<sub>v</sub>β-SH3 domain resolved in BN-PAGE (4-20% gradient) under different treatments. Ca<sub>v</sub>β-SH3 in native conditions (lane 1) and after 30 min incubation with DTT (lane 2) or SDS (lane 3). Lane 4 was loaded with Ca<sub>v</sub>β-SH3 concatamer construct. *B*, Size exclusion chromatography profile from Superdex 200 10/30 column (GE Healthcare Life Sciences) of purified Ca<sub>v</sub>β-SH3 C113A. The elution volume for molecular mass standards is shown. 1, void volume and 2, 3 and 4 denotes the elution volume of Albumin (67 kDa), Ovalbumin (43 kDa), and Ribonuclease A (13.7 kDa), respectively. *C*, Same as *A* but for Ca<sub>v</sub>β C113A SH3 in native conditions (lane 1) and after 30 min incubation with DTT (lane 2) or SDS (lane 3). Lane 4 was loaded with Ca<sub>v</sub>β-SH3 concatamer construct as control.

#### **8.4.2 $\text{Ca}_V\beta_{2a}$ -SH3 C113A dimerization-deficient mutant associates with dynamin but does not promote endocytosis**

Wild-type  $\text{Ca}_V\beta_{2a}$ -SH3 interacts with dynamin and promotes internalization of cardiac  $\text{Ca}_V1.2$  channels expressed in *Xenopus laevis* oocytes (Gonzalez-Gutierrez *et al.*, 2007). To examine the ability of  $\text{Ca}_V\beta_{2a}$ -SH3 dimerization-deficient mutant to interact with dynamin we expressed HA-tagged dynamin (HA-dynamin) in tsA201 cells and perform coimmunoprecipitation assays with  $\text{Ca}_V\beta_{2a}$ -SH3 C113A and wild-type  $\text{Ca}_V\beta_{2a}$ -SH3 as control. Immunoprecipitation of HA-dynamin coprecipitates wild-type  $\text{Ca}_V\beta_{2a}$ -SH3 and  $\text{Ca}_V\beta_{2a}$ -SH3 C113A to a similar extent (Fig 8.2A), indicating that substitution of cysteine 113 impairs does not prevent binding to dynamin. Here as in previous reports (Gonzalez-Gutierrez *et al.*, 2007;Hidalgo *et al.*, 2006) we used gating currents measurements which result from the charge movement ( $Q_{on}$ ) of a defined number of charged residues that lead to channel opening during activation (Bezanilla and Stefani, 1998). The total charge moved, that is proportional to the number of channel in the plasma membrane, is obtained by integrating the area down the gating current (Fig. 8.2B). A strict correlation between number of channels assessed by  $Q_{on}$  and by immunoassay using epitope-tagged channels has already been established elsewhere (Hidalgo *et al.*, 2006). Injection of wild-type  $\text{Ca}_V\beta_{2a}$ -SH3 into oocytes expressing  $\text{Ca}_V1.2$  channels decreases dramatically  $Q_{on}$  while injection of  $\text{Ca}_V\beta_{2a}$ -SH3 C113A results in no significant changes (Fig. 8.2B). It appears then that binding of  $\text{Ca}_V\beta_{2a}$ -SH3 to dynamin is required but not sufficient to promote endocytosis. Formation of  $\text{Ca}_V\beta_{2a}$ -SH3 dimers emerges as a crucial step. Dynamin uses GTP hydrolysis to generate the force required for scission of newly formed vesicles from the plasma membrane during endocytosis (Marks *et al.*, 2001). The GTPase activity can be

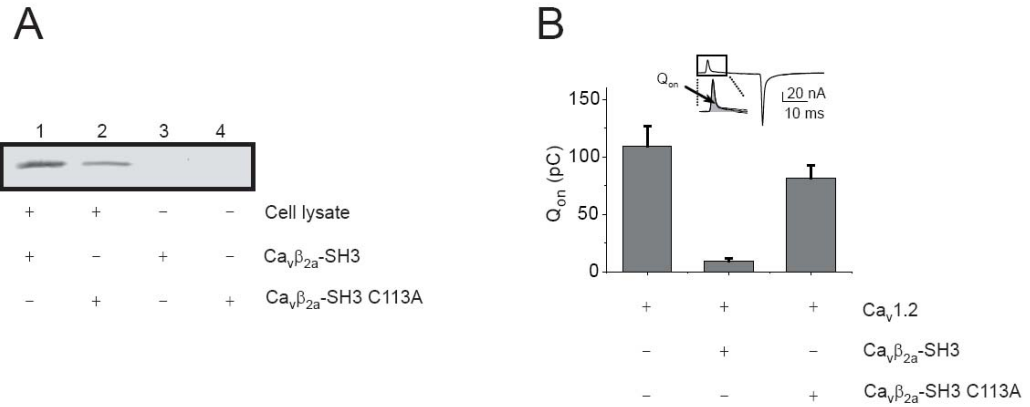


**Fig. 8.2. Association with dynamin and endocytosis activity of wild type  $\text{Ca}_v\beta_{2a}\text{-SH3}$  and  $\text{Ca}_v\beta_{2a}\text{-SH3 C113A}$  dimerization-deficient mutant.** *A*, Western blot of the coprecipitation assay of His<sub>6</sub>-Ca<sub>v</sub>β-SH3 and His<sub>6</sub>-Ca<sub>v</sub>β-SH3 C113A with HA-dynamin expressed in tsA201 cells. Cell lysate from cells expressing HA-dynamin was incubated with either His<sub>6</sub>-Ca<sub>v</sub>β-SH3 (lane 1) or His<sub>6</sub>-Ca<sub>v</sub>β-SH3 C113A (lane 2) and immunoprecipitated with anti-HA antibody (Roche Applied Sciences). Bound proteins were eluted with SDS loading buffer, resolved in SDS-PAGE and analyzed by western blot using anti-His antibody. For lane 3 and 4, cells lysate were replaced by buffer. *B*, Average  $Q_{\text{on}}$  from Ca<sub>v</sub>1.2-expressing oocytes before ( $109.4 \pm 17.8$  pC,  $n=11$ ) and after Ca<sub>v</sub>β<sub>2a</sub>-SH3 ( $8.8 \pm 2.8$  pC,  $n=12$ ) or Ca<sub>v</sub>β<sub>2a</sub>-SH3 C113A injection ( $81.7 \pm 10.7$  pC,  $n=17$ ).  $Q_{\text{on}}$  was measured by integrating gating current during a step near reversal potential for barium as shown in the inset.

stimulated by several factors including self-assembly and binding to SH3-domain containing proteins (Gout *et al.*, 1993; Warnock *et al.*, 1996; Zheng *et al.*, 1996). Dimerization of Ca<sub>v</sub> $\beta$ <sub>2a</sub>-SH3 may facilitate dynamin self-assembly and thus endocytosis.

#### **8.4.3 Concatameric Ca<sub>v</sub> $\beta$ <sub>2a</sub>-SH3 113A rescues endocytosis**

If dimerization through cysteine bridge formation at position 113 is crucial for Ca<sub>v</sub> $\beta$ <sub>2a</sub>-SH3 endocytic function we expect that spatially confining two Ca<sub>v</sub> $\beta$ <sub>2a</sub>-SH3 C113A molecules by joining them together may rescue this function. We engineered a concatameric version of Ca<sub>v</sub> $\beta$ <sub>2a</sub>-SH3 C113A by covalently linking two Ca<sub>v</sub> $\beta$ <sub>2a</sub>-SH3 C113A molecules in a single open reading frame and compare its effect with a wild type Ca<sub>v</sub> $\beta$ <sub>2a</sub>-SH3 concatamer. Association to dynamin was preserved in wild type and mutant concatamers (Fig. 8.3A). Injection of wild type Ca<sub>v</sub> $\beta$ <sub>2a</sub>-SH3 concatamer into Ca<sub>v</sub>1.2-expressing *Xenopus* oocytes reduced Q<sub>on</sub> as efficient as its monomeric counterpart does, indicating that the idea that no major structural rearrangements were induced by linking the two molecules together (Fig. 8.3B). In contrast to its monomeric version, Ca<sub>v</sub> $\beta$ <sub>2a</sub>-SH3 C113A concatamer downregulate Ca<sub>v</sub>1.2 channels (Fig. 8.3C). Thus, Ca<sub>v</sub> $\beta$ <sub>2a</sub>-SH3 C113A concatamer rescues the ability of the wild-type protein to promote endocytosis which is loss in Ca<sub>v</sub> $\beta$ <sub>2a</sub>-SH3 C113A monomer. These findings reinforce the idea that dimerization of Ca<sub>v</sub> $\beta$ <sub>2a</sub>-SH3 is required for its role in mediating endocytosis.

#### **8.4.4 $\text{Ca}_v\beta$ forms dimers**

After establishing the functional relevance of  $\text{Ca}_v\beta_{2a}$ -SH3 we explored the ability of the full length  $\text{Ca}_v\beta$  to form dimers using BN-PAGE and pull down assays. We rationalized that dimerization may constitute a molecular switch contributing to the functional plasticity of  $\text{Ca}_v\beta$ .  $\text{Ca}_v\beta_{2a}$  resolved in BN-PAGE also exhibits two protein populations suggesting the coexistence of monomers and dimers (Fig. 8.4A). However, neither treatment with DTT nor with SDS leads to disaggregation of the higher molecular weight complex. Consistently, incorporation of the C113A mutation in the full-length protein ( $\text{Ca}_v\beta$  C113A) did not change the protein migration in the BN-PAGE suggesting that the oligomer state is stabilized by additional interactions beside SH3-SH3 contacts (data not shown). Moreover,  $\text{Ca}_v\beta$  C113A exhibit same endocytic activity as the wild type protein (data not shown).

To investigate dimer formation in intact cells we generated a  $\text{Ca}_v\beta$  fused to either the yellow fluorescence protein (YFP- $\text{Ca}_v\beta$ ) or to the strep tacin II<sup>TM</sup> tag (Strep- $\text{Ca}_v\beta$ ) and coexpressed them in tsA201 cells. Strep- $\text{Ca}_v\beta$  pulled down specifically YFP- $\text{Ca}_v\beta$  indicating that  $\text{Ca}_v\beta$  dimers are formed inside the cell (Fig. 8.4B).

It has been established that one molecule of  $\text{Ca}_v\beta$  suffices for calcium channel function modulation (Dalton *et al.*, 2005). However,  $\text{Ca}_v\beta$  down-regulates only calcium channels that lack the highly conserved AID site but not wild type channels indicating that only the unbound form is able to promote endocytosis (Gonzalez-Gutierrez *et al.*, 2007). This mechanism would provide a very efficient quality control mechanism assuring functional fitness and survival of the channel in the plasma

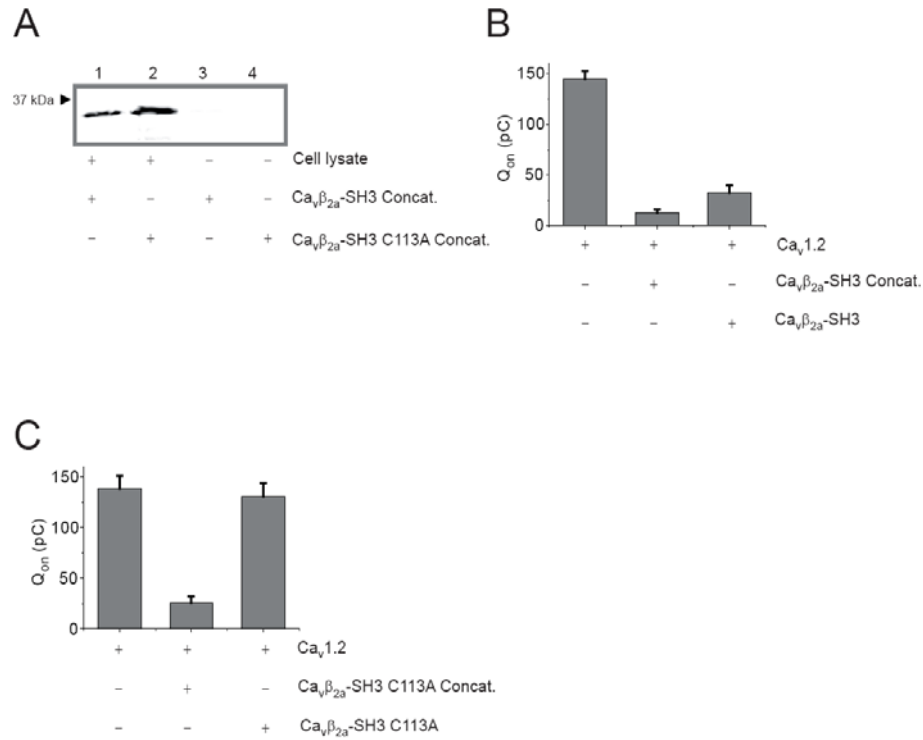


**Fig. 8.3. Association with dynamin and endocytosis activity of wild type Ca<sub>v</sub>β<sub>2a</sub>-SH3 and Ca<sub>v</sub>β<sub>2a</sub>-SH3 C113A concatamers.** *A*, Western blot of the coprecipitation assay of His<sub>6</sub>-Ca<sub>v</sub>β-SH3 concatamer and His<sub>6</sub>-Ca<sub>v</sub>β-SH3 C113A concatamer with HA-dynamin expressed in tsA201 cells as in Fig. 2A. *B*, Average Q<sub>on</sub> from Ca<sub>v</sub>1.2-expressing oocytes before (144.6 ± 7.72 pC, n=12) and after injection of either Ca<sub>v</sub>β<sub>2a</sub>-SH3 concatamer (12.8 ± 2.8 pC, n=10) or Ca<sub>v</sub>β<sub>2a</sub>-SH3 monomer (32.8 ± 7.1 pC, n=10). *C*, Average Q<sub>on</sub> from Ca<sub>v</sub>1.2-expressing oocytes before (137.9 ± 13.0 pC, n=15) and after injection of either Ca<sub>v</sub>β<sub>2a</sub>-SH3 C113A concatamer (25.9 ± 5.7 pC, n=17) or Ca<sub>v</sub>β<sub>2a</sub>-SH3 C113A monomer (130.4 ± 13.6 pC, n=16). Q<sub>on</sub> was calculated as in Fig. 2B.

membrane. We envision that free  $\text{Ca}_v\beta$  dimerizes and its association with  $\text{Ca}_v\alpha_1$  pore forming subunit regulates its oligomerization state. This predicts that pre-association of  $\text{Ca}_v\beta$  with the AID would impair its endocytic ability by preventing dimerization of  $\text{Ca}_v\beta$ . We coinjected  $\text{Ca}_v\beta_{2a}$  alone and pre-incubated with loop I-II of  $\text{Ca}_v\alpha_1$  that encompasses the AID site in oocytes expressing  $\text{Ca}_v1.2$  channels lacking the AID site.

Association of  $\text{Ca}_v\beta$  with AID indeed prevented internalization of  $\text{Ca}_v1.2 \Delta\text{AID}$  channels (Fig 8.4C). Thus it appears likely that dimerization of  $\text{Ca}_v\beta$  plays a relevant role in determining the multifunctionality of this protein.

#### **8.4.5 Speculation**

Dimerization is an important event in signal transduction and plays a crucial role in signaling events at the plasma membrane (Klemm *et al.*, 1998). We propose that dimerization of  $\text{Ca}_v\beta$  regulates the functional switch of  $\text{Ca}_v\beta$  from calcium channel modulator to endocytosis activator. This is consistent with the yet well-established one-to-one stoichiometry of  $\text{Ca}_v\alpha_1$ - $\text{Ca}_v\beta$  interaction that modulates calcium channels function (Dalton *et al.*, 2005) and the reversible nature of this interaction (Hidalgo *et al.*, 2006).  $\text{Ca}_v\beta$  would bind the channel as monomer and when dissociates may interact with dynamin, dimerize and promote endocytosis (Fig 8.5). Whereas the whole picture is certainly still incomplete, our findings constitute a first step towards unveiling the molecular basis of  $\text{Ca}_v\beta$  functional versatility. They outline a novel mechanism for the functional plasticity of  $\text{Ca}_v\beta$  which clearly has become a multifunctional regulatory protein besides modulation of calcium channels (Hidalgo *et al.*, 2007).

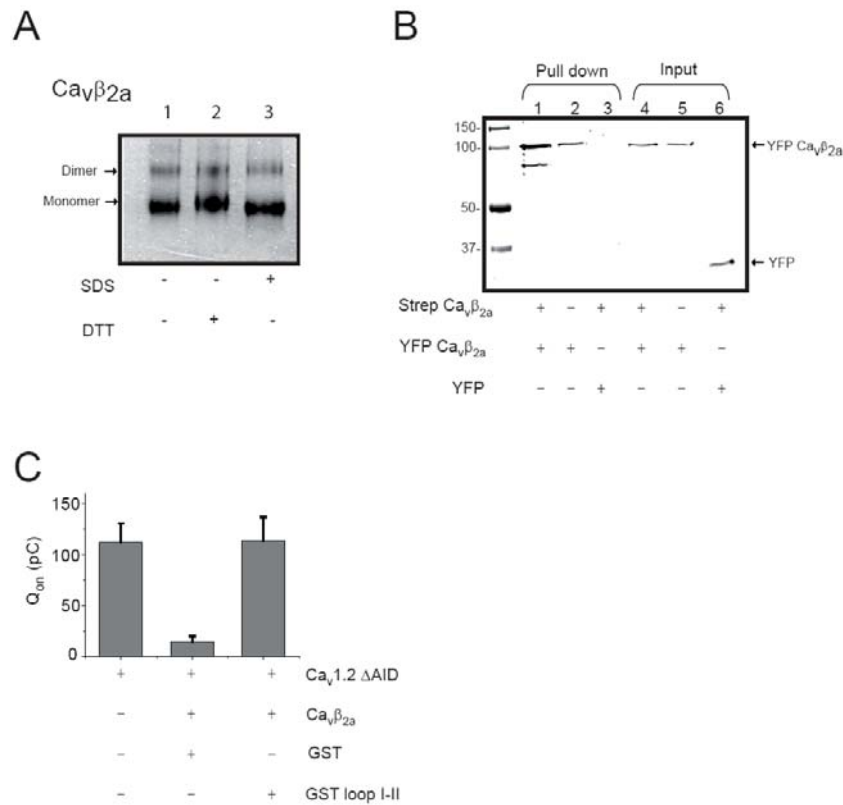


**Fig. 8.4. BN-PAGE and pull down assays of Ca<sub>v</sub>β<sub>2a</sub>.** *A*, Ca<sub>v</sub>β<sub>2a</sub> domain resolved in BN-PAGE (4-20% gradient) under different treatments. Ca<sub>v</sub>β<sub>2a</sub> in native conditions (lane 1) and after 30 min incubation with DTT (lane 2) or SDS (lane 3). *B*, Pull down assay using Strep-Ca<sub>v</sub>β<sub>2a</sub> as bait and YFP-Ca<sub>v</sub>β<sub>2a</sub> as prey expressed in tsA201 cells. Bound proteins were eluted with SDS loading buffer, resolved in SDS-PAGE and visualized by fluorescence scanning. Lane 1-3, pull down assay using: lane 1, Strep-Ca<sub>v</sub>β<sub>2a</sub> and YFP-Ca<sub>v</sub>β<sub>2a</sub>; lane 2, YFP-Ca<sub>v</sub>β<sub>2a</sub> alone and lane 3, Strep-Ca<sub>v</sub>β<sub>2a</sub> and YFP. Lane 4-6, crude extract from cell expressing: lane 4, Strep-Ca<sub>v</sub>β<sub>2a</sub> and YFP-Ca<sub>v</sub>β<sub>2a</sub>; lane 5, YFP-Ca<sub>v</sub>β<sub>2a</sub> alone and lane 6, Strep-Ca<sub>v</sub>β<sub>2a</sub> and YFP. *C*, Average Q<sub>on</sub> from Ca<sub>v</sub>1.2 ΔAID-expressing oocytes before (112.1 ± 19.1 pC, n=19) and after injection of Ca<sub>v</sub>β<sub>2a</sub> either pre-incubated with GST (14.3 ± 5.2 pC, n=19) or with GST fused to loop I-II of Ca<sub>v</sub>α<sub>1</sub> encompassing AID site (113.7 ± 23.2 pC, n=20).



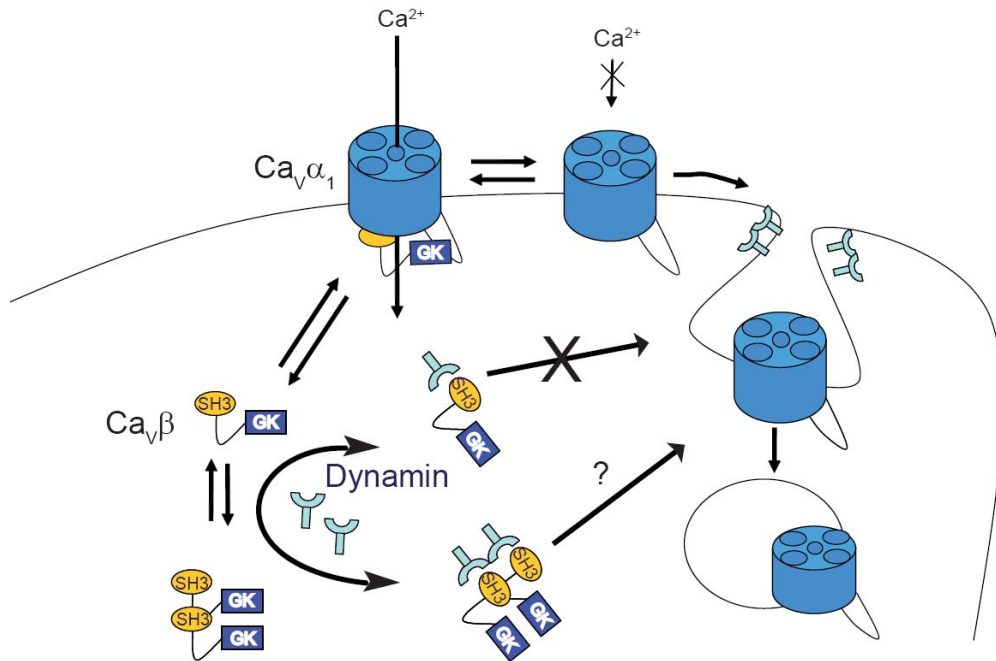


**Fig. 8.5. Model for the functional switch of  $\text{Ca}_v\beta$  from calcium channel modulator to endocytosis activator.**  $\text{Ca}_v\beta$  binds as a monomer to the AID site located within the intracellular loop joining domain I and II of  $\text{Ca}_v\alpha_1$ . For simplicity the other loops were removed). Dissociation of  $\text{Ca}_v\beta$  allows its interaction with dynamin and dimerization. Only interaction of the dimeric form of  $\text{Ca}_v\beta$  with dynamin with would leads to endocytosis. The mechanism by which this interaction results in vesicle internalization remains to be investigated.

## **ACKNOWLEDGEMENTS**

We thank Dr. Christoph Fahlke for insightful discussion: This study was supported by grants from the Deutsche Forschung Gemeinschaft (DFG) (FOR 450, TP1, to PH.)

The authors declare no competing financial interests.

## **8.5 References**

1. Arikath J and Campbell KP (2003) Auxiliary subunits: essential components of the voltage-gated calcium channel complex. *Curr Opin Neurobiol*, **13**, 298-307.
2. Berggren PO, Yang SN, Murakami M, Efanov AM, Uhles S, Kohler M, Moede T, Fernstrom A, Appelskog IB, Aspinwall CA, Zaitsev SV, Larsson O, de Vargas LM, Fecher-Trost C, Weissgerber P, Ludwig A, Leibiger B, Juntti-Berggren L, Barker CJ, Gromada J, Freichel M, Leibiger IB, and Flockerzi V (2004) Removal of Ca<sup>2+</sup> channel beta3 subunit enhances Ca<sup>2+</sup> oscillation frequency and insulin exocytosis. *Cell*, **119**, 273-284.
3. Bezanilla F and Stefani E (1998) Gating currents. *Methods Enzymol*, **293**, 331-352.
4. Catterall WA (2000) Structure and regulation of voltage-gated Ca<sup>2+</sup> channels. *Annu Rev Cell Dev Biol*, **16**, 521-555.
5. Chen YH, Li MH, Zhang Y, He LL, Yamada Y, Fitzmaurice A, Shen Y, Zhang H, Tong L, and Yang J (2004) Structural basis of the alpha1-beta subunit interaction of voltage-gated Ca<sup>2+</sup> channels. *Nature*, **429**, 675-680.
6. Dalton S, Takahashi SX, Miriyala J, and Colecraft HM (2005) A single CaV $\beta$  can reconstitute both trafficking and macroscopic conductance of voltage-dependent calcium channels. *J Physiol*, **567**, 757-769.
7. Dolphin AC (2003) Beta subunits of voltage-gated calcium channels. *J Bioenerg Biomembr*, **35**, 599-620.

8. Gonzalez-Gutierrez G, Miranda-Laferte E, Neely A, and Hidalgo P (2007) The Src Homology 3 Domain of the beta-Subunit of Voltage-gated Calcium Channels Promotes Endocytosis via Dynamin Interaction. *J Biol Chem*, **282**, 2156-2162.
9. Gonzalez-Gutierrez G, Miranda-Laferte E, Nothmann D, Schmidt S, Neely A, and Hidalgo P (2008) The guanylate kinase domain of the {beta}-subunit of voltage-gated calcium channels suffices to modulate gating. *Proc Natl Acad Sci U S A*, **105**, 14198-14203.
10. Gout I, Dhand R, Hiles ID, Fry MJ, Panayotou G, Das P, Truong O, Totty NF, Hsuan J, Booker GW, and . (1993) The GTPase dynamin binds to and is activated by a subset of SH3 domains. *Cell*, **75**, 25-36.
11. Hibino H, Pironkova R, Onwumere O, Rousset M, Charnet P, Hudspeth AJ, and Lesage F (2003) Direct interaction with a nuclear protein and regulation of gene silencing by a variant of the Ca<sup>2+</sup>-channel beta 4 subunit. *Proc Natl Acad Sci U S A*, **100**, 307-312.
12. Hidalgo P, Gonzalez-Gutierrez G, Garcia-Olivares J, and Neely A (2006) The alpha 1-beta subunit interaction that modulates calcium channel activity is reversible and requires a competent alpha -interaction domain. *J Biol Chem*, **281**, 24104-24110.
13. Hidalgo P and Neely A (2007) Multiplicity of protein interactions and functions of the voltage-gated calcium channel beta-subunit. *Cell Calcium*, **42**, 389-396.

14. Klemm JD, Schreiber SL, and Crabtree GR (1998) Dimerization as a regulatory mechanism in signal transduction. *Annu Rev Immunol*, **16**, 569-592.
15. Marks B, Stowell MH, Vallis Y, Mills IG, Gibson A, Hopkins CR, and McMahon HT (2001) GTPase activity of dynamin and resulting conformation change are essential for endocytosis. *Nature*, **410**, 231-235.
16. Neely A, Garcia-Olivares J, Voswinkel S, Horstkott H, and Hidalgo P (2004) Folding of active calcium channel beta(1b) -subunit by size-exclusion chromatography and its role on channel function. *J Biol Chem*, **279**, 21689-21694.
17. Niepmann M and Zheng J (2006) Discontinuous native protein gel electrophoresis. *Electrophoresis*, **27**, 3949-3951.
18. Opatowsky Y, Chen CC, Campbell KP, and Hirsch JA (2004) Structural analysis of the voltage-dependent calcium channel beta subunit functional core and its complex with the alpha 1 interaction domain. *Neuron*, **42**, 387-399.
19. Owen DJ, Wigge P, Vallis Y, Moore JD, Evans PR, and McMahon HT (1998) Crystal structure of the amphiphysin-2 SH3 domain and its role in the prevention of dynamin ring formation. *EMBO J*, **17**, 5273-5285.
20. Pragnell M, De Waard M, Mori M, Tanabe T, Snutch TP, and Campbell KP (1994) Calcium channel  $\beta$ -subunit binds to a conserved motif in the I-II cytoplasmic linker of the  $\alpha_1$ -subunit. *Nature*, **368**, 67-70.

21. Van Petegem F., Clark KA, Chatelain FC, and Minor DL, Jr. (2004) Structure of a complex between a voltage-gated calcium channel beta-subunit and an alpha-subunit domain. *Nature*, **429**, 671-675.
22. Warnock DE, Hinshaw JE, and Schmid SL (1996) Dynamin self-assembly stimulates its GTPase activity. *J Biol Chem*, **271**, 22310-22314.
23. Wigge P, Kohler K, Vallis Y, Doyle CA, Owen D, Hunt SP, and McMahon HT (1997) Amphiphysin heterodimers: potential role in clathrin-mediated endocytosis. *Mol Biol Cell*, **8**, 2003-2015.
24. Wigge P and McMahon HT (1998) The amphiphysin family of proteins and their role in endocytosis at the synapse. *Trends Neurosci*, **21**, 339-344.
25. Zheng J, Cahill SM, Lemmon MA, Fushman D, Schlessinger J, and Cowburn D (1996) Identification of the binding site for acidic phospholipids on the pH domain of dynamin: implications for stimulation of GTPase activity. *J Mol Biol*, **255**, 14-21.

## **Acknowledgments**

*I would like to thank Dr. Patricia Hidalgo, for the experience transmitted, her advices, her confidence, her help and her support during all these years and for give me the chance to work in this project.*

*I also would like to thank Prof. Dr Christoph Fahlke for the opportunity to work in his lab and have the chance to learn of his experience.*

*I thank too Dr Giovanni Gonzalez-Gutierrez for his unconditional friendship and help in the lab and life in general.*

*I also would like to thank Silke Schmidt for her excellent technical assistance in many of the experiments that were presented here.*

*Thanks to Prof Dr. Alan Neely for share with me his experience in electrophysiology and in cut open.*

*I thank all my colleagues of our group for the nice moments that we had together through all these years and for all the help that they gave me in many aspects.*

*I also would like to thank my family and all my friends in Hannover and around the world for support me and be worry about me and my work.*

*Thanks*

## **Curriculum Vitae**

### **Erick Miranda Laferte**

Auf dem Lärchenberge 14C. 2G.

30161, Hannover, Germany

Born on September, 14<sup>th</sup> of 1974 at Havana (Cuba)

### **Graduated of:**

**1997: *Bachelor in Science in Biochemistry at University of Havana.***

**2003: *Master in Science in Biochemistry of Proteins at University of Havana.***

### **List of Publications**

**Miranda-Laferte E**, Gonzalez-Gutierrez G, Schmidt S, Neely A and Hidalgo P (2009) Dimerization of the Src Homology 3 domain of the voltage-gated calcium channel  $\beta$ -subunit regulates endocytosis. Manuscript in preparation to be submitted to ***EMBO Reports***.

Gonzalez-Gutierrez G, **Miranda-Laferte E**, Contreras G, Neely A and Hidalgo P (2009). Swapping the I-II intracellular linker between L-type  $\text{Ca}_v1.2$  and R-type  $\text{Ca}_v2.3$  high-voltage gated calcium channels exchanges activation attributes. **Channels** in press.



Gonzalez-Gutierrez G, **Miranda-Laferte E**, Nothmann D, Schmidt S, Neely A and Hidalgo P (2008). The guanylate kinase domain of the  $\beta$ -Subunit of Voltage-gated calcium channels suffices to modulate gating. *Proc. Natl. Acad. Sci. USA*. 105(37):14198-14203.

Gonzalez-Gutierrez G, **Miranda-Laferte E**, Naranjo D, Hidalgo P and Neely A (2008). Mutations of non-conserved residues within the calcium channel  $\alpha 1$ -interaction domain inhibit  $\beta$ -subunit potentiation. *Journal of General Physiology*. 132(3): 383-395.

**Miranda-Laferte E\***, Gonzalez-Gutierrez\* G, Neely A and Hidalgo P (2007). The Src Homology 3 domain of the  $\beta$ -Subunit of Voltage-gated Calcium Channels promotes endocytosis via dynamin interaction. *Journal of Biological Chemistry*. 282(4): 2156-2162. (\*First author with equal contribution)

### **Stays and Formation**

**2006-2009**: PhD Student. Institute of Neurophysiology. Hannover Medicine School. (MHH). Hannover. Germany.

**2008**: Visiting scientist. Centre for Neuroscience of Valparaiso. University of Valparaiso. Chile

**2005-2006**: Research Assistant. Institute of Physiology. RWTH University. Aachen. Germany.

**2001-2003**: Master studies in Biochemistry at University of Havana.

**1999:** Visiting scientist. International Institute of Genetics and Biophysics of Naples. Italy.

**1997-2004:** Research Assistant, Molecular Biology Laboratory. Plant Health Research Institute, Havana, Cuba.

**1995-1997:** Undergraduate student, Molecular Biology Laboratory. National Centre for Animal and Plant Health. Havana. Cuba

**1992-1997:** Diploma studies in Biochemistry at University of Havana.